A BIOCHEMICAL AND GENETIC INVESTIGATION OF REDOX-ACTIVE TRANSITION METAL ION HOMEOSTASIS

A Dissertation

Presented to the Faculty of the Graduate School

of Cornell University

in Partial Fulfillment of the Requirements for the Degree of

Doctor of Philosophy

by

Gregory Thomas Smaldone

January 2012

A BIOCHEMICAL AND GENETIC INVESTIGATION OF REDOX-ACTIVE TRANSITION METAL ION HOMEOSTASIS

Gregory Thomas Smaldone, Ph.D.

Cornell University 2012

Iron and copper are essential trace nutrients required for cell growth and proliferation. In excess, these metals pose a serious threat to the cell, either by interacting with oxygen species, generating free radicals, or by replacing other metal cofactors within the metal binding sites of enzymes. For these reasons, it is of vital importance that bacteria be able to tightly control the intracellular concentrations of both iron and copper. In *Bacillus subtilis*, a Gram positive model soil bacterium, this control is exerted via a number of uptake, efflux, and storage systems.

Iron limitation is answered by means of a newly discovered sRNA mediated iron-sparing system. Using global analytical techniques, I identified the regulon of the iron-sparing response; mediated by the Fur regulated small RNA A (FsrA) and the Fur regulated basic proteins (FbpABC). In times of iron starvation, the mRNAs of iron binding targets are post-transcriptionally affected by their interaction with the iron-sparing response elements. Through this regulatory process, FsrA and its chaperones prioritize iron usage within the cell during iron starvation, ensuring that newly acquired iron is earmarked for essential functions. I also characterized the direct repression of a single target of the iron-sparing response, the iron-utilizing lactate oxidoreductase operon, *lutABC*. The regulation of this operon was shown to be dependent on the expression of FsrA as well as the translation of the RNA chaperone-like peptide,

FbpB. The iron responsive regulation of the *lut* operon plays an important role in the cell's ability to grow and form biofilms on lactate as a carbon source in iron limiting environments.

Finally, I characterized how the cell senses and responds to copper accumulation via the copper sensitive operon repressor, CsoR, and not the previously identified copper regulator YhdQ. I determined the high affinity binding of CsoR to a site overlapping the copper efflux operon, *copZA*, repressing its expression when copper is bound.

The work presented here furthers our understanding of how *B. subtilis* regulates and responds to changing levels of iron and copper.

BIOGRAPHICAL SKETCH

Gregory Thomas Smaldone was born 29 October 1982 in Neptune, New Jersey and was raised in nearby Millstone Township. From an early age his parents, Donald and Lesyle, ensured he had a full and enriching education, providing him with books on every subject. They instilled in him the importance of personally supplementing one's formal education.

Upon completion of his high school education at Christian Brothers Academy, Greg attended Cook College at Rutgers, The State University of New Jersey in New Brunswick. While studying there, he took a particular interest in the biological sciences, particularly biochemistry and molecular biology. Professor Donald Kobayashi offered Greg a research position studying gene regulation in *Pseudomonas fluorescens*, introducing him to the importance of microbiology in our fundamental understanding of life. Greg graduated with highest honors in 2005 with a B.S. in Biotechnology.

Upon attaining his degree, Greg decided to pursue a doctorate in biochemistry at Cornell University. There he joined the laboratory of Professor John D. Helmann and studied the regulation of copper and iron homeostasis in *Bacillus subtilis*. With the competition of his doctorate, Greg will be relocating to Davis, California where he will begin postdoctoral research in the developmental program of *Myxococcus xanthus*.

For Mom, Dad, Stephen, Marcy, and Shamoni

ACKNOWLEDGEMENTS

There are many people to which I owe a great debt. They have helped guide me through both my life and my scientific career.

To John Helmann, thank you for your support and guidance these past five years. You taught me that skillful communication is as important as thorough experimentation. To Ahmed Gaballa, thank you for your time, energy, patience, and expertise. Without you productivity in the lab would grind to a halt. To Letal Salzberg, you are an invaluable colleague and a selfless friend. Thank you for always offering your honest opinion. To my family, thank you for providing the strength and foundation for all my past and future successes. Most importantly, thank you to Shamoni Maheshwari. You are my best friend and motivation. I could not have finished this without you. Lastly, thanks to the Helmann lab members past and present, my committee members Jim Shapleigh and Brian Crane, the Microbiology department, and the field of Biochemistry, Molecular, and Cell Biology for your support.

TABLE OF CONTENTS

LIST OF TABLES

LIST OF FIGURES

CHAPTER 1

CONTROLLING REDOX-ACTIVE TRANSITION METALS: IRON AND COPPER HOMEOSTASIS IN BACTERIA

Bacteria require metal ions as essential co-factors for many cellular proteins as both structural and enzymatic centers [4, 41, 70] and hence have evolved many high affinity transport systems to obtain them from the environment. However, once acquired, high concentrations of many metals can result in toxic overload. Iron and copper are two of these essential metals that participate in major cellular processes such as respiration, DNA biosynthesis, and the tricarboxylic acid cycle. While the toxicity of iron and copper has been empirically observed, we have only recently begun to understand the biological mechanisms underlying this toxicity.

The main themes in metal homeostasis revolve around uptake, efflux, and the control of "free" metal levels within the cytosol. These activities are orchestrated on a transcriptional level by a suite of metalloregulators which each respond to a specific metal. This chapter will summarize our current knowledge of these systems as they pertain to iron and copper.

1.1 Iron

1.1.1 Regulation

The best characterized examples of iron metalloregulators are the ferric uptake regulator (Fur) protein family present in *Escherichia coli* and *Bacillus subtilis* and the diphtheria toxin regulator (DtxR) family proteins which control iron home-

ostasis in many high GC Gram positive bacteria.

Fur is a global regulator controlling the transcription of a suite of genes necessary for iron uptake, storage, sparing and utilization. Fur was first characterized in *E. coli* as a histidine-rich protein of 148 amino acid residues and a molecular mass of 17 kDa, acting as a divalent metal-dependent DNA-binding protein [8, 58]. These studies put forth the model of a dimeric regulator that binds Fe^{2+} and mediates repression of target genes under iron-replete conditions. Repression is driven by the binding of the two dimers to a specific "Fur-box," a 19 bp consensus sequence made up of two overlapping 7-1-7 inverted repeats. This motif is present at the promoters of target genes and Fur binding blocks the access of the transcriptional machinery to the downstream genes [9, 38]. With the identification of this consensus sequence, it became possible to search annotated genomes for candidate Fur regulated genes. In *B. subtilis*, the model Gram-positive microorganism, 20 operons (39 genes) have been identified both bioinformatically and experimentally as belonging to the Fur regulon [10], many of which constitute systems important iron uptake.

DtxR is similar to Fur both structurally and functionally. Both proteins contain an N-terminal DNA binding domain similar to that of the CAP family of proteins, followed by a metal binding domain [138]. Functionally, DtxR also regulates the expression of genes responsible for siderophore biosysnthesis, uptake and iron sparing [126, 150]. These similarites speak to the possible evolutionary relationship of Fur and DtxR. However, important differences do separate the two into distinct families. Unlike Fur, DtxR has an unordered C-terminal domain of unknown function and DtxR shares little to no sequence similarity with Fur [65]. DtxR and its family members (IdeR, *Mycobacterium tuberculosis*; SirR,

Staphylococcus epidermidis) require iron as a co-repressor *in vivo*, but other divalents can also act similarly *in vitro* [28, 42, 66, 116] albeit at much higher levels, suggesting Fe^{2+} is indeed the physiologically relevent co-repressor [28, 133].

1.1.2 Iron uptake systems

The iron acquisition systems regulated by Fur and DtxR are used for scavenging iron from the environment under iron limiting conditions. In *B. subtilis*, this includes the use of iron chelating siderophores such as bacillibactin, enterobactin, ferrioxamine, and ferrichrome [110]. These compounds are able to bind ferric iron making it soluble in aqueous solution so that it can then enter the cell via ATP-binding cassette (ABC) transporter complexes with a relative specificity for a given substrate [106]. In addition, elemental iron and iron citrate uptake systems are also employed. In *B. subtilis*, there are four energy-requiring ABC transporter complexes: YfmCDEF, FhuD-FhuBGC-YusV, YfiY-YfiZA-YusV, and FeuABC, involved in the uptake of at least seven iron-acquiring chelators [106, 110]. These complexes consist of a membrane anchored binding protein specific for the ferri-siderophore, gated integral permease proteins that open once the binding protein delivers the ferri-siderophore, and the ATP-binding cassette protein that interacts with the permease and hydrolyzes ATP to fuel the action of the permease protein [5]. It is also common for the cell to produce ABC transporters for siderophores that it does not produce endogenously. Of the siderophores listed above, only bacillibactin is produced and secreted by *B. subtilis*. It is recognized and taken up by the FeuABC ABC transport complex [106]. *B. subtilis* can also pirate extracellularly iron bound siderophores produced by other bacteria for its own use [110]. This is useful to the cell in an iron

starved environment where there may be competition from other bacteria.

1.1.3 Cellular toxicity

When cellular iron interacts with either superoxide or hydrogen peroxide species (which both are mildly physiologically reactive) a highly reactive and extremely damaging hydroxyl radical results [5, 154]. The following is a simplified representation of what is most likely taking place *in vivo*:

$$Fe^{2+} + H_2O_2 \Rightarrow Fe^{3+} + OH^- + {}^{\cdot}HO$$

The Fenton reaction resulting in a hydroxyl radical is coupled with iron reduction leading to the catalytic production of ${}^{\cdot}HO$ (known as the Haber-Weiss cycle). This reaction can also take place while Fe^{2+} is bound to a ligand as a co-factor [154]. Once reactive oxygen species are generated, they can cause damage to iron-sulfur clusters, protein carbonylation, cystine/methionine oxidation, membrane lipid peroxidation, and DNA damage [34, 45]. Due to the fact that iron is a major contributor to redox stress, there is significant regulatory cross-talk between iron homeostasis and oxidative stress resistance [34].

1.2 Control of iron levels in the cytosol

1.2.1 Iron storage systems

In *B. subtilis*, "free" iron accumulation is managed by a set of specialized storage proteins known as the mini-ferritins [68], which include DNA protection during starvation protein (Dps) and MrgA [5]. These proteins are comprised of 12 subunits that assemble to form a spherical protein shell with an internal cavity that functions as an iron storage reservoir (≈500 iron atoms in Dps). Dps and MrgA are thought to store iron in a similar fashion; taking up soluble ferrous iron and oxidizing it to the ferric form for storage. Preliminary results suggest that *B. subtilis* Dps can indeed store iron and function as an iron reservoir (RM Heinneman and JD Helmann, unpublished results). While similar in structure, Dps and MrgA are differentially regulated by σ^B, the general stress response sigma factor, and PerR, the peroxide sensing regulator, respectively [5, 49]. Once iron is stored, the free iron content of the cell will drop, protecting the cell from oxidative damage [5]. When iron becomes limiting, it is hypothesized that it can be mobilized from the mini-ferritins. This may, along with the iron-sparing response, allow for survival during times of iron starvation.

1.2.2 The iron-sparing response

Bioinformatic searches for additional Fur regulon members identified a strong consensus Fur-box (16 of 19) in the intergenic region between *ykuI* and *ykuJ* [50]. This was interesting since *ykuJ* expression did not appear affected by iron levels [50]. Upon closer inspection of the region, consensus -35 and -10 σ^A promoter

elements were identified [50]. In addition, an inverted repeat, indicating the presence of a strong stem-loop structure, followed by a stretch of Ts was also identified, denoting a ρ-independent terminator. These features are all consistent with the presence of a small non-coding RNA [152]. Subsequently, this transcript was named the Fur-regulated small RNA A (FsrA). FsrA measures 80 nucleotides in length, is transcribed from the identified σ^A promoter, and was confirmed to be an iron-responsive sRNA [50].

A similarly regulated sRNA, RyhB, has been well characterized in *E. coli* and was shown to negatively regulate a number of "low-priority" iron-utilizing genes including superoxide dismutase (*sodB*), succinate dehydrogenase (*sdhCDAB*), fumarase (*fumA*), bacterioferritin (*bfr*), and ferritin (*ftnA*) [96]. RyhB is expressed as a 90-nt transcript observed during growth in minimal media and at late stationary phase [6, 96]. The model for RyhB activity, termed the iron-sparing response, accounts for the apparent activation of several genes by Fur under repressive conditions [10, 59]. The model proposes that when iron levels are low, Fur repression is lifted and iron-uptake is increased. At the same time the RyhB transcript is expressed, repressing the production of "low-priority" iron-containing proteins and allowing the newly imported iron to be shuttled to essential iron-requiring functions [75, 96]. This regulation is mediated by the sRNA binding directly to target mRNA. The model also hypothesizes that the function of the sRNA is to adjust iron flux within the cell, modulating the flow of free iron during iron-replete or -deplete conditions. An example of iron flux remodeling by RyhB has been demonstrated with *E. coli* enterobactin biosynthesis. The direct repression of *cysE* translation by RyhB leads to the reduction of CysE activity. CysE encodes serine acetyltransferase, an enzyme that uses serine as a substrate for cysteine biosynthesis, and its repression allows serine to

be used preferentially for enterobactin synthesis [123].

The many sRNAs that have been identified to date utilize a number of diverse regulatory methods. The first sRNA identified was 6S RNA which is unique because it is the only one known to regulate transcription by interacting directly with RNA polymerase [148]. 6S RNA is a double stranded RNA with an unpaired region and is expressed as the cell enters stationary phase. It mimics the open complex of a σ^{70} promoter and binds specifically to σ^{70} loaded RNA polymerase, titrating it away from chromosomal promoters [148]. However, it does not bind RpoS (σ^{38}, stationary phase) loaded RNA polymerase, leading to an increase in genes transcribed from stationary promoters and a decrease in genes transcribed from vegetative promoters [54]. Another, more common regulatory method is degradation of the target mRNA by interaction with the sRNA [87]. This is exemplified by degradation of the *E. coil* superoxide dismutase (*sodB*) mRNA when bound to RyhB. In this case, the sRNA possesses a short sequence similar to the target mRNA, the two initially bind forming what is known as a "kissing complex," followed by the formation of a more stable RNA duplex which is then identified and degraded by RNase E [117]. Further evidence suggests that specific conserved regions of the sRNAs are of particular importance when directing its binding to mRNA targets [53, 114]. Target transcripts are often predicted to pair with the sRNA at the ribosome binding region or overlapping the start codon. Interference with the translational machinery can occur even without the degradation of the transcript. This was illustrated by the 109 nucleotide sRNA Spot 42 and its target *galK* in *E. coli* [105]. Spot 42 is transcribed in response to growth on glucose. It binds to the *galK* transcript restricting access of the ribosomes, effectively stopping translation. Conversely, it is also possible for the sRNA to relieve inhibitory mRNA secondary structure

that interferes with translation. This is the case with the RpoS transcript, which is positively regulated by both the RprA (cell wall stress) and the DsrA (low temperature) sRNAs [54].

With the advent of next generation sequencing techniques, sRNA identification has entered a new era. Deep sequencing has uncovered hundreds of new sRNAs in *E. coli*, *B. subtilis*, *Staphylococcus aureus*, and *Salmonella* species to mention a few [74, 128, 143, 144]. With their discovery, more variations on the above mentioned regulatory themes are being characterized with ever increasing speed.

In many instances, sRNAs have been shown to require a protein chaperone, known as Hfq, for their function [3]. Hfq was originally identified as a host factor required for the replication of the RNA phage Qβ in *E. coli* and as an RNA binding protein. It has a hexameric doughnut shaped structure with a central hole of about 12Å in diameter [127]. Hfq homologs have been identified in numerous bacteria and are highly conserved [16]. The sRNAs bind to the inner surface of the central opening in a circular fashion, suggesting that RNA could be threaded through, denaturing any secondary structure present [127]. Studies have shown that Hfq binds to, and is necessary for, the regulatory activity of a number of trans-acting sRNAs. RNA binding facilitates either a change in the structure of the sRNA, allowing it to interact with its target, or increases the accessibility of the sRNA by bringing it into close proximity with its target [3]. Surprisingly, the *B. subtilis* Hfq homolog, *ymaH*, has yet to be demonstrated as necessary for the function of any sRNAs. In fact, while implicated initially in the regulation of arginine catabolism, it was later demonstrated that sRNA SR1 functions independently of YmaH [62, 63]. Our previous data shows that YmaH

is not required for the repression of FsrA targets (KB Song and JD Helmann, unpublished results). However, while YmaH may not be playing a co-regulatory role in these specific examples, recent RNAseq experiments have demonstrated the association of YmaH with a number of known sRNA and their corresponding targets in *B. subtilis* (WC Winkler, personal communication). This suggests that YmaH may act as a chaperone with other sRNAs or that there might be additional chaperones with overlapping functions.

Interestingly, our findings suggest that two members of the Fur regulon, *ydbN* and *mrgC*, initially believed to be sRNAs themselves, might actually encode protein chaperones for FsrA. Comparison of *ydbN* and *mrgC* with the genome sequences of other *Bacilli* demonstrated nucleotide sequence conservation at the first and second codon positions, but not the third, suggesting that these transcripts are translated [50]. The translated products of *ydbN* and *mrgC* (renamed *fbpAB* and *fbpC* for Fur-regulated basic protein) are all basic in nature, suggesting a possible nucleic acid binding ability. Closer inspection of *fbpAB*, both *in silico* and via western analysis has revealed that it is a bi-cistronic operon [50]. This suggests that these proteins may work together in a single complex, but does not rule out independent action of both FbpA and FbpB (as presented in Chapter 3). Our working hypothesis is that these genes encode chaperones for FsrA, regulating a different subset of genes under varying environmental conditions (Chapters 2 and 3).

1.2.3 Iron binding metallochaperones and efflux

Much less is known regarding how iron is directed to protein complexes or extruded from the cell. There is currently only one example of a chaperone involved in the delivery of iron to the site of iron-sulfur cluster assembly [40]. Iron loaded *E. coli* IscA provides iron for the iron-sulfur cluster assembly via IscU in the presence of L-cysteine and cysteine desulfurase (IscS) *in vitro*. IscA has an iron association constant of 3.0×10^{19} M^{-1} and is resistant to oxygen damage [39]. This proved to be physiologically relevant since it was demonstrated that IscA can indeed acquire iron from the iron chelator citrate and deliver it to Fe-S centers [40].

Only one example of an iron efflux has been identified to date: the *E. coli* FieF, ferrous iron efflux transporter [55]. Expression of the efflux pump is dependent upon iron concentration, yet it is not regulated by Fur. This discovery was important because it represented the first example of iron detoxification via efflux in any microorganism [55].

1.3 Copper

1.3.1 Regulation

Two of the best described copper sensing metalloregulators are the MerR family member copper efflux regulator, CueR, and the copper sensitive operon repressor, CsoR [115].

CueR-type regulators, which regulate copper response genes in *E. coli*, have homologs in a number of *Bacillus* species [130]. Activation by CueR occurs after it binds Cu^+. This leads to a structural rearrangement of CueR, turning this bound repressor into an activator of gene expression [113]. Activated CueR causes DNA twisting of the long promoter spacer, thus aligning the -10 and -35 regulatory elements to the same face of the DNA helix, allowing for the binding of the sigma factor and RNA polymerase [113]. In *E. coli*, CueR regulates the expression of *copA*, a Cu^+-translocating P-type ATPase, and *cueO*, a multi-copper oxidase [122]. CueR has an unusually high affinity for copper binding, within the zeptomolar range, corresponding to less than one atom of free copper per cell (which supports the hypothesis that copper toxicity is not due to oxidative stress) [24]. It was initially thought that *B. subtilis* CueR controlled expression of *copZ*, a copper chaperone, and *copA*, a CPx-type efflux ATPase [51]. However, this was later refuted and regulation of these genes was assigned to a CsoR-type regulator (Chapter 4) [90, 129]. Therefore, the function of CueR in *B. subtilis* remains unknown, although recent finding may point towards a possible role as a silver or gold sensing metalloregulator [76, 134, 136].

CsoR was first described in *Mycobacterium tuberculosis* and homologs have been found in *B. subtilis* and *Listeria monocytogenes* [33, 90, 129]. Recent studies have also identified a paralog in *M. tuberculosis* which regulates a copper-protective metallothionein, MymT [46].

CsoR is a tetrameric protein with two monomers each forming a stable homodimer and adopting an antiparallel four-helix bundle structure [88]. Each CsoR homodimer binds two equivalents of Cu^+. The structure of CsoR represents a novel regulatory family, with a DNA binding motif never before ob-

served for metalloregulators [88]. When copper is in excess, DNA bound CsoR binds Cu^{+}. The binding of copper changes the structure of CsoR, leading to its disassociation from the DNA, thus relieving repression of the efflux operon [88, 129].

1.3.2 Copper uptake systems

Copper uptake is largely uncharacterized in bacteria, but some systems have been studied. In *Enterococcus hirae*, *copA* is believed to encode a Cu^{+} transporting ATPase, acquiring copper under deplete conditions [108, 109]. *Pseudomonas syringae* CopCD has also been implicated in the uptake of Cu^{2+} [7, 32]. In other systems, such as *E. coli* and *B. subtilis*, copper uptake has been described, but specific energy dependent copper uptake has yet to be directly demonstrated. One recent study has identified YcnJ as a copper uptake pump in *B. subtilis* under the control of CsoR [26]. YcnJ exhibits moderate sequence similarity to CopCD (28%), with homology to the copper binding sites of CopC and to the transmembrane domain of the inner-membrane transport protein CopD [26].

There is one example of an analogous bacterial siderophore molecule specific for the extracellular binding and uptake of copper. This molecule, called a chalkophore, was identified in the methane-oxidizing bacterium *Methylosinus trichospoium*, and was named methanobactin [94]. It is a fluorescent 1.2-kDa peptide secreted into the environment which coordinates copper via a dual nitrogen- and sulfur-donating system [81]. Methanobactin is of major importance to *M. trichospoium* due to the unusually high copper demand in the biosynthesis of methane monooxygenase.

1.3.3 Cellular toxicity

Copper toxicity was initially believed to be due to the same mechanism as described for iron since it too is able to catalyze the Fenton reaction [94]. A sulfhydryl depletion mechanism resulting in lipid, protein, and nucleic acid damage *in vitro* had also been proposed as an alternative to the Fenton reaction [130]. However, more recent findings suggest an alternate *in vivo* copper toxicity mechanism; measurements of free copper levels within the cell demonstrated extremely low to non-existent amounts, making the Fenton or the sulfhydryl depletion mechanisms highly unlikely [24]. Also, copper-loaded *E. coli* has been demonstrated to be less sensitive to hydrogen peroxide killing than *E. coli* grown without copper [92]. Surprisingly, high copper levels actually protect the cell against iron-mediated oxidative killing via hydrogen peroxide [92]. Taken together, this suggests a toxicity mechanism independent of oxidative stress. The most recent mechanism proposed for copper toxicity is an enzymatic active site substitution [27]. Copper has been shown *in vitro* and *in vivo* to specifically displace iron in the iron-sulfur centers of isopropylmalate dehydratase of *E. coli*, effectively blocking the synthesis of branch chain amino acids [91]. The destabilization of iron-sulfur cluster formation by copper has also been demonstrated in *B. subtilis*, disrupting the generation of all iron-sulfur producing and containing proteins [27].

1.4 Control of copper levels in the cytosol

1.4.1 Copper binding metallochaperones

When dealing with internalized copper, due to its highly redox-active nature, cells ensure that it remains bound to metallochaperones when not incorporated into enzymes. This limits the exposure of copper to oxygen species as well as to other transition metal binding centers, thus limiting oxidative damage to the cell as well as deleterious metal ion substitution [60].

The ubiquitous copper chaperone has a critical biological function; it transports copper in the cytosol to the utilization sites of copper dependent proteins. Homologs of the bacterial chaperone, CopZ, have been well characterized in yeast (Atx1p), plants (CCH), nematodes (CUC-1), and humans (HAH1) demonstrating the importance of this mode of copper delivery and cellular protection [67, 82, 86, 146, 153]. Additional copper chaperones including the *B. subtilis* Sco, which plays a role in the insertion of copper into heme-copper oxidases [12], and *Thermus thermophilus* PCu_AC, which selectively inserts copper into ba_3 oxidase [2], have also been well characterized.

The current model for chaperone delivery proposes that the copper bound chaperone is subject to attack/exchange by the recipient protein ligands [60]. In other words, the exchange is a competitive process between the two binding sites of the chaperone and the recipient protein. In the case of the CopZA complex, the high affinity chaperone CopZ specifically interacts with the CPx-ATPase CopA in a transient manner. The higher affinity cysteinyl sulfurs of the CxxC motif within CopA attack the copper bound to CopZ, resulting in the

transfer of copper to CopA and regeneration of the apo-form of the chaperone, which is able to once again bind and deliver copper ions [60].

1.4.2 Copper efflux

The best understood copper efflux pumps are CopB of *E. hirae* and CopA of *B. subtilis* [130]. These two systems belong to the P- and the CPx-type ATPases respectively, responsible for pumping both transition- and heavy-metal ions across the cytosolic membrane [89, 131]. The P-type ATPases are so named due to the phosphorylation of a conserved DKTGT motif. The CPx- type is a subgroup of the P-type and possess a highly conserved CPx (where x is either C or H) motif in its sixth transmembrane domain [131]. The ATPase pumps in these families can transport a wide range of metal ions including heavy metals; the monovalent Cu^{+} and Ag^{+} and the divalent Co^{2+}, Cd^{2+}, Zn^{2+}, Hg^{2+}, and Pb^{2+}. CopB confers copper resistance by expelling excess copper it receives via specific interaction with the cytosolic CopZ chaperone. The repression of *copB*, mediated by the CopY repressor (member of the BlaI transcriptional regulatory family), is lifted when the levels of copper bound CopZ become high [130].

The concentration of periplasmic copper in *E. coli* is mediated by the *cus* system. This copper efflux system consist of CusA, an inner membrane pump; CusB, the periplasmic protein; CusC, a trimeric outer membrane protein; and CusF, a periplasmic copper chaperone [122]. The structure of the *cus* system is similar to TolC, suggesting a model where CusA, B, and C interact to form a periplasmic spanning channel. CusF interacts with this complex in the periplasm, donating its bound copper ion into the channel for extrusion into the

external environment [83].

1.5 Concluding remarks

The essential, yet toxic nature of iron and copper makes it is vitally important for the cell to closely regulate their concentrations within the cytosol. A number of systems have evolved to do just this and include uptake, chaperoning, storage, and sparing systems, the expression of which is orchestrated by specific metalloregulators.

Regulation of iron homeostasis is mainly achived through the repression of uptake and the allocation of iron within the cell either into iron storage systems, which can then be made available during iron limiting conditions, or the distribution of newly acquired iron to essential functions through the iron sparing response. Copper homeostasis, on the other hand, centers on efflux systems and sequestration of cellular copper via binding to copper-specific chaperones, which also act to direct this metal to proteins requiring it for activity.

While this introductory chapter is by no means an exhaustive characterization of all methods used to regulate metal ion levels within the cell, hopefully it grants some insight into the complexity and importance of iron and copper homeostasis. Chapter two will introduce, in more detail, the *B. subtilis* iron-sparing response. It will define those genes that are post-transcriptionally controlled by the sRNA FsrA as identified using transcriptomic and other global regulatory analyses. It will also demonstrate the important role the iron-sparing response plays in the regulation of central metabolism and, specifically, the TCA cycle. Lastly, it will take a closer look at the iron-sparing regulation of a specific

gene, *dctP*, and define the role it plays in metabolism.

Chapter three will describe the regulation of the lactate utilization operon, *lutABC*, by both FsrA and the chaperone-like FbpB. This study demonstrates an independent role for the small basic peptide FbpB, which supports the hypothesis that the Fbp proteins help to specifically target FsrA to different subsets of its regulon.

Chapter four will describe genetic and biochemical approaches used to identify CsoR as the copper response repressor of the *copZA* efflux operon in *B. subtilis*. This is important since it not only characterizes a member of a newly discovered family of metalloregulators, but also corrects a previously published report claiming CueR (YhdQ) as the regulator of copper homeostasis in *B. subtilis*.

The work presented in these chapters advances our understanding of how *B. subtilis* negotiates the complex balance between its requirement for these metal co-factors and the inherent dangers posed by uncontrolled levels of iron and copper within the cell.

CHAPTER 2

A GLOBAL INVESTIGATION OF THE *BACILLUS SUBTILIS* IRON-SPARING RESPONSE IDENTIFIES MAJOR CHANGES IN METABOLISM[1]

2.1 Summary

The *Bacillus subtilis* ferric uptake regulator (Fur) protein is the major sensor of cellular iron status. When iron is limiting for growth, derepression of the Fur regulon increases the cellular capacity for iron uptake and mobilizes an iron-sparing response mediated, in large part, by a small non-coding RNA named FsrA. FsrA functions together with three small, basic proteins (FbpABC) to repress many "low-priority" iron-containing enzymes. We have used transcriptome analyses to define the scope of the iron-sparing response and to define subsets of genes also dependent on FbpA, FbpB, or FbpC for their repression. Enzymes of the tricarboxylic acid cycle, including aconitase and succinate dehydrogenase, are major targets of FsrA-mediated repression and, as a consequence, flux through this pathway is significantly decreased under conditions mimicking iron limitation.

[1]Gregory T. Smaldone, Olga Revelles, Uwe Sauer, Haike Antelmann, and John D. Helmann. Journal of Bacteriology. (Under revision). G.T.S. carried out the strain construction, microarray assays, growth assays, and western blots. O.R. carried out the absolute metabolic flux assays and physiological parameter assays. H.A. carried out the northern blots. G.T.S., U.S., and J.D.H. analyzed the results. G.T.S. and J.D.H. wrote the manuscript.

2.2 Introduction

The tricarboxylic acid (TCA) cycle is a central pathway of *Bacillus subtilis* metabolism. The flux of carbon through the TCA cycle generates ATP through substrate level phosphorylation and by the generation of reducing equivalents that feed the electron transport chain. TCA cycle intermediates also serve as biosynthetic precursors for numerous amino acids, heme, and other key metabolites [18, 30, 57, 72, 149]. Citric acid, if released from cells, can also play a role in metal ion homeostasis by facilitating the uptake of cations including Fe^{3+}, Mg^{2+}, and Mn^{2+} [84, 110]. Since the TCA cycle is central to many biosynthetic and metabolic processes, several regulators exact tight control over the expression of TCA cycle enzymes including both global (CcpA, CodY, and TnrA) and pathway specific (CcpC, RocR, and GltC) regulators [132]. To this list, we can now add the ferric uptake regulator (Fur).

Fur has dual roles in iron homeostasis. Under iron-limiting growth conditions, derepression of numerous Fur-regulated operons [10] allows synthesis of iron uptake pathways [20, 102, 110]. Many other genes were downregulated in the *fur* mutant [10], including several with roles in central metabolism. Many of the genes downregulated in the *fur* mutant result from the actions of a Fur-regulated sRNA A (FsrA) and three small, Fur-regulated basic proteins (FbpABC)[50]. These effectors repress the translation of target genes and thereby contribute to an iron-sparing response [50]. This response enables the cell to prioritize iron usage by reducing the synthesis of low priority, iron-containing proteins as first proposed for *Escherichia coli* where it is mediated by RyhB and Hfq [96]. The *B. subtilis* iron-sparing response was defined by proteomics and was observed to include at least two enzymes involved in the TCA

cycle, aconitase, and succinate dehydrogenase [50].

Metabolomics studies have also implicated a role for Fur in regulation of the TCA cycle. Fischer and Sauer observed that a null mutation of *fur* produced one of the greatest growth defects among the 137 strains tested and this was correlated with a significantly (23%) reduced flux through the TCA cycle and a 3-fold reduction in citrate synthase activity [47]. These dramatic effects contrasted with the minimal changes noted in the vast majority of strains, consistent with the notion that *B. subtilis* has a very robust metabolism: there are sufficient opportunities for metabolic rerouting that most mutations tested did not lead to measurable growth effects. Although these previous results indicated that the *fur* mutation had significant effects on TCA cycle activity, it was not determined whether this decreased flux was causal for the reduced growth rate, or whether the effects of Fur on TCA cycle activity were direct or indirect.

Here, we extend our characterization of the FsrA-mediated iron-sparing response using transcriptomic, fluxomic, and molecular genetic analyses. Our results suggest that iron limitation leads to a physiologically significant repression of the TCA cycle. The Fur-regulated FsrA sRNA is complementary to the leader regions of the *sdh* operon and *citB* genes. Mutations that eliminate iron-sparing response effectors restore efficient growth and increase TCA cycle flux in a *fur* mutant background. Comparison of transcriptome changes and metabolic fluxes in cells lacking FsrA or various Fbp proteins supports a model in which iron-sparing involves complex, combinatorial effects of FsrA and the three small chaperone-like proteins, FbpA, B, and C.

2.3 Materials and Methods

2.3.1 Bacterial strains, media, and growth conditions

Bacterial strains used in this study are listed in Table 2.1. *Escherichia coli* DH5α was used for routine DNA cloning [124]. *B. subtilis* CU1065 strains were constructed by using long-flanking homology PCR [21]. Erythromycin (1 μg/mL) and lincomycin (25 μg/mL) [for MLS (macrolide-lincosamide-streptomycin B) resistance], spectinomycin (100 μg/mL), kanamycin (10 μg/mL), and chloramphenicol (5 μg/mL) were used for the selection of various *B. subtilis* strains unless otherwise indicated. Liquid media were inoculated from an overnight preculture and incubated at 37°C with shaking at 225 rpm. Growth media used in this study include LB medium, modified competence medium (MC), minimal growth medium (MOPS-based with glucose carbon source; MM), fumarate minimal growth medium (MOPS-based with 2% fumarate carbon source; fumarate MM), succinate minimal growth medium (MOPS-based with 2% succinate as carbon source; succinate MM), Belitsky minimal medium, and M9 minimal growth medium [19, 25, 61, 80, 137]. For ^{13}C-labelling experiments, cultures were grown in 250-mL baffled shake flasks containing 20 mL citrate-amended M9, supplemented either with 100% (wt/wt) [1-^{13}C]glucose (99%: Cambridge Isotope Laboratories) or with a mixture of 20% (wt/wt) [U-^{13}C]glucose (99%: Cambridge Isotope Laboratories) and 80% (wt/wt) natural abundance glucose. Citrate (3.4 mM) is required in these studies to increase iron availability and thereby decrease the expression of the Fur regulon in wild-type cells (data not shown).

Table 2.1: Bacterial strains and plasmids used in A GLOBAL INVESTIGATION OF THE *BACILLUS SUBTILIS* IRON-SPARING RESPONSE IDENTIFIES MAJOR CHANGES IN METABOLISM

Strain or plasmid	Relevant Characteristic(s)	Source or reference
***B. subtilis* strains**		
CU1065	W168 *att* SPβ *trpC2* (”Wild Type”)	[142]
HB2501	CU1065 *fur::kan*	[10]
HB5733	CU1065 *fur::kan fsrA::cat*	[50]
HB5735	CU1065 *fur::kan fbpAB::tet*	[50]
HB5737	CU1065 *fur::kan fbpC::MLS*	[50]
HB5750	CU1065 *fur::kan fsrA::cat fbpC::MLS*	[50]
HB5751	CU1065 *fur::kan fsrA::cat fbpAB::tet*	[50]
HB5752	CU1065 *fur::kan fsrA::cat fbpAB::tet fbpC::MLS*	[50]
HB8264	CU1065 *fur::kan fbpAB::tet fbpC::MLS*	[50]
HB12551	CU1065 *amyE::dctP*-FLAG(pPL82)	This study
HB12558	CU1065 *fur::kan amyE::dctP*-FLAG(pPL82)	This study
HB12562	CU1065 *dctP::*pMUTIN-FLAG	This study
HB12563	CU1065 *fur::kan dctP::*pMUTIN-FLAG	This study
HB12564	CU1065 *fur::kan fsrA::cat dctP::*pMUTIN-FLAG	This study
HB12573	CU1065 *fur::kan fsrA::cat amyE::fsrA*	This study
***E. coli* strains**		
DH5α	ϕ Δ(*lacZ*)M15 Δ(*argF-lac*)U169 *endA1 recA1 hsdR17* (r_K^- m_K^+) *deoR thi-1 supE44 gyrA96 relA1*	[124]
Plasmids		
pDG1730	Integration vector into *amyE* locus	BGSC
pMUTIN-FLAG	Integration vector at locus generating a C-terminal FLAG tagged ORF	BGSC
pPL82	IPTG inducible (P_{spac}(hy)) integration vector into *amyE* locus	[119]

2.3.2 DNA manipulations

Routine molecular biology procedures were performed as previously described [124]. Isolation of *B. subtilis* chromosomal DNA and transformation were carried out as previously described [36]. Restriction enzymes, DNA ligase, and DNA polymerases were all used according to manufacturer's instructions (New England Biolabs). Site directed mutagenesis was done by PCR and overlap extension according to [69].

For FsrA complementation, *fsrA* was PCR amplified to include its native promoter and terminator stem loop and inserted between the *Eco*RI and *Bam*HI sites of pDG1730 [56]. The construct was then integrated ectopically at the *amyE* locus.

The inducible *dctP*-FLAG construct was generated by PCR amplification of the *dctP* gene including the RBS directly upstream of the start codon in the forward primer and by addition of the FLAG epitope tag sequence on the reverse primer so as to generate a C-terminal translationally fused FLAG epitope. This amplified product was cloned between the *Xba*I and *Cla*I sites of the pPL82 expression vector and integrated into the *amyE* locus [119]. The pMUTIN-FLAG *dctP* construct was generated by PCR amplification of the *dctP* open reading frame excluding the start and stop codons and remaining in frame at the 3′ end. Addition of *Kpn*I and *Cla*I sites, to the forward and reverse primers respectively, allowed for the integration of the amplified product into the multicloing site of the pMUTIN-FLAG vector. This generated a C-terminal FLAG epitope tagged *dctP* gene when integrated into the *B. subtilis* genome at its native locus. The sequences for all mutant constructs were verified by DNA sequencing (Cornell Life Sciences Core Laboratories Center).

2.3.3 RNA isolation and microarray analysis

Strains CU1065 (WT), HB2501 (*fur*), HB5733 (*fur fsrA*), HB5735 (*fur fbpAB*), HB5737 (*fur fbpC*), and HB8264 (*fur fbpABC*) were inoculated into LB and grown at 37°C with vigorous shaking until an $OD_{600} \approx 0.4$ (Spectronic 21), and RNA isolation was performed using the RNeasy mini kit (Qiagen). RNA was DNase treated with Turbo DNA-free (Ambion) and precipitated overnight. The RNA was dissolved in RNase-free water and quantified using a NanoDrop spectrophotometer (Nanodrop Tech. Inc., Wilmington, DE). RNA was isolated from three biological replicates.

cDNA synthesis was performed using the SuperScript Plus indirect cDNA labeling system (Invitrogen) as per the manufacturer's instructions with 20 μg of total RNA and then purified using the Qiagen MiniElute kit (Qiagen, Maryland) and quantified with NanoDrop. Total cDNA was labeled overnight with Alexa Fluor 555 or Alexa Fluor 647 (Invitrogen), purified using the Qiagen MiniElute kit, and quantified with NanoDrop. Equal amounts (100 to 150 pmol) of labeled cDNA (*fur*/WT, *fur*/*fur fsrA*, *fur*/*fur fbpAB*, *fur*/*fur fbpC*, and *fur*/*fur fbpABC*) were combined to a final volume of 15 μL, and 1 μL salmon sperm DNA (10 mg/mL; Invitrogen) plus 16 μL 2× hybridization buffer (50% formamide, 10× SSC (1× SSC is 0.15 M NaCl, 0.015 M sodium citrate), 0.1% sodium dodecyl sulfate (SDS)) were added. The cDNA mix was denatured at 95°C and hybridized for 16 to 18 h at 42°C to DNA microarray slides which had been prehybridized for at least 30 min at 42°C in 1% bovine serum albumin, 5× SSC, 0.1% SDS, washed in water, and dried. Following hybridization the slides were washed sequentially in 2× SSC plus 0.1% SDS for 5 min at 42°C, 2× SSC plus 0.1% SDS for 5 min at room temperature, 2× SSC for 5 min at room tempera-

ture, and 0.2× SSC for 5 min at room temperature and finally dipped in water and spun until dry. Arrays were scanned using a GenePix 4000B array scanner (Axon Instruments, Inc.). Our arrays are based on a *B. subtilis* oligonucleotide library manufactured by Sigma-Genosys consisting of 4,128 oligonucleotides (65-mers) representing 4,106 *B. subtilis* genes, 10 control oligonucleotides (from *E. coli* and Brome mosaic virus), and 12 random oligonucleotides. A single oligonucleotide was designed to represent each of the *B. subtilis* genes as annotated in the genome data, release R16.1 (26 April 2001), at the SubtiList website (http://genolist.pasteur.fr/SubtiList/) [107]. The arrays were printed onto poly-L-lysine-coated Corning CMT-Gap slides at the W.M. Keck Foundation Biotechnology Resource Laboratory, Yale University. Each array contains 8,447 features corresponding to duplicates of each open reading frame-specific oligonucleotide, additional oligonucleotides of control genes, and 50% dimethyl sulfoxide blank controls.

Raw data files were produced from the scanned images using the GenePix Pro 4.0 software package (GPR files), and the red/green fluorescence intensity values were normalized such that the ratio of medians of all features was equal to 1. The normalized data were exported to Excel for analysis. The data sets were filtered to remove those genes that were not expressed at levels significantly above background under either condition (sum of mean fluorescence intensity, <100). For analysis, we filtered to identify those genes that were altered at least 2.0-fold in signal intensity in the average of the three biological replicates.

All original raw data files were deposited into the GEO accession viewer database as series GSE27416.

2.3.4 Hierarchical clustering analysis

Hierarchical clustering was performed using Cluster 3.0 [37] from transcriptome datasets derived from this work. After hierarchical clustering, the output was visualized using TreeView [43]. Studies were carried out using those genes that were at least 1.25-fold repressed in the *fur* mutant (relative to WT) and also at least 2.0-fold induced in any one of the four strains altered in components of the iron-sparing response. Genes considered in the analysis must have an unfiltered fold-change calculation for three of the four microarray experiments. Genes where expression levels are strongly affected by growth rate (encoding ribosomal proteins, rRNA, and purine and pyrimidine synthesis enzymes) were excluded from the analysis.

2.3.5 Bioinfomatic analysis of FsrA pairing with putative targets

Predicted targets of the iron-sparing response from [50] or from the transcriptome analysis described in this study were selected for pairing analysis. Secondary structure models were predicted by joining a region encompassing the translation initiation region (TIR; from ≈ -60 to +10 nts from the start of translation) of each mRNA to the FsrA sequence via a short linker (ten CA repeats). Secondary structures predicted using mFold [162] were examined for extended pairing between the TIR and FsrA. If pairing was observed, the interaction was extended and refined using RNAhybrid [121].

2.3.6 Northern blot experiments

B. subtilis wild type CU1065, *fur*, *fur fsrA* and *fur fbpABC* cells were grown in Belitsky minimal medium [137] and samples were harvested for RNA isolation at an OD_{500} of 0.4, 1.0, and 2.0 corresponding to the exponential growth, transition phase and stationary phase respectively. RNA isolation and Northern blot analyses were performed as described previously [151]. Hybridizations specific for *sdhA*, *citB*, and *lutB* were performed with the digoxigenin-labeled RNA probes synthesized *in vitro* using T7 RNA polymerase from T7 promoter containing internal PCR products of the respective genes using the following primer pairs: CATCAAACCCATACGTGCTG - *citB*-for; CTAATACGACTCACTATAGGGAGATACGTCGTAAATCCGCCTTC - *citB*-T7-rev; CGGGAATCATCTTTGGAAAA - *sdhA*-for; CTAATACGACTCACTATAGGGAGAAGCGCTCCATTAACTCCTGA - *sdhA*-T7-rev; GAAGGAAGGCTGTGAAGTCG - *lutB*-for; CTAATACGACTCACTATAGGGAGACCAAGTCCGAATGCTTTCAT - *lutB*-T7-rev.

2.3.7 Analytical techniques and sample preparation

Maximum specific growth rate, biomass yield on glucose, specific glucose consumption and by-product formation rates were determined by regression analysis during the exponential growth phase in batch cultures. Glucose and acetate concentration were determined from culture supernatants along the growth curve on an HPLC HP1100 system (Agilent Technologies, Santa Clara, USA). Detection was performed using refractive index for glucose and a UV detector at 240 nm for acetate. Cellular dry weights were calculated from the OD_{600}

values multiplied by a conversion factor that was previously determined [160].

2.3.8 Metabolic flux analysis

^{13}C-based flux analysis takes advantage of the fact that alternative pathways scramble and cleave the substrates' carbon backbone differently before they converge on the same intermediate. To carry out this analysis, mass spectrometry is employed to trace patterns of stable isotopes in protein-bound amino acids from growing micro-organisms for extended periods on ^{13}C-labled substrates [160]. To assess ^{13}C patterns in proteinogenic amino acids, cell pellets from 5 mL of culture aliquots were harvested during growth at an OD_{600} of 1, hydrolyzed in 6M HCl, and derivatized with N-(ter-butyldimethylsilyl)-methyltrifluoroacetamide as described elsewhere [160]. Derivatized amino acids were analyzed for ^{13}C-labeling patterns with a series 8000 gas-chromatograph (GC) combined with an MD800 mass spectrometer (MS) (Fisons Instruments). The GC-MS-derived mass isotope distributions of proteinogenic amino acids were then corrected for naturally occurring isotopes. Flux ratio analysis and subsequent ^{13}C-constrained net flux analysis were conducted by using the software package FiatFlux [160, 161]. Ratios of converging fluxes were directly calculated from ^{13}C patterns and then used together with measured physiological rates as constraints to estimate the flux distribution from the stoichiometric matrix. Fluxes into biomass were calculated from the known metabolite requirements for macromolecular compounds and the growth rate-dependent RNA and protein contents [44]. Using the FiatFlux software, the sum of the weighted square residuals of the constraints from both metabolite balances and flux ratios were minimized using the MATLAB function, and the residuals were weighed by di-

viding through the experimental error [160]. The computation was repeated at least five times with randomly chosen initial flux distributions to ensure identification of the global minimum. Two independent experiments have been analyzed.

2.3.9 Growth curve generation and comparison

Fresh single colonies were picked from selective LB plates and cultivated statically at 30°C overnight in 5 mL MM. They were then shifted to 37°C shaking and grown to mid-exponential phase ($OD_{600} \approx 0.4$; Spectronic 21). Cells were recovered from 1 mL of each culture, washed in 0.75 mL 0.88% NaCl then resuspended and diluted to a standard OD_{600} of 0.1 (Perkin Elmer) in 0.88% NaCl. 30 μL of cells were inoculated into 170 μL of either fumarate MM or succinate MM in a 100-well microtitre plate and growth was monitored with shaking at 37°C using a BioScreen C plate reader.

2.3.10 Western blot analysis

Strains for western blot analysis were grown overnight in 1 mL LB broth + MLS (when appropriate) at 37°C shaking. 0.5 mL overnight culture was inoculated into 50 mL LB broth, grown to an $OD_{600} \approx 0.4$ (Spectronic 21), and spun down at 5000 rpm for 5 min in an Eppendorf 5804R swinging bucket rotor centrifuge. The pellet was resuspended in 1 mL of MM supplemented with 0.2 mM KPO_4 (pH 7.0), 40 mM $MnCl_2$ and 1 mM $FeSO_4$ (MMa) and centrifuged for 2 min at 5,900× g. The pellet was then resuspended in 1 mL of MMb (1× *Bacillus* salts

[19], 40 mM MOPS (pH 7.4), 2% (wt/vol) glucose) and centrifuged for 2 min at 5,900× g. The pellet was then resuspended in 1 mL of MMa with the addition of 20% sucrose and 1 mg/mL lysozyme and incubated shaking at 37°C for 40 min. Formation of protoplasts was verified by microscopy and the protoplasts were centrifuged for 4 min at 4,600× g at 4°C. The protoplasts were resuspended in 200 μL TBS (50 mM Tris-HCl (pH 7.4), 150 mM NaCl, 1 mM EDTA, 1 mM DTT, and 0.1 mM PMSF), briefly sonicated, and then ultracentrifuged at 45,000 rpm for 30 min (TLA 100.3 fixed-angle rotor for a Beckman TL-100 ultracentrifuge) to separate the membrane and cytoplasmic fractions. The membrane fraction was resuspended in 200 μL TBS. A Bradford assay was carried out on the membrane fraction to determine total recovered protein and 10 μg of total protein was used for SDS-PAGE. Protein levels were detected after membrane transfer and western blot analysis using commercially obtained anti-FLAG primary antibodies (Sigma).

2.4 Results and Discussion

2.4.1 Scope of the FsrA-dependent iron-sparing response as monitored at the transcriptome level

Under conditions of iron sufficiency, the *fsrA*, *fbpAB*, and *fbpC* operons are repressed and their products inactive. We therefore used a *fur* mutant strain, in which these genes are constitutively derepressed [10, 50], as the starting point for our analysis. This strain expresses an iron-sparing response in which multiple iron-dependent proteins are repressed. In most cases tested previously,

this translational repression was accompanied by a decrease in steady state mRNA levels [50]. We therefore focused our attention on those genes with reduced mRNA levels in the *fur* mutant as visualized by transcriptomics (Fig. 2.1, *fur*/WT). Since the level of decrease in steady state mRNA levels is often quite small, we selected all genes with mRNA levels reduced by at least 1.25-fold in a *fur* mutant (corresponding to less than 2% of coding regions). The resulting set of genes included most of those previously identified as targets of the iron-sparing response [50].

To determine whether down-regulation is mediated by the *fsrA*, *fbpAB*, or *fbpC* operons, we compared the transcriptome of a *fur* mutant with strains additionally inactivated for one or more components of the iron-sparing response. Of the 116 genes with at least a 1.25-fold reduction in mRNA levels, 78 displayed an increase in mRNA in a background lacking one or more of the effectors of the iron-sparing response. Cluster analysis of those genes that were at least 2.0-fold up-regulated (relative to the *fur* mutant) in any one of four genetic backgrounds tested allows us to define clusters of coordinately regulated genes. These genes sets can be interpreted as representing mRNA targets directly affected by the Fur-regulated FsrA small RNA (cluster *R*) and the subsets where FsrA regulation additionally requires FbpAB and/or FbpC (clusters *RAB* and *RABC*) (Fig. 2.1). In some cases, regulation by FbpC appeared to be at least partially independent of FsrA (cluster *C*).

Consistent with our previous findings for the *sdh* operon [50], mutation of *fsrA* in a *fur* mutant background leads to significant up-regulation and the effects of FsrA on expression are largely independent of FbpABC (cluster *R*). *leuC* and *pdh* also belong to cluster *R*. SdhCBA and PdhABCD both play a role in

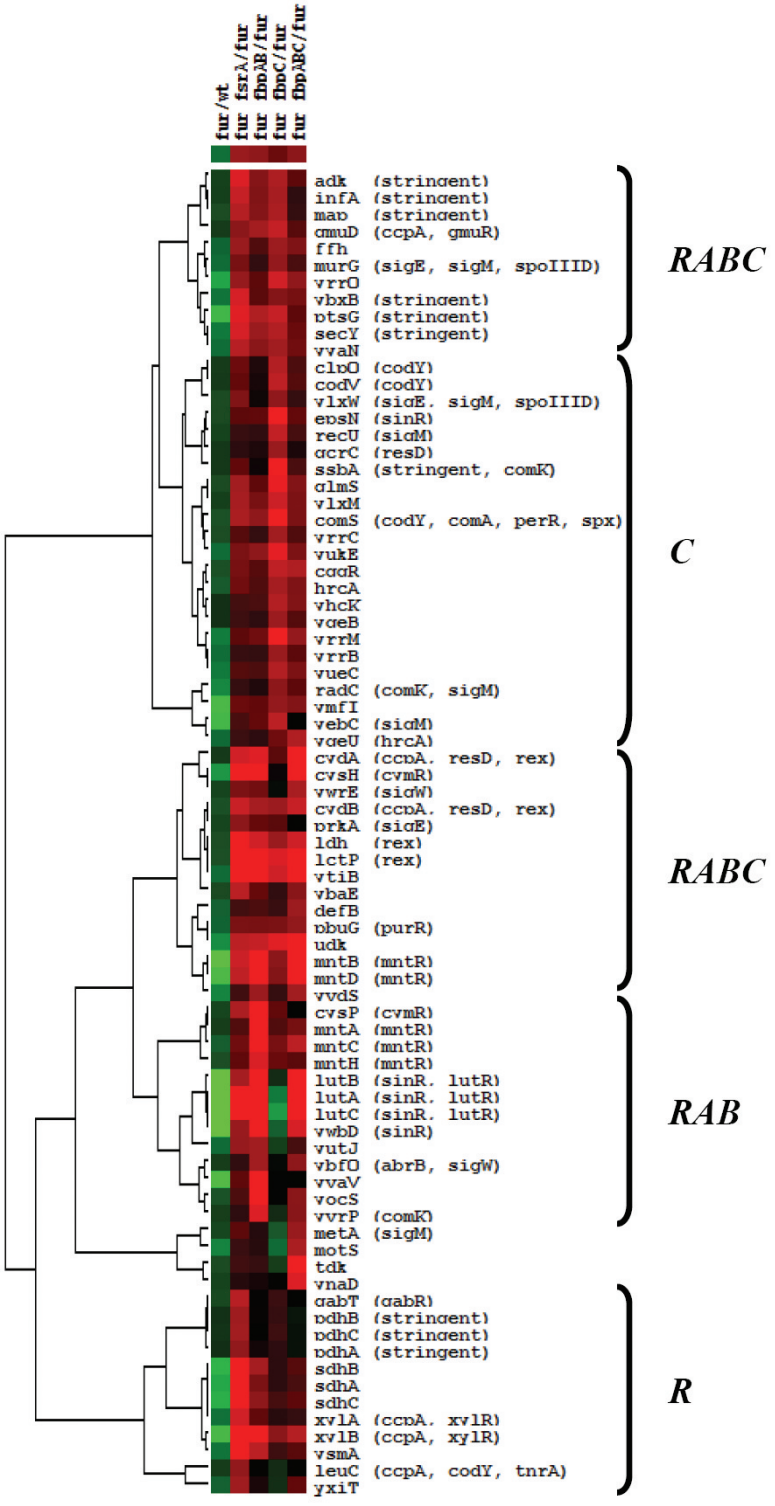
fur/wt
fur fsrA/fur
fur fbpAB/fur
fur fbpC/fur
fur fbpABC/fur
adk (stringent)
infA (stringent)
map (stringent)
gmuD (ccpA, gmuR)
ffh
murG (sigE, sigM, spoIIID)
yrrO
ybxB (stringent)
ptsG (stringent)
secY (stringent)
yvaN
clpC (codY)
codV (codY)
ylxW (sigE, sigM, spoIIID)
epsN (sinR)
recU (sigM)
gcrC (resD)
ssbA (stringent, comK)
glmS
ylxM
comS (codY, comA, perR, spx)
yrrC
yukE
cggR
hrcA
yhcK
ygeB
yrrM
yrrB
yueC
radC (comK, sigM)
ymfI
yebC (sigM)
ygeU (hrcA)
cydA (ccpA, resD, rex)
cysH (cymR)
ywrE (sigW)
cydB (ccpA, resD, rex)
prkA (sigE)
ldh (rex)
lctP (rex)
ytiB
ybaE
defB
pbuG (purR)
udk
mntB (mntR)
mntD (mntR)
yvdS
cysP (cymR)
mntA (mntR)
mntC (mntR)
mntH (mntR)
lutB (sinR, lutR)
lutA (sinR, lutR)
lutC (sinR, lutR)
ywbD (sinR)
yutJ
ybfO (abrB, sigW)
yvaV
yocS
yvrP (comK)
metA (sigM)
motS
tdk
ynaD
gabT (gabR)
pdhB (stringent)
pdhC (stringent)
pdhA (stringent)
sdhB
sdhA
sdhC
xylA (ccpA, xylR)
xylB (ccpA, xylR)
ysmA
leuC (ccpA, codY, tnrA)
yxiT
RABC
C
RABC
RAB
R

Figure 2.1

Figure 2.1: Hierarchical cluster analysis of transcriptional changes in iron-sparing response mutant strains. A hierarchical cluster analysis (generated using Treeview) representing genes at least 1.25-fold repressed in the *fur* vs. WT microarray experiment and induced at least 2.0-fold in at least one of the following conditions: *fur* vs. *fur fsrA*, *fur* vs. *fur fbpAB*, *fur* vs. *fur fbpC*, or *fur* vs. *fur fbpABC*. Clusters with similar regulatory patterns are indicated by brackets and represent genes mostly affected by FsrA (*R*), FbpC (*C*), FsrA and FbpAB (*RAB*), and FsrA and FbpABC (*RABC*). Red intensity indicates increasing expression while green intensity indicates decreased expression. Black indicates no change or no data for the gene/array indicated. Genes are listed to the right of the cluster and the corresponding regulators (where known) are indicated to the right of each gene.

carbon metabolism and their activities are expected to be correlated with the activity of the TCA cycle. We note that *leuC* is the penultimate gene of the *ilv-leu* operon and the LeuC protein was previously found to be strongly repressed in an FsrA-dependent manner by proteomics studies [50]. All genes of the *ilv-leu* operon were not represented in our transcriptome studies which could be due to the complex RNA processing that occurs for this primary transcript [93].

Most of the other genes up-regulated in the *fur fsrA* mutant (compared to *fur* alone) appeared to be also (variably) up-regulated in the *fur fbpAB* and/or *fur fbpC* mutants (clusters *RAB* and *RABC*). This may mean that the regulation of these targets is indirect or, alternatively, that FsrA action on these targets is stimulated by or requires one or more of these basic proteins as co-regulators. For example, the *lutABC* operon is in the *RAB* cluster which reflects the fact that translational repression of this mRNA requires both FsrA and the FbpB protein (Smaldone *et al.*, ms. in revision).

For most operons that appear to be under FsrA and FbpABC control (clusters *RAB* and *RABC*) neither the mechanism nor the physiological relevance of the noted regulation is yet established. As expected, many of the target operons encode known or likely metalloproteins. Examples include the metalloprotein Map (methionine aminopeptidase) and the iron-containing enzyme CydAB (a 3-heme containing cytochrome bd) [77]. It has been hypothesized that Map and its paralog, YlfG, both function as methionine aminopeptidases each requiring a different metal cofactor [158]. The regulation of *map* as part of the iron-sparing response, as well as studies demonstrating activity for Fe^{2+}-metallated Map orthologs [157, 159], suggests that the Map cofactor may be iron.

A third cluster (cluster *C*) includes genes where FbpC appears to play a dom-

inant role in regulation. This cluster includes the *eps* operon, encoding functions for extracellular polysaccharide biosynthesis, and the *qcrABC* operon responsible for the production of the Fe-S containing cytochrome c. An interesting feature of the genes in this cluster is that their dependence on FbpC is generally greater than on FsrA. This is not consistent with a simple model in which FbpC acts together (in the same pathway) with FsrA and suggests that FbpC (either as a transcript or as the peptide product) has additional regulatory activity.

To confirm the results observed in the transcriptome studies, we performed northern blot analysis of selected operons (Fig. 2.2). We included aconitase (*citB*) in this analysis since previous results suggested that it was a target for the iron-sparing response [50], although this was not apparent in the DNA microarray-based analysis (this gene signal was not reliably detected with these microarrays). In each case tested, the level of mRNA was reduced significantly in the *fur* mutant strain and this reduction was, in most cases, dependent on the FsrA sRNA since mRNA levels returned to near wild-type levels in the *fur fsrA* double mutant. Moreover, these results again highlight the combinatorial complexity as also apparent in our proteome data [50]. In some cases, the mRNA levels returned to near wild-type levels in mutants lacking one or more Fbp proteins instead of, or in addition to, the *fsrA* mutant strain.

2.4.2 Bioinfomatic analysis supports a direct role for FsrA at many targets

In most bacterial systems, small trans-acting RNAs function by annealing at or near the translation initiation region (TIR) [87]. Subsequent to hybrid forma-

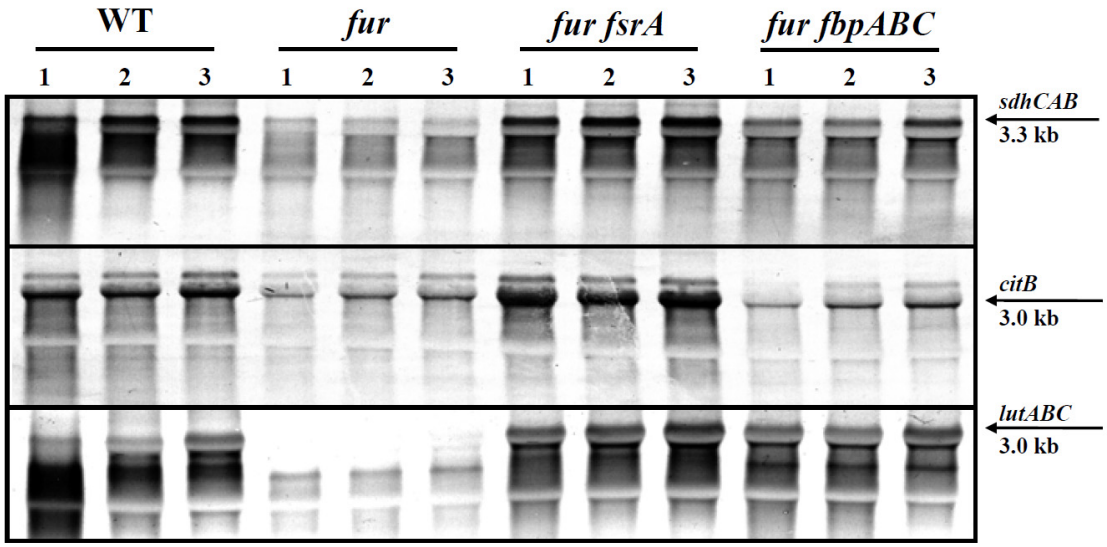

Figure 2.2: Northern analysis of selected FsrA regulon members. Equal amounts of total RNA isolated from wild type and *fur*, *fur fsrA*, and *fur fbpABC* mutant strains were hybridized with antisense RNA probes specific for *sdhA*, *citB*, and *lutB* as indicated. Cells were grown in Belitsky minimal medium and harvested at an OD_{500} of 0.4, 1.0, and 2.0 corresponding to the log phase (lane 1), transition phase (lane 2), and stationary phase (lane 3). The arrows point to the expected size of the specific transcripts.

tion, the duplex RNA can be targeted for degradation which can account for the observed reduction in steady-state mRNA levels [87]. Moreover, mRNAs that are not actively translated often have a shorter half-life than those that are being translated [22].

In an initial attempt to understand the mechanism behind the regulation by *fsrA*, we sought to determine if FsrA was complementary to the TIR of various mRNA targets. Using both mFold and RNAhybrid, pairings were predicted that could account for the translational repression of several targets (Fig. 2.3). For consistency, the free energy values for regions of pairing limited to 20 nt in length were compared unless much more extensive pairing was observed. It is interesting to note that all of the pairings presented here involve a C-rich unstructured loop region of FsrA [50] and regions overlapping the RBS of the target operon. This suggests that FsrA may nucleate interaction with its targets via this open loop structure. Similar C-rich motifs have been described in *S. aureus* sRNAs and are predicted to act in a similar manner [53].

2.4.3 FsrA decreases flux through the TCA cycle

The repression of the Sdh complex by FsrA, together with the down-regulation noted for aconitase (CitB) and pyruvate dehydrogenase (Pdh), suggests that the iron-sparing response may significantly perturb carbon metabolism and, specifically, the TCA cycle. This is consistent with prior results demonstrating that a *fur* mutant strain has reduced flux through the TCA cycle [47]. We performed ^{13}C-based flux analysis [125] to determine if the reduced TCA cycle activity is due to FsrA and/or FbpABC. For this purpose, ^{13}C-labelling experiments with

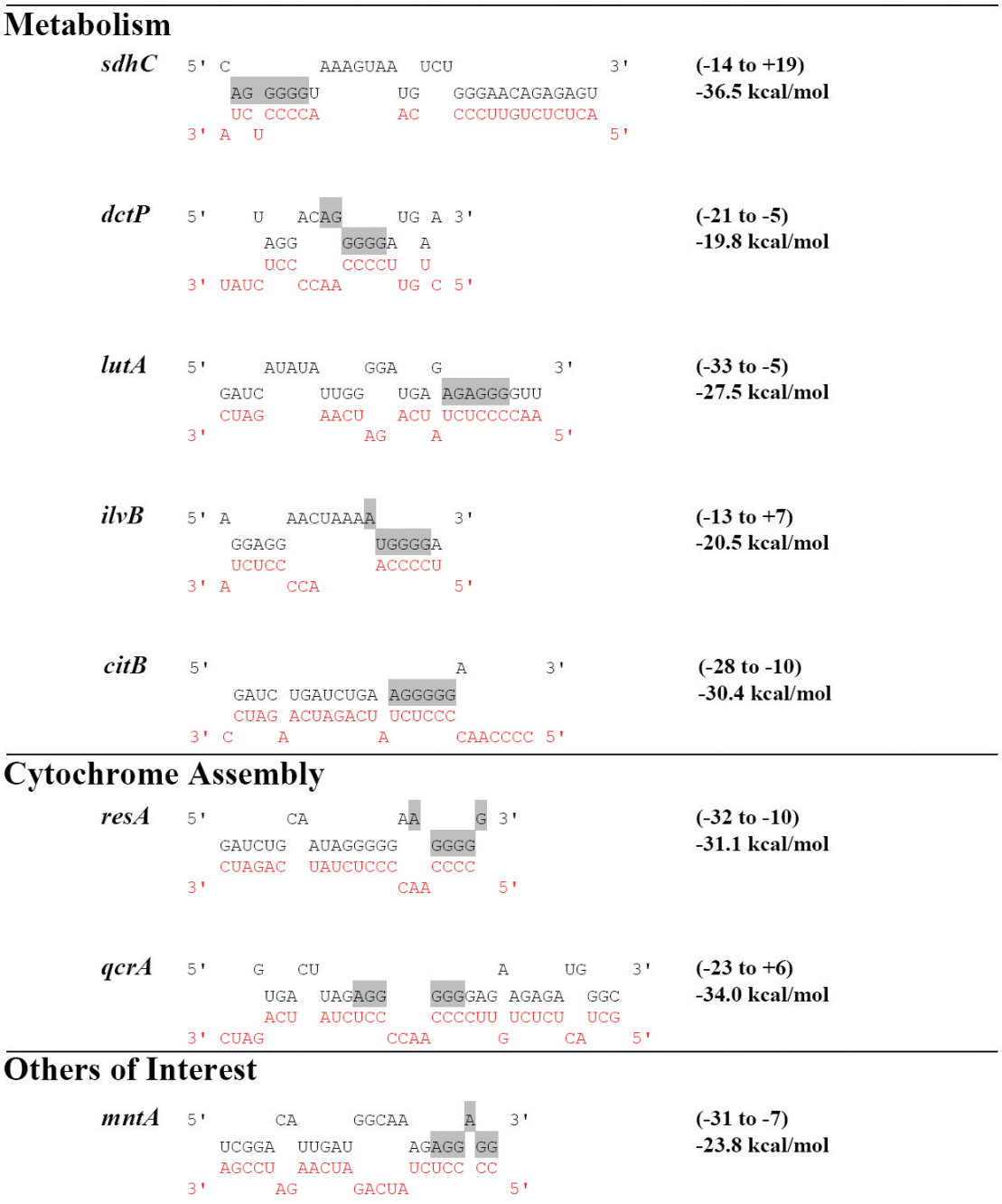

Figure 2.3: Predicted RNA pairings for selected FsrA regulon members. Pairings between the TIR of the indicated target mRNA (black, 5′ to 3′) and FsrA (red, 3′ to 5′) are illustrated and organized by common function. The region of interaction corresponding to the TIR is numbered relative to the AUG of the corresponding gene and the putative RBS is highlighted in grey. The change in free energy of the corresponding pairing is listed to the right of each model. The pairing for *sdhC* was previously reported in [50].

exponentially growing cultures were carried out in medium containing 80% natural abundance glucose and 20% [U-^{13}C]glucose and, in another series, with 100% [1-^{13}C]glucose. A complete net-flux distribution for the wild-type strain and its isogenic mutants is given in Figure 2.5 and selected fluxes are shown in Figure 2.4.

The most apparent perturbations in the flux analysis are due to the *fur* mutation (relative to WT) and are best observed in glycolysis and the TCA cycle (Fig. 2.5 and Fig. 2.4). The *fur fsrA* mutant, but not the *fur fbpAB* or *fur fbpC*, generally reverts the *fur* flux phenotype to wild-type levels, and this is most notable for the TCA cycle-related fluxes (Fig. 2.4). In contrast, fluxes through the pentose phosphate pathway remained at a relatively constant level (Fig. 2.5).

Consistent with previous data [47], and with the altered fluxes through the TCA cycle, the *fur* mutation roughly halves the growth rate on glucose as the sole carbon source (Table 2.2). Mutating *fsrA* in the *fur* mutant background partially restores the growth phenotype, but a full restoration of rapid growth in only achieved in those *fur fsrA* mutants that are additionally lacking either FbpAB, FbpC, or all three (Table 2.2). These results provide further evidence that FbpAB and FbpC have physiological functions independent of FsrA. Whereas these small proteins were proposed to act, at least in part, as chaperones to facilitate FsrA-mediated translational repression [50], these data suggest that they may also act in conjunction with other sRNAs or their transcripts may themselves function as sRNAs. Collectively, these data clearly show that FsrA directly affects metabolic fluxes and, in particular, targets the TCA cycle. The restoration of comparatively rapid growth in a *fur fsrA* double mutant supports a model in which the poor growth of the *fur* mutant results directly from the

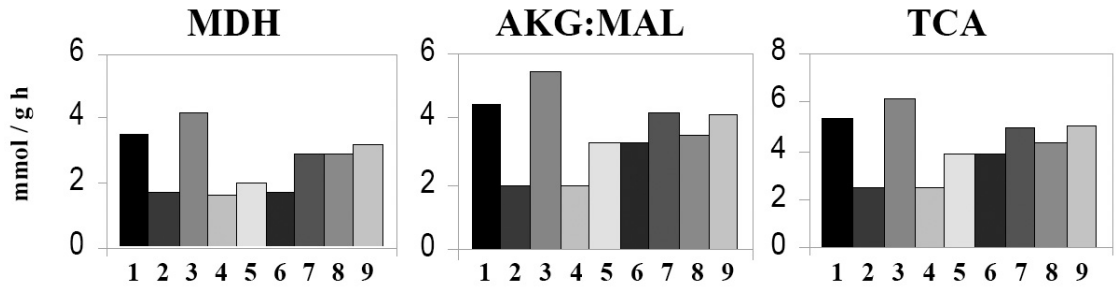

Figure 2.4: Selected absolute metabolic fluxes in *B. subtilis* mutants during exponential growth in glucose batch culture. Selected fluxes are given for the enzymes that catalyze the indicated reactions: MDH, flux measured from malate to oxaloacetate; AKG:MAL flux measured from α-ketoglutarate to malate; and TCA, flux through the TCA cycle. Strains tested for flux analysis are as follows: 1. WT, 2. *fur*, 3. *fur fsrA*, 4. *fur fbpAB*, 5. *fur fbpC*, 6. *fur fbpABC*, 7. *fur fsrA fbpC*, 8. *fur fsrA fbpAB*, and 9. *fur fsrA fbpABC*. One of two replicate experiments is shown. Generally, the 95% confidence intervals were between 10 and 15% of the values shown for the major fluxes. Larger confidence intervals were estimated for reactions with low fluxes.

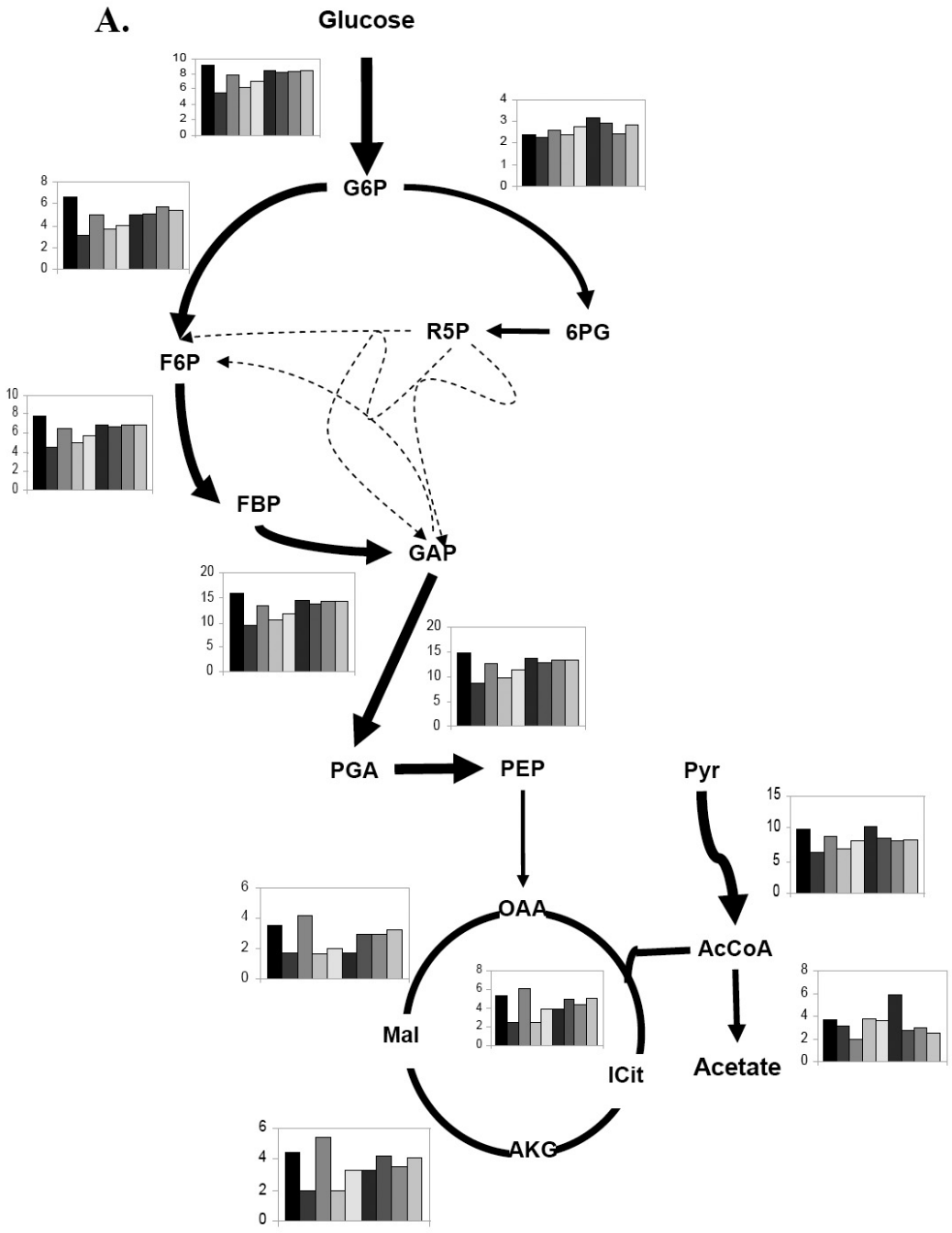
A.
Glucose
G6P
6PG
R5P
F6P
FBP
GAP
PGA
PEP
Pyr
OAA
AcCoA
Acetate
Mal
ICit
AKG

Figure 2.5

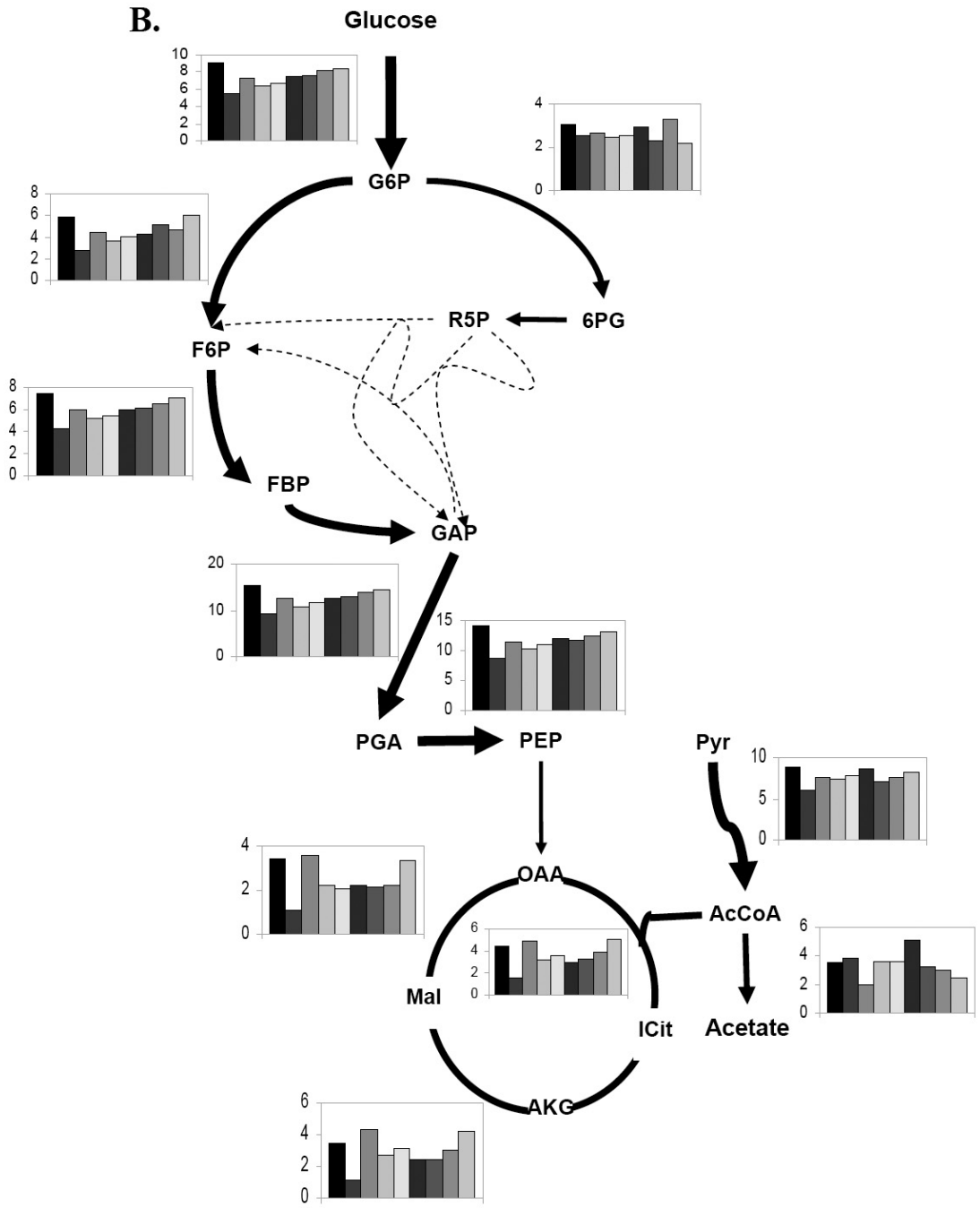
B.
Glucose
G6P
6PG
R5P
F6P
FBP
GAP
PGA
PEP
Pyr
OAA
AcCoA
Mal
ICit
Acetate
AKG

Figure 2.5

Figure 2.5: Absolute metabolic fluxes in *B. subtilis* mutants during exponential growth in glucose batch culture. *B. subtilis* strains used for flux analysis listed from left to right as follows: WT, *fur*, *fur fsrA*, *fur fbpAB*, *fur fbpC*, *fur fbpABC*, *fur fsrA fbpC*, *fur fsrA fbpAB*, and *fur fsrA fbpABC* mutants. The presented fluxes are from two independent experiments and were obtained by ^{13}C-constrained flux analysis using the software FiatFlux [161]. **A**. and **B**. represent two replicate experiments. Abbreviations used are as follows: G6P, Glucose-6-P; 6PG, Gluconate-6-P; F6P, Fructose-6-P; FβP, Fructose-1,6-bis-P; R5P, Ribulose-5-P; GAP, Glyceraldehyde-3-P; PGA, 3-P-glycerate; PEP, Phospoenolpyruvate; OAA, Oxaloacetate; Mal, Malate; iCit, iso-citrate; AKG, α-ketoglutarate; and AcCoA, Acetyl-CoA. Generally, the 95% confidence intervals were between 10 and 15% of the values shown for the major fluxes. Larger confidence intervals were estimated for reactions with low fluxes.

iron-sparing response and the consequent down-regulation of several central metabolic enzymes including Sdh and CitB.

2.4.4 Role of DctP in C_4-dicarboxylate uptake and utilization

Down-regulation of Sdh can explain our previous observation that a *fur* mutant strain grows very poorly on minimal medium with succinate as carbon source. However, we have also observed that a *fur* mutant is severely impaired in growth on fumarate [50], which is the product of the Sdh reaction. A hint to a possible mechanism is provided from earlier transcriptome studies which indicated that a C_4-dicarboxylate permease (DctP) is strongly down-regulated in a *fur* mutant [10]. We therefore hypothesized that the inability to grow on succinate or fumarate might be due to repression of DctP rather than (or in addition to) Sdh.

To monitor the effects of *fur* and the iron-sparing response on DctP levels, western blot analysis was used with strains expressing a DctP-FLAG protein. A marked reduction in the level of DctP-FLAG was observed in the membrane fractions of the *fur* mutant compared to WT (Fig. 2.6). Protein levels increased with the additional mutation of *fsrA* (Fig. 2.6), but not in strains mutant for *fbpAB* or *fbpC* (data not shown). This indicates that *dctP* (which was not reliably detected in our microarray studies) is likely a member of Cluster *R* (as is the *sdh* operon) and primarily regulated by FsrA. Consistent with this hypothesis, the inability of a *fur* mutant to grow on succinate or fumarate can be rescued in a *fur fsrA* double mutant strain, but not by a *fur fbpAB* or *fur fbpC* double mutant strain (Fig. 2.7A, 2.7B, and data not shown).

Table 2.2: Physiological parameters of *B. subtilis* growth on citrate supplemented M9 medium

Strain	**Growth rate (μ)**	**Biomass yield g(g glucose)$^{-1}$**	**Glucose uptake (mmol g^{-1} h^{-1})**	**Acetate secretion**
WT	0.64 ± 0.01	0.42 ± 0.09	9.7 ± 2.0	3.8 ± 0.7
fur	0.36 ± 0.02	0.35 ± 0.05	7.0 ± 1.3	3.0 ± 0.5
fur fsrA	0.50 ± 0.01	0.36 ± 0.02	7.8 ± 0.5	2.0 ± 0.2
fur fbpC	0.44 ± 0.00	0.32 ± 0.02	6.1 ± 0.3	3.8 ± 0.8
fur fbpAB	0.42 ± 0.04	0.40 ± 0.05	6.4 ± 1.2	2.7 ± 1.0
fur fbpABC	0.41 ± 0.01	0.36 ± 0.01	8.4 ± 2.0	4.3 ± 1.5
fur fsrA fbpC	0.61 ± 0.03	0.51 ± 0.04	7.4 ± 1.8	3.2 ± 0.8
fur fsrA fbpAB	0.65 ± 0.04	0.50 ± 0.04	7.8 ± 0.9	2.9 ± 0.1
fur fsrA fbpABC	0.64 ± 0.03	0.43 ± 0.07	8.3 ± 1.6	2.5 ± 0.6

To directly test if regulation of *dctP* was responsible for these growth effects, we generated an IPTG inducible *dctP*-FLAG construct and integrated it ectopically in WT and *fur* mutant strains. Growth of both strains was measured after 24 hours in both succinate MM and fumarate MM with and without the addition of 1.0 mM IPTG. Induction of *dctP*-FLAG led to significant restoration of growth in fumarate MM, but not in succinate MM (Fig. 2.7C). This suggests that repression of DctP is, at least in part, limiting for growth on fumarate. Conversely, induction of DctP is not sufficient to overcome the growth restriction on succinate, presumably because FsrA additionally represses *sdhCBA*.

2.5 Concluding Remarks

Transcriptome analysis of the *fur* mutant strain compared to wild type reveals derepression of those genes repressed by Fur (including many operons encoding iron uptake functions) and down-regulation of numerous other operons, consistent with prior studies [10]. The discovery of the iron-sparing response, mediated by FsrA and/or FbpABC, provides a mechanistic explanation for much of this down-regulation: mRNAs that are targeted by the FsrA sRNA for translational repression are presumably degraded more rapidly which thereby reduces the steady state mRNA level.

The genes targeted by the iron-sparing response include those encoding aconitase (*citB*), succinate dehydrogenase (*sdhCBA*), and C_4-dicarboxylate permease (*dctP*) which all may affect fluxes through the TCA cycle (Fig. 2.8). The results presented here confirm that these effects, as observed in transcriptomics and noted previously in proteomics studies [50], are indeed responsible for a

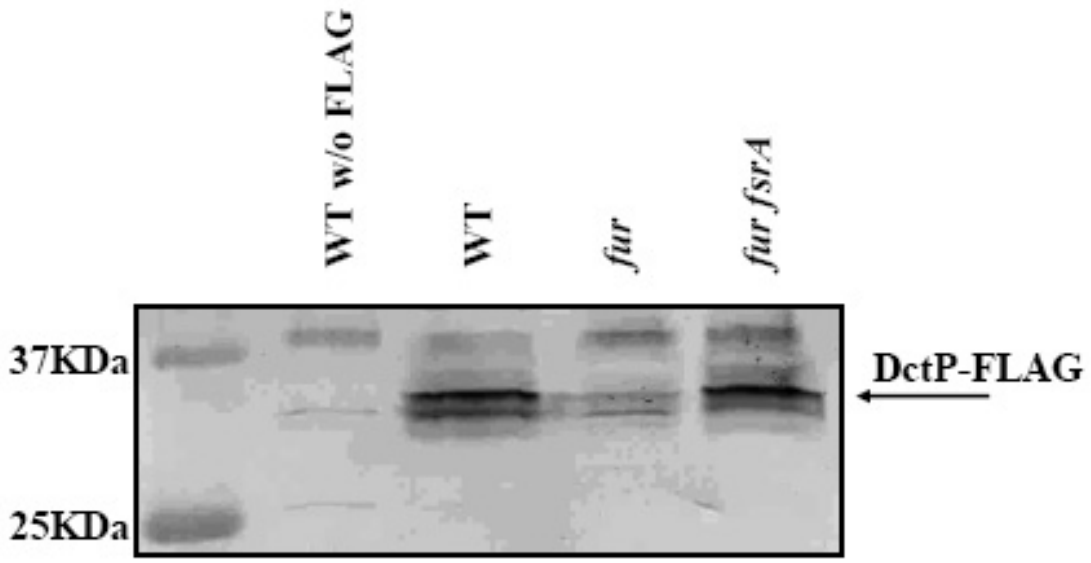

Figure 2.6: Western analysis of DctP-FLAG. Western blot analysis was used to monitor the expression of DctP-FLAG in various mutant backgrounds. 10 μg total protein from membrane fractions was loaded per lane. Each lane is labeled with the strain background and a wild type strain carrying no FLAG construct was included as a negative control. Development was carried out with anti-FLAG primary antibody and alkaline phosphatase linked secondary anti-rabbit antibody.

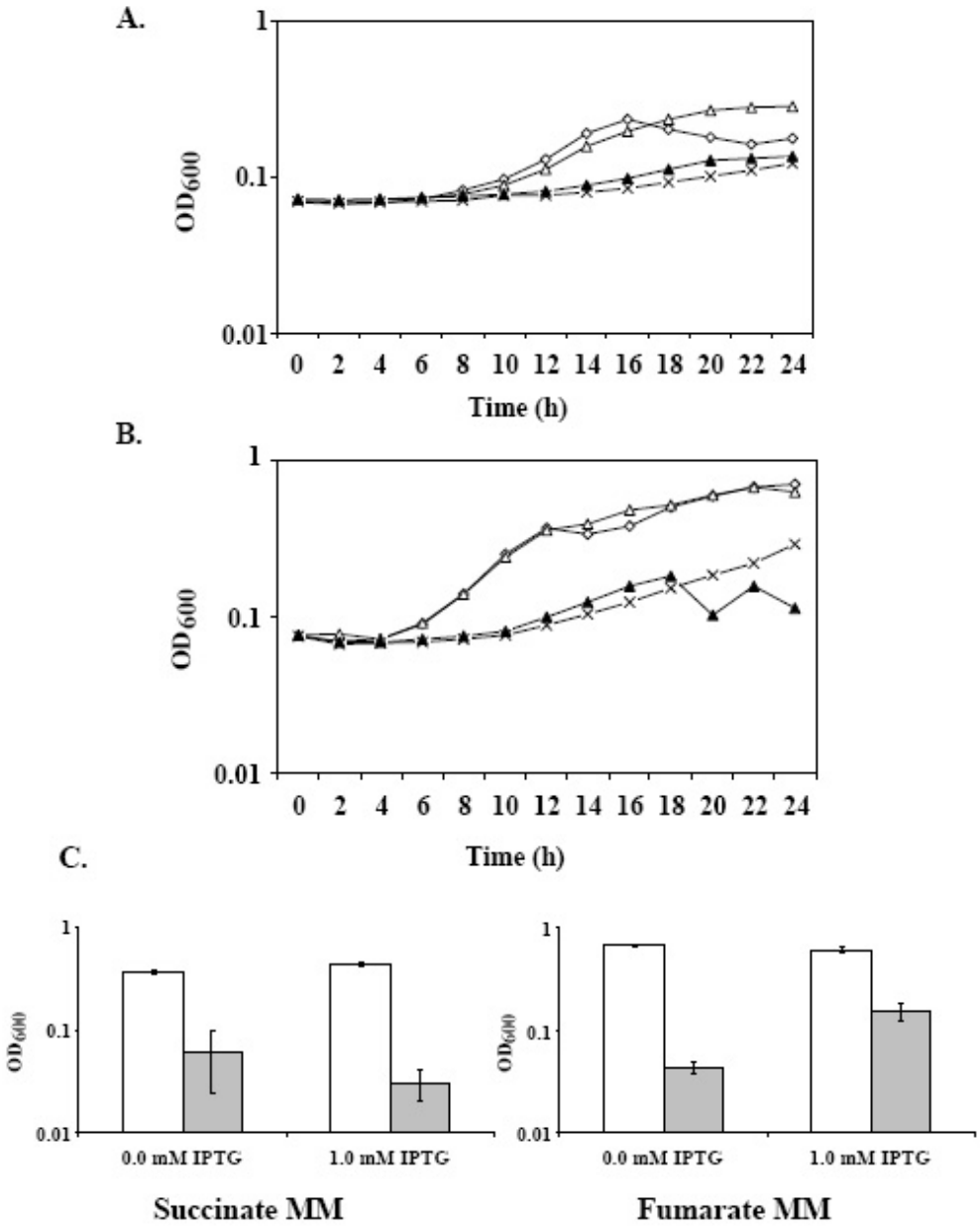

Figure 2.7: Growth phenotypes of selected mutant strains. **A**. Growth curves of mutant strains affected in the iron-sparing response in succinate MM. The strains used in this experiment are as follows: WT (open diamond); *fur* (cross); *fur fsrA* (open triangle); and *fur fsrA +fsrA* (filled triangle). **B**. Growth curves of mutant strains affected in the iron-sparing response in fumarate MM. Strain designations are as in Panel A. **C**. Comparison of growth in succinate MM and fumarate MM. Column labels indicate amount of IPTG added. Columns represent final OD_{600} after 24 hours of growth at 37°C. The strains used in this experiment are as follows: WT +P_{spac}-*dctP*-FLAG (white); and *fur* +P_{spac}-*dctP*-FLAG (grey).

substantially reduced flux through the TCA cycle. The repression of TCA cycle enzymes is physiologically significant: the *fur* mutant has a reduced growth rate and yield on glucose and is unable to grow on either succinate or fumarate as carbon source. The inability to grow on fumarate may result, at least in part, from down-regulation of the DctP dicarboxylate uptake protein. This may also reduce the ability to grow on succinate but increasing DctP expression does not allow growth on succinate suggesting that repression of Sdh is also limiting. Our results further highlight the complex nature of the *B. subtilis* iron sparing response which, though largely dependent on the FsrA sRNA, additionally involves the poorly characterized FbpABC proteins postulated to function (at least in part) as RNA chaperones.

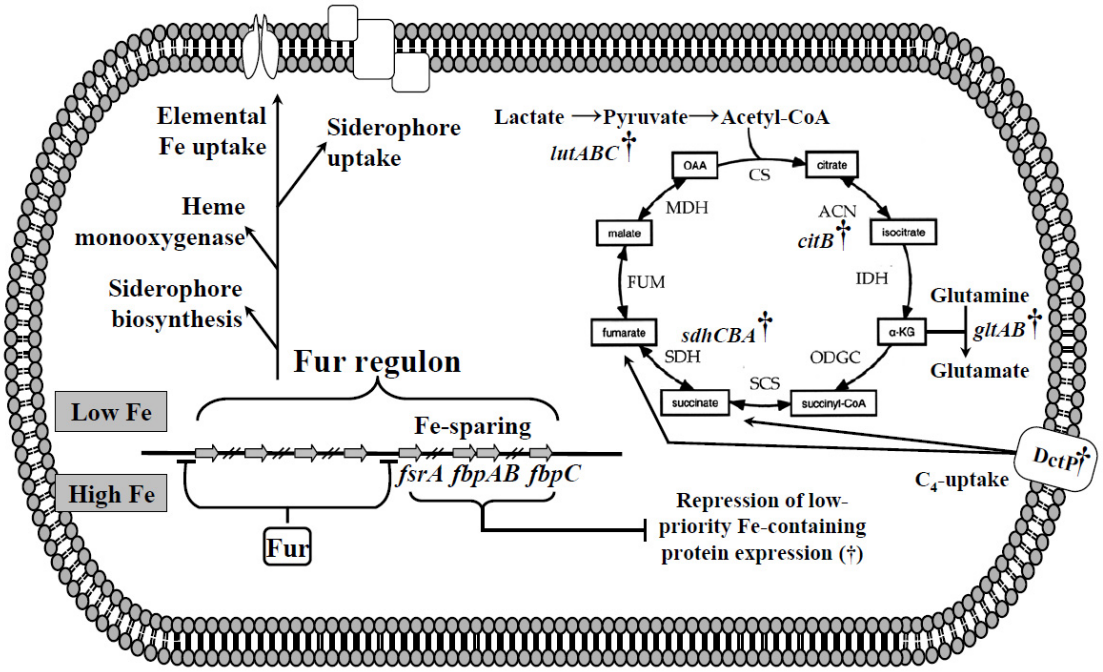

Figure 2.8: An integrated model of metabolism regulation by Fur and the iron-sparing response effectors FsrA, FbpA, FbpB, and FbpC. This model depicts the cellular response of *Bacillus subtilis* under iron replete and deplete conditions. Under high iron conditions, Fur enacts repression on its regulon including uptake and iron-sparing. Under low iron conditions, repression is lifted and iron uptake is turned on along with the iron-sparing response. Iron-sparing in turn represses expression of low-priority iron-containing proteins. Those transcripts or their protein products repressed by iron-sparing that have an effect on carbon metabolism are indicated by a dagger (†).

CHAPTER 3

THE FSRA SRNA AND FBPB PROTEIN MEDIATE THE IRON-DEPENDENT INDUCTION OF THE *BACILLUS SUBTILIS* LUTABC IRON-SULFUR CONTAINING OXIDASES [1]

3.1 Summary

The *Bacillus subtilis* ferric uptake regulator (Fur) protein regulates iron homeostasis and directly represses more than 20 operons. Fur indirectly regulates many more genes including those controlled by the small, non-coding RNA FsrA. FsrA translationally represses numerous target genes and, for at least some targets, appears to function in conjunction with one or more of three small, basic proteins known as FbpA, FbpB, and FbpC. The lactate-inducible *lutABC* operon encodes iron sulfur-containing enzymes required for growth on lactate. We here demonstrate that a *fur* mutant strain grows poorly on lactate due to an FsrA-dependent repression of LutABC synthesis. Growth is restored in an *fsrA* mutant and also partially restored by mutation of the *fbpAB* operon. Genetic studies indicate that the 48 amino acid FbpB protein, but not FbpA, contributes to regulation of *lutABC*. FbpB appears to function by increasing the efficiency of FsrA-targeting to the *lutABC* mRNA since the role of FbpB can be bypassed by modest up-regulation of FsrA. These results provide support for a model in which FbpB, and perhaps other Fbp proteins, act as RNA chaperones for FsrA.

[1] Gregory T. Smaldone and John D. Helmann. Journal of Bacteriology. (Under revision).

3.2 Introduction

Iron is an essential element for nearly all living cells, but due to the insolubility of ferric hydroxides it is a limiting nutrient in many environments [5]. Bacteria have developed a variety of mechanisms for optimizing growth under iron-limiting conditions including the production of siderophores and uptake systems for iron and iron complexes [147]. The ferric uptake repressor (Fur) represses expression of iron uptake systems in response to iron sufficiency. Originally described in *Escherichia coli*, Fur orthologs are found in both Gram negative and Gram positive bacteria, including *Bacillus subtilis* and related pathogens such as *Staphylococcus aureus* and *Listeria monocytogenes* [64].

In addition to the role of Fur as a repressor of iron uptake, several observations suggest that, at least in *E. coli*, there are further layers of regulation. First, Fur also functions, directly or indirectly, as an activator of expression for proteins that contain iron (e.g. iron superoxide dismutase, ferritin). Second, a *fur* null mutant strain has reduced total cellular iron levels, despite the constitutive expression of uptake functions [1]. Third, *fur* mutants have a variety of other phenotypes, including an inability to grow on succinate and related dicarboxylate compounds. Many of these additional phenotypes are due to the actions of a Fur-repressed small RNA which, under iron-limiting conditions, mediates repression of iron-containing proteins [96, 97]. This sRNA, named RyhB, works in conjunction with a global chaperone Hfq to regulate succinate dehydrogenase, aconitase, fumarase, and Fe superoxide dismutase [98]. This system functions as an iron-sparing response and enables the cell to prioritize the usage of this limiting element by the selective repression of low priority, iron-consuming proteins. More recently, it has been appreciated that RyhB can also activate the

translation of functions needed for siderophore biosynthesis [118, 123].

A functionally analogous iron-sparing response system was recently identified in *B. subtilis* which includes the Fur-regulated sRNA A (FsrA) and three small, Fur-regulated basic proteins (FbpABC). In this initial study, the global effects of this sRNA and these small proteins on gene expression were monitored by proteomics [50]. This work led to the unexpected finding that the effects of an *fsrA* deletion could in several cases be mimicked by deletion of one or more of the genes encoding FbpA, B, or C. This led to the proposal that these small proteins might function as chaperones to target FsrA to specific transcripts. Altogether, approximately 20 operons were implicated as being down-regulated in response to iron limitation [50].

Of the many FsrA-regulated operons, *yvfVWyvbY* was amongst the most strongly derepressed in a *fur fsrA* double mutant when compared to the *fur* single mutant as monitored by both transcriptomic and proteomic approaches [50]. This operon was recently renamed *lutABC* and shown to encode a lactate utilization system important for growth and biofilm formation in *B. subtilis* [23]. In this study, we demonstrate that translational repression of *lutABC* involves FsrA, which is complementary to the translation initiation region corresponding to the +18-46 nt relative to the +1. FbpB, but neither FbpA nor FbpC, functions to enhance FsrA-mediated repression. The stimulatory effect of FbpB is not needed if FsrA expression is elevated by insertion of an ectopic copy of FsrA, consistent with a model in which FbpB functions as an RNA chaperone.

3.3 Materials and Methods

3.3.1 Bacterial strains, media, and growth conditions

Bacterial strains used in this study are listed in Table 3.1. *Escherichia coli* DH5α was used for routine DNA cloning [124]. *B. subtilis* CU1065 derivatives were constructed by allelic replacement using long-flanking homology PCR [21]. Mutations generated in *B. subtilis* CU1065 were transferred to *B. subtilis* NCIB3610 by SPP1 phage transduction as described previously [156]. Erythromycin (1 μg/mL) and lincomycin (25 μg/mL) [for MLS (macrolide-lincosamide-streptomycin B) resistance], spectinomycin (100 μg/mL), kanamycin (10 μg/mL), neomycin (10 μg/mL), and chloramphenicol (5 μg/mL) were used for the selection of various *B. subtilis* strains unless otherwise indicated. Liquid media were inoculated from overnight pre-culture and incubated at 37°C with shaking at 225 rpm. Growth media used in this study include LB medium, modified competence medium (MC), MSgg medium, lactate MSgg (MSgg with lactate replacing glycerol at the same concentration), minimal growth medium (MOPS-based with glucose carbon source; MM), and lactate minimal growth medium (MOPS-based with 2% DL-lactate carbon source; lactate MM) [19, 25, 80].

3.3.2 DNA manipulations

Routine molecular biology procedures were performed as described [124]. Isolation of *B. subtilis* chromosomal DNA and transformation were carried out as described [36]. Restriction enzymes, DNA ligase, and DNA polymerases were

Table 3.1: Bacterial strains and plasmids used in THE FSRA SRNA AND FBPB PROTEIN MEDIATE THE IRON-DEPENDENT INDUCTION OF THE *BACILLUS SUBTILIS* LUTABC IRON-SULFUR CONTAINING OXIDASES

Strain or plasmid	Relevant Characteristic(s)	Source or reference
***B. subtilis* strains**		
CU1065	W168 *att* SPβ *trpC2* (”Wild Type”)	[142]
NCBI3610	Marburg savage strain	[31]
HB2501	CU1065 *fur::kan*	[10]
HB5733	CU1065 *fur::kan fsrA::cat*	[50]
HB5735	CU1065 *fur::kan fbpAB::tet*	[50]
HB5751	CU1065 *fur::kan fsrA::cat fbpAB::tet*	[50]
HB7371	NCBI3610 *fur::kan*	This study
HB7374	NCBI3610 *fur::kan fsrA::cat*	This study
HB7379	NCBI3610 *fur::kan fbpAB::spc*	This study
HB7381	NCBI3610 *fur::kan fsrA::cat fbpAB::spc*	This study
HB7497	CU1065 *fur::kan fbpAB::tet amyE::*pSWEET-FbpA-FLAG *lutA::*pMUTIN-FLAG	This study
HB7498	CU1065 *fur::kan fbpAB::tet amyE::*pSWEET-FbpB-FLAG *lutA::*pMUTIN-FLAG	This study
HB12510	CU1065 *fur::kan fsrA::cat thrC::fsrA*	This study
HB12511	CU1065 *fur::kan fbpAB::tet thrC::fbpAB*	This study
HB12520	CU1065 *fur::kan lutB::*pMUTIN-FLAG	This study
HB12521	CU1065 *fur::kan lutC::*pMUTIN-FLAG	This study
HB12522	CU1065 *fur::kan fbpAB::tet lutB::*pMUTIN-FLAG	This study
HB12523	CU1065 *fur::kan fbpAB::tet lutC::*pMUTIN-FLAG	This study
HB12524	CU1065 *lutA::*pMUTIN-FLAG	This study
HB12525	CU1065 *lutB::*pMUTIN-FLAG	This study
HB12526	CU1065 *fur::kan fsrA::cat lutA::*pMUTIN-FLAG	This study
HB12527	CU1065 *fur::kan fsrA::cat lutB::*pMUTIN-FLAG	This study
HB12528	CU1065 *fur::kan fsrA::cat lutC::*pMUTIN-FLAG	This study
HB12529	CU1065 *fur::kan fsrA::cat fbpAB::tet lutA::*pMUTIN-FLAG	This study
HB12530	CU1065 *fur::kan fsrA::cat fbpAB::tet lutB::*pMUTIN-FLAG	This study
HB12531	CU1065 *fur::kan fsrA::cat fbpAB::tet lutC::*pMUTIN-FLAG	This study
HB12532	CU1065 *fur::kan lutA::*pMUTIN-FLAG	This study
HB12533	CU1065 *fur::kan fbpAB::tet lutA::*pMUTIN-FLAG	This study
HB12534	CU1065 *lutC::*pMUTIN-FLAG	This study
HB12579	CU1065 *fur::kan fbpAB::tet thrC::fbpAB lutA::*pMUTIN-FLAG	This study
HB12580	CU1065 *fur::kan fbpAB::tet thrC::fbpAB* ACG A *lutA::*pMUTIN-FLAG	This study
HB12581	CU1065 *fur::kan fbpAB::tet thrC::fbpAB* ACG B *lutA::*pMUTIN-FLAG	This study
HB12582	CU1065 *fur::kan fbpAB::tet thrC::fbpAB* ACG AB *lutA::*pMUTIN-FLAG	This study
HB12594	CU1065 *fur::kan fbpAB::tet amyE::fsrA*	This study
***E. coli* strains**		
DH5α	ϕ Δ(*lacZ*)M15 Δ(*argF-lac*)U169 *endA1 recA1 hsdR17* (r_K^- m_K^+) *deoR thi-1 supE44 gyrA96 relA1*	[124]
Plasmids		
pDG1730	Integration vector into *amyE* locus	BGSC
pDG1731	Integration vector into *thrC* locus	BGSC
pSWEET	Xylose inducible integration vector into *amyE* locus	[15]
pMUTIN-FLAG	Integration vector at locus generating a C-terminal FLAG tagged ORF	BGSC

all used according to manufacturer's instructions (New England Biolabs). Site directed mutagenesis was done by PCR and overlap extension according to Ho *et al*. [69].

For complementation of *fsrA* and *fbpAB*, the genes were PCR amplified to include their native promoters and terminator stem loops. The amplicons were inserted between the *Eco*RI-*Bam*HI and *Hind*III-*Eco*RI sites of pDG1731, respectively [56]. The constructs were then integrated ectopically at the *thrC* locus. A second construct was also made for *fsrA* complementation using pDG1730 for integration into the *amyE* locus.

For the Lut-FLAG constructs, the *lutA*, *lutB*, and *lutC* genes were individually PCR amplified and inserted into the *Hind*III-*Cla*I, *Kpn*I-*Cla*I, and *Hind*III-*Kpn*I sites of the pMUTIN-FLAG vector, respectively [78]. The resulting constructs express a translation fusion with C-terminal FLAG epitope tag. Strains were constructed via Campbell integration at the gene locus.

The xylose-inducible FbpA-FLAG construct was generated by PCR amplification of the *fbpA* gene (*fbpA* is the ORF upstream and including part of the misannotated gene *ydbN*; [50]) including the upstream RBS in the forward primer and by addition of the FLAG epitope tag sequence on the reverse primer so as to generate a C-terminal translationally fused FLAG epitope. The FbpB-FLAG construct was generated in the same fashion, by PCR amplification of *fbpB* [50] including a putative RBS upstream in the first primer, and by adding the FLAG epitope to the second primers to generate a C-terminal translationally fused FLAG epitope. These modified PCR products were cloned between the *Pac*I and *Bam*HI sites of pSWEET [15] and integrated into *amyE*. The sequences for all mutant constructs were verified by DNA sequencing (Cornell Life Sciences

Core Laboratories Center).

3.3.3 Growth curve generation and comparison

Fresh single colonies were picked from selective LB plates and cultivated statically at either 25°C or 30°C overnight in 5 mL MM. They were then shifted to 37°C shaking and grown to mid-exponential phase ($OD_{600} \approx 0.4$; Spectronic 21). Cells were recovered from 1 mL of each culture, washed in 0.75 mL 0.88% NaCl then resuspended and diluted to a standard OD_{600} of 0.1 (Perkin Elmer lambda-2 spectrophotometer) in 0.88% NaCl. 30 μL of cells were inoculated into 170 μL lactate MM in a 100-well microtitre plate and growth was monitored with shaking at 37°C using a BioScreen C plate reader.

3.3.4 Western blot analysis

50 mL cultures were inoculated from overnight LB broth starter cultures and grown to mid-log ($OD_{600} \approx 0.4$; Spectronic 21) in LB broth. Cells were recovered by centrifugation at 5000 rpm for 5 min in an Eppendorf 5804R swinging bucket rotor centrifuge. Cells were frozen overnight at -20°C, thawed, and resuspended in 0.5 mL 50 mM Tris-HCl (pH 7.4), 150 mM NaCl, 1 mM EDTA, 1 mM DTT, and 0.1 mM PMSF. Cells were then sonicated for 3× 8 s bursts with at least one min on ice between each burst. Crude extract was clarified by centrifugation at 14,000 rpm at 4°C. Bradford assay was used to quantify total protein within the crude extract and 10 μg of total protein was used for SDS-PAGE. Protein levels were detected after membrane transfer and western blot analysis us-

ing commercially obtained anti-FLAG primary antibodies (Sigma) and alkaline phosphatase linked secondary anti-rabbit antibody.

3.3.5 Colony morphology assay

For assays of colony architecture on solid agar MSgg medium, cells were cultivated overnight in 1 mL LB broth with appropriate antibiotic selection, diluted 1:100 into 5 mL LB, and grown to mid-exponential phase ($OD_{600} \approx 0.4$, Spectronic 21). 10 μL of each culture was then spotted onto solid MSgg and lactate MSgg. They were then incubated at room temperature for at least 120 hours. Colonies were imaged on plates using a Canon PowerShot SD600 digital camera.

3.4 Results

It has been previously demonstrated that the *lutABC* operon plays a major role in *B. subtilis* growth on lactate as a sole carbon source [23]. Bioinformatic analyses suggest that LutA, B, and C may function as a complex of 4Fe-4S-containing oxidases [23]. Two members of this proposed protein complex (LutB and LutC) were also observed in proteomic studies to be strongly repressed in response to iron limitation as part of the Fur-regulated iron-sparing response [50]. We therefore sought to define the roles of the Fur-regulated small RNA FsrA and the co-regulated small, basic proteins FbpABC on *lutABC* expression.

3.4.1 Mutation of *fsrA* or *fbpAB* enables growth of a *fur* mutant on lactate

Consistent with repression of LutABC as part of a Fur-regulated iron-sparing response, a *fur* mutant strain demonstrates reduced growth in lactate MM (Fig. 3.1A). This inability to grow on lactate is due to FsrA since growth is restored in the *fur fsrA* double mutant (Fig. 3.1A). We also observed a partial rescue of growth in the *fur fbpAB* mutant strain, consistent with prior proteomic analysis of LutB and LutC protein expression levels [50]. As expected, disruption of *lutABC* also led to an inability to grow on lactate as a sole carbon source in all mutant backgrounds tested (data not shown), which confirms the key role for this operon in lactate utilization [23].

Complementation experiments demonstrate that provision of an ectopic copy of *fbpAB* to a *fur fbpAB* double mutant restores the poor growth characteristic of the *fur* mutant (Fig. 3.1A). Similarly, an ectopic copy of *fsrA* in a *fur fsrA* double mutant complements the phenotype and leads to even worse growth than in a *fur* mutant (Fig. 3.1A). The lack of growth exhibited by the *fur fsrA* strain complemented with *fsrA* was unexpected, but suggested that FsrA levels might be higher when expressed from an ectopic locus. To test this hypothesis, we measured FsrA levels using quantitative primer extension analysis. Indeed, FsrA levels when complemented ectopically were approximately 1.6-fold (±0.3) higher than when expressed from the native locus in a *fur fsrA amyE::fsrA* background. Significantly, the presence of an additional copy of *fsrA* at an ectopic locus (leading to a 2- to 3-fold increase in FsrA levels compared to the native locus alone) bypasses the requirement for *fbpAB* for eliciting a growth restriction on lactate (Fig. 3.1B). Together, these results suggest that *fsrA* and *fbpAB*

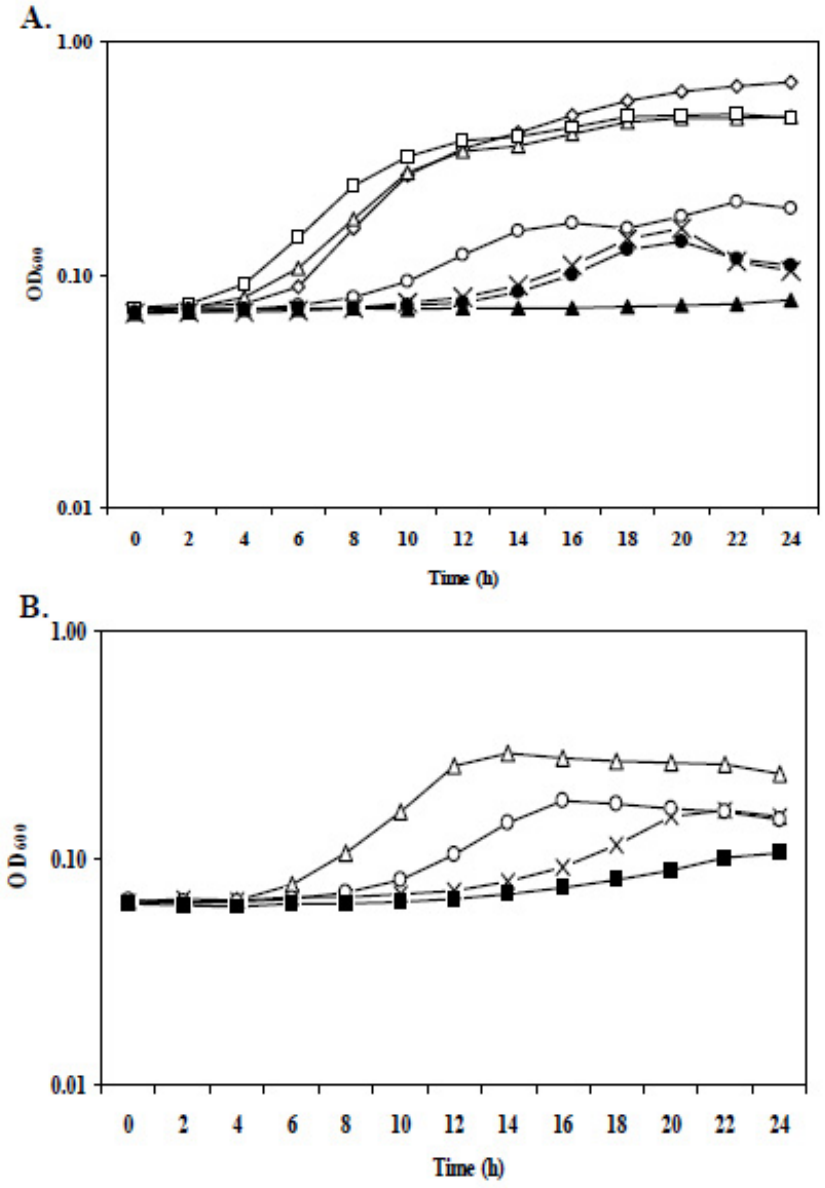

Figure 3.1: Growth on lactate minimal medium is reduced in a *fur* mutant and restored by mutations in both *fsrA* and *fbpAB*. Growth curves of the indicates strains in lactate MM. **A**. The strains used were: WT (open diamond); *fur* (cross); *fur fsrA* (open triangle); *fur fbpAB* (open circle); *fur fsrA fbpAB* (open square); *fur fsrA +fsrA* (filled triangle); and *fur fbpAB +fbpAB* (filled circle). **B**. The strains used were: *fur* (cross); *fur fsrA* (open triangle); *fur fbpAB* (open circle); and *fur fbpAB +fsrA* (filled square).

co-regulate expression of *lutABC* as described below.

3.4.2 Fur and the iron-sparing response affect colony morphology on lactate minimal medium

Mutation of the *lutABC* operon was previously shown to affect colony morphology when grown on lactate minimal medium [23]. In these experiments, complex colony morphology is used as a surrogate for the differentiation of multiple cell types as occurs during biofilm formation as described previously [23, 79, 101]. In order to test if *fsrA* or *fbpAB* regulation plays a role in the ability to develop complex colony architecture we generated a set of isogenic strains (Table 3.1) in the NCIB3610 background which is known to form robust biofilms. In this background, neither the *fur* nor the *fur fsrA* mutants were able to form complex structures on lactate medium although they were relatively unimpaired in growth and differentiation on MSgg medium (Fig. 3.2). We also observed that a *fur fbpAB* strain partially restores the ability to form such structures, while the *fur fsrA fbpAB* triple mutant strain restores the wild type phenotype. These results support the suggestion that lactate utilization is important for growth and therefore elaboration of complex colony architecture on this medium.

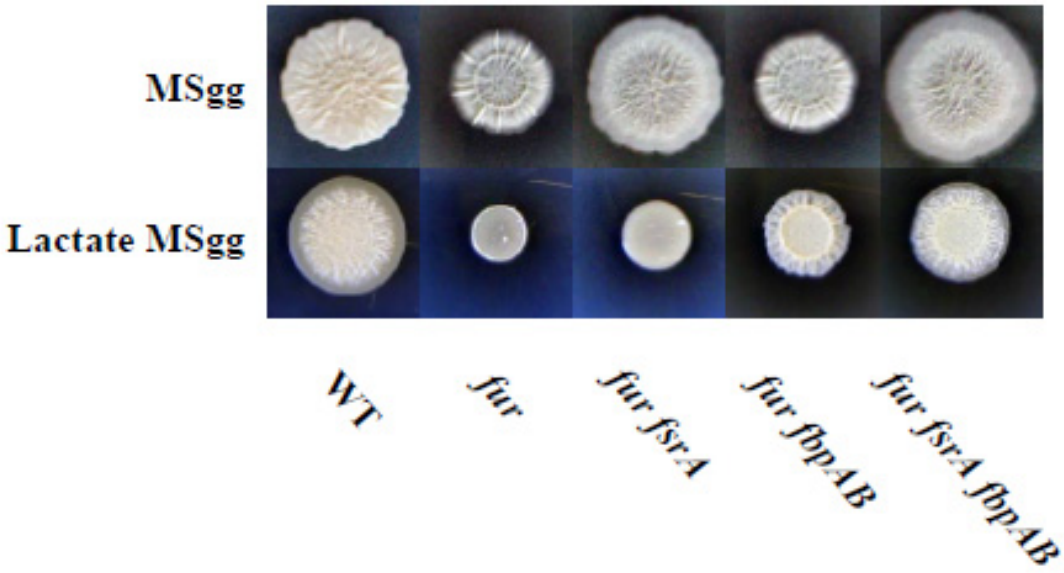

Figure 3.2: Colony morphology on lactate medium. Colony morphology of NCIB3610 derived strains as observed on MSgg medium plus 0.5% lactate in place of glycerol. Images shown here were taken after 120 hours of growth at room temperature.

3.4.3 Mutation of *fsrA* or *fbpAB* restores expression LutA, LutB, and LutC in a *fur* mutant background

Western blot analysis demonstrates a marked reduction in the protein level of LutA-FLAG, LutB-FLAG, and LutC-FLAG in the *fur* mutant strain compared to the levels in the WT (Fig. 3.3). Consistent with the lactate MM growth data, protein expression levels in the *fur* mutant background increase with the additional mutation of either *fsrA* or *fbpAB*(Preliminary indications whose effects are further verified in Fig. 3.4 and Fig. 3.5). We did not observe any further effect on the expression of the FLAG-tagged Lut protein levels in the *fur fsrA fbpAB* triple mutant strain consistent with a model in which *fsrA* and *fbpAB* are working within the same pathway to regulate LutABC expression.

3.4.4 FbpB, not FbpA, co-regulates LutABC expression

In general, we have investigated the effects of the *fbpA* and *fbpB* genes together due to the fact that they are small overlapping coding sequences expressed from a common promoter with a single Fur box. We previously reported phylogenomic comparisons that reveal a pattern of degenerate third codon position base substitutions suggesting that both FbpA and FbpB are translated [50], although this does not exclude the possibility that the *fbpAB* transcript might function in addition as a regulatory RNA. Their co-regulation suggests that FbpA and FbpB may interact to form a multimeric complex, but it is also possible that they function independently.

To determine whether FbpA, FbpB, or both are needed for *lutABC* regula-

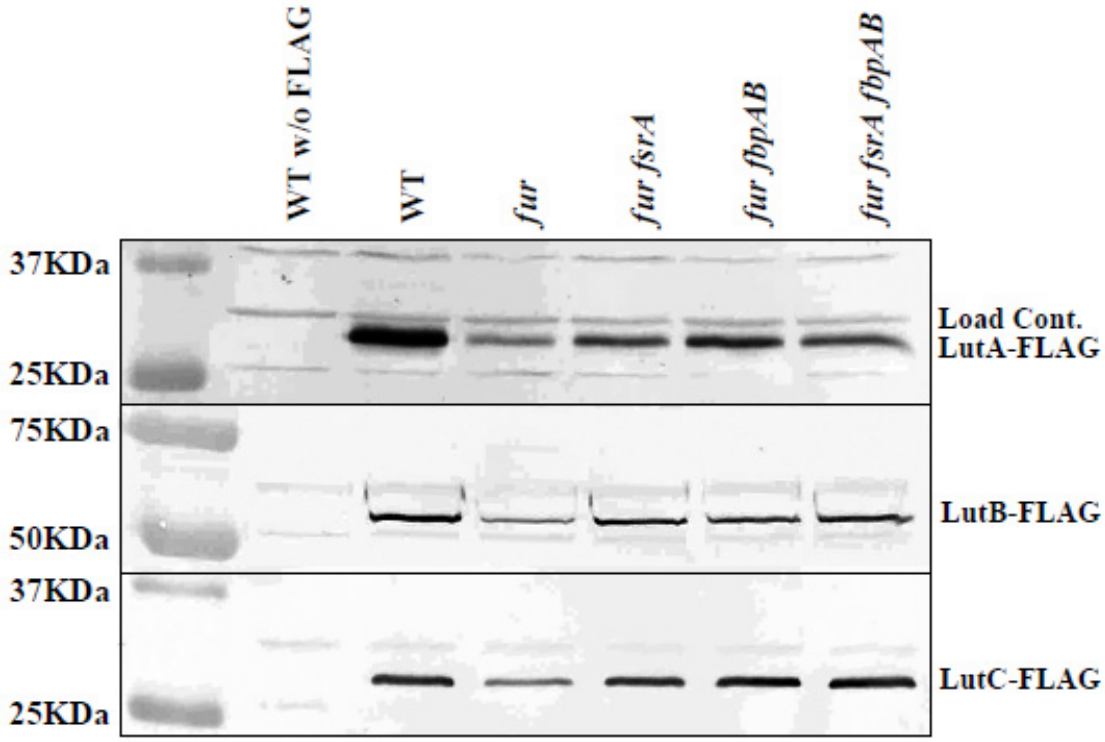

Figure 3.3: Repression of the *lutABC* operon involves both *fsrA* and *fbpAB*. Western blot analysis of LutA-FLAG (top panel), LutB-FLAG (middle), and LutC-FLAG (bottom) expression in mutant strains was carried out with 10 μg total crude extract loaded per lane (an unidentified cross-reactive band that also serves as a loading control is indicated). Each lane is labeled with the relevant genotype of the strain background. A wild type strain carrying no FLAG tag construct is in the left lane as a negative control.

tion we complemented the *fur fbpAB* mutant strain with constructs in which the start codon of *fbpA*, *fbpB*, or both was altered from ATG to an ACG. This change leaves the transcript sequence largely unchanged, yet prevents translation of the encoded peptides (Fig. 3.4A). Note that the start codon mutation in *fbpB* is a silent mutation with respect to the sequence of the FbpA product. As expected, translation of LutA-FLAG was repressed in the *fur* mutant, restored with the mutation of *fbpAB*, and repressed in the *fur fbpAB* complemented strain (Fig. 3.4B). In addition, we observed derepressed levels of LutA-FLAG in the *fur fbpAB +fbpAB* ACG B strain (indicating a lack of complementation), whereas repression was restored in the *fur fbpAB +fbpAB* ACG A complemented strain. These results suggest that the FbpB peptide, but not FbpA, is needed for the translational repression of LutA-FLAG. They further suggest that the two genes are not translationally coupled: FbpB translation is not dependent on translation of FbpA.

To confirm that FbpB was sufficient for co-regulation of LutA-FLAG, both FbpA and FbpB were FLAG-tagged and expressed in a *fur* mutant (constitutively expressing FsrA) from an ectopic locus using a xylose-inducible promoter. Expression of FbpA and FbpB was observed by western blot, as demonstrated previously [50]. As predicted, repression of LutA-FLAG was observed upon induction of FbpB-FLAG, but not FbpA-FLAG (Fig. 3.5).

3.4.5 FbpB enhances the activity of FsrA

Our epistasis studies suggest that the FsrA sRNA and FbpB function in the same pathway for *lutABC* repression. Specifically, growth of a *fur* mutant and ex-

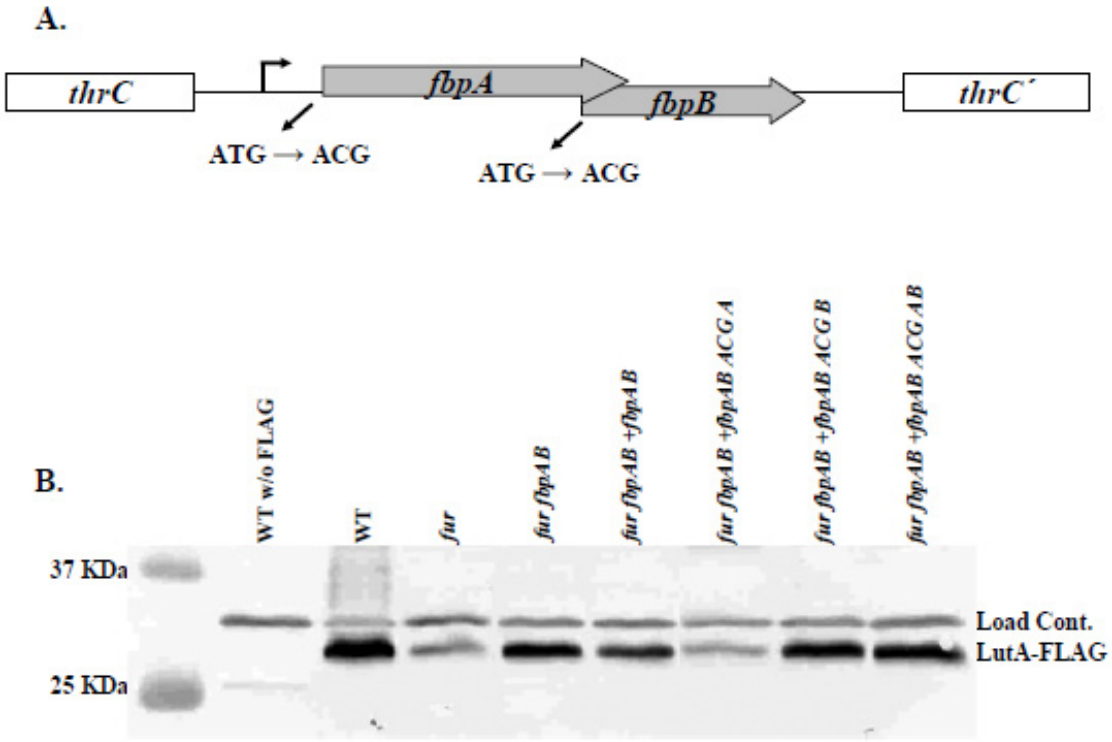

Figure 3.4: Regulation of LutA-FLAG expression requires translation of FbpB but not FbpA. **A**. Illustration of the start codon mutations generated in an ectopically integrated copy of the *fbpAB* operon. **B**. Western blot of LutA-FLAG in various mutant strains was carried out with 10 μg total crude extract loaded per lane.

Figure 3.5: Induction of FbpB-FLAG protein is sufficient to restore repression of LutA-FLAG expression in an *fbpAB* mutant. Western blot of LutA-FLAG in various strain backgrounds was carried out with 10 μg total crude extract loaded per lane. Each lane is labeled with the mutant background and a wild type strain carrying no FLAG tag construct was included as control. Lanes are also labeled to indicate growth with either 0 or 2% xylose to induce expression of FbpA-FLAG or FbpB-FLAG.

pression of Lut proteins is fully restored by an *fsrA* mutation and there is no additional effect of mutating *fbpB*. In general, the effect of the *fbpB* (or *fbpAB*) mutation on growth and Lut expression is less dramatic than that observed with *fsrA*. These results are consistent with a model in which FbpB, which is a 48 amino acid basic peptide, interacts with FsrA, the target RNA, or both to facilitate their annealing or to stabilize the FsrA transcript much as Hfq does for sRNA-mediated gene regulation in *E. coli* [50, 95, 104, 141]. This model is consistent with the observation that when expression of FsrA is elevated, by integration of a second copy at an ectopic locus, growth restriction on lactate was observed even in the absence of FbpB (Fig. 3.1B).

3.5 Discussion

Interest in the *lutABC* operon was initially motivated by its identification in transcriptome studies as a target for SinR, the master regulator of biofilm formation in *B. subtilis* [29]. Bioinformatic and physiological studies subsequently defined a role for the *lutABC* operon in growth and biofilm formation on media where lactate is the carbon source. Induction of *lutABC* is mediated by the LutR repressor which responds to lactate as an inducer [23]. In addition to this complex transcriptional regulation, the studies here add a new layer of post-transcriptional control: translational repression mediated by the FsrA sRNA aided by the FbpB RNA chaperone.

The precise role played by the LutABC gene products during growth and biofilm differentiation is still unknown. It is interesting to note that during maturation of *B. cereus* biofilms there is marked increase in *lctE* (lactate dehydroge-

nase) expression between 2 and 18 hrs. of growth [112]. This possibly indicates that oxygen is limiting in the deeper layers of aerobic biofilms [155], and those cells experiencing anoxic conditions switch to a fermentative metabolism and produce lactate. In *B. subtilis*, *lctE* is both strongly induced and essential under anaerobic conditions [35]. Thus, induction of *lutABC* under biofilm inducing conditions allows for a fitness advantage for cells at all levels of the biofilm both by removing an acidic waste product from the fermentative zone and by providing an energy source to those cells still in the oxic zone.

3.5.1 Mechanism of iron-mediated induction of LutABC synthesis

The predicted products of all three genes in the *lutABC* operon contain putative iron-sulfur clusters and resemble oxidoreductases [85]. Under iron replete growth conditions, synthesis of these proteins would consume iron from the available cytosolic pool. However, in times of severe iron limitation synthesis of this non-essential lactate-utilization pathway would be an unnecessary draw on that pool. Therefore, repression of *lutABC* translation under iron-limited growth conditions, as mediated by FsrA and FbpB, will allow iron to be directed to higher priority target proteins. The small, basic Fur-regulated proteins (FbpA, FbpB, and FbpC) were previously postulated to function together with FsrA, possibly by acting as RNA chaperones [50]. This model is supported by the results herein which demonstrate that it is the FbpB peptide that is important in the case of the *lutABC* operon and that this effect can be bypassed by increased expression of the FsrA sRNA. The roles of the other putative chaper-

ones, and whether they work independently or in a combinatorial manner, is not yet clear.

3.6 Concluding Remarks

The results presented here allow us to revise the model of regulation at the *lutABC* operon. Pairing predictions between FsrA and the 5'UTR of the *lutABC* transcript reveal an extended interaction surrounding and including the ribosome-binding site (Fig. 3.6A). We therefore propose a model wherein FsrA binds at the 5'UTR of the *lutABC* operon aided by the small basic RNA chaperone FbpB (Fig. 3.6B). The repression exerted here is a second level of regulation occurring post-transcriptionally, subsequent to the regulation of SinR/SinI and LutR.

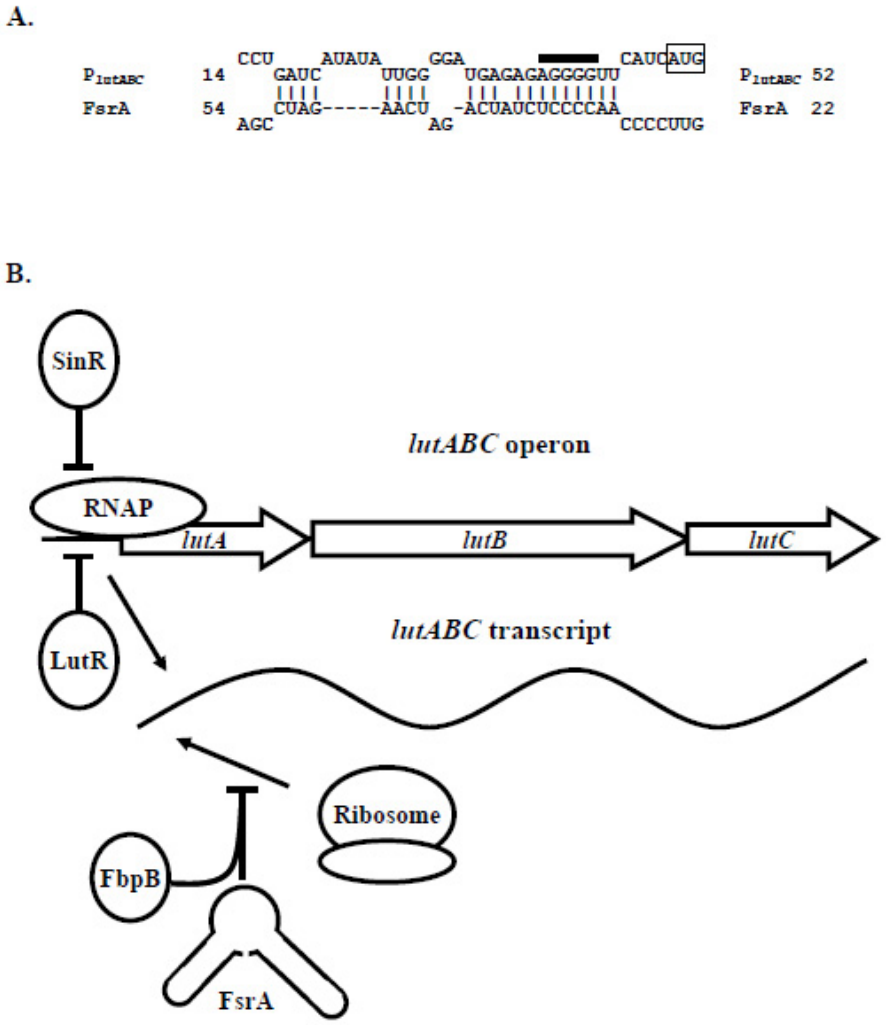

Figure 3.6: Model of the iron-sparing response repression of the *lutABC* operon. **A**. Illustration of the predicted pairing between the *lutABC* 5′UTR (above) and the sRNA FsrA (below). The RBS is indicated by the solid black bar and the AUG start codon is indicated by a black box. RNAs are numbered relative to the transcription start site (+1). **B**. Summary of the multiple levels of regulation at the *lutABC* operon. Arrows represent the processes of transcription and translation and bars represent repression at either the transcriptional or post-transcriptional levels

CHAPTER 4

CSOR REGULATES THE COPPER EFFLUX OPERON *COPZA* IN *BACILLUS SUBTILIS*[1]

4.1 Summary

The adaptation of *Bacillus subtilis* to elevated levels of copper ions requires the copper-inducible *copZA* operon encoding a copper chaperone and efflux ATPase. Here we identify CsoR (formerly YvgZ) as the copper-sensing repressor that regulates the *copZA* operon. CsoR binds with high affinity to an operator site overlapping the *copZA* promoter and its binding is specifically inhibited by copper salts. As previously described, the YhdQ (CueR) protein also binds to the *copZA* regulatory region, but genetic experiments indicate that this protein is not responsible for the copper-dependent regulation of this operon.

4.2 Introduction

Metals are essential cofactors for many enzymic reactions within the cell. Yet, at high concentrations, many metals become toxic. Toxicity can arise from metal ions binding inappropriately to metal-binding sites in enzymes, thereby inhibiting activity, or by the generation of reactive oxygen species that can damage the genetic, enzymic and structural components of the cell [73, 140]. Thus, it is vitally important for the cell to closely regulate metal concentrations within the cytoplasm. When limited for metal ions, many bacteria express high-affinity

[1]Gregory T. Smaldone and John D. Helmann. Microbiology. (2007). 153:4123-4128

uptake systems. Conversely, when metals are in excess the cell will often express specific efflux systems or metal-storage proteins. The regulated expression of metal homeostasis mechanisms, including both uptake and efflux systems, is controlled by metalloregulatory proteins that sense metal availability within the cytosol.

Copper is an essential element for *Bacillus subtilis* aerobic respiration because it is a cofactor for heme-copper oxidases, the terminal enzymes in the respiratory pathway [99]. The pathways responsible for the uptake of copper are not yet defined, but copper present in the cytosol appears to be tightly chaperoned. The Sco chaperone characterized in yeast, humans and bacteria (YpmQ in *B. subtilis*) mediates the insertion of copper into the Cu_A copper center of cytochrome c oxidase [99]. It has also recently been suggested that Sco may play a role in the insertion of copper into the Cu_B centers of the heme-copper oxidases, and may play a more general role as a copper chaperone for other metalloproteins [12].

When copper is present in excess, a specific efflux system encoded by the *copZA* operon is induced [52]. Strong induction of *copZA* was noted in the presence of copper salts, but not other metals tested, and the CopZA system was shown to be required for resistance to high levels of copper [52]. CopZ functions as a copper chaperone to deliver copper to CopA, a CPx-type efflux ATPase [14, 120]. Structural analyses have allowed visualization of *B. subtilis* Sco, CopZ and the N-terminal domain of CopA, thereby affording a detailed look at the molecular mechanics of copper homeostasis in this model organism [11, 14, 13].

The regulatory proteins controlling the expression of these copper homeostasis proteins are not as well defined. Previously, we identified a MerR-type regulatory protein (YhdQ; previously renamed CueR) as a candidate regulator

for the *copZA* operon [51]. Here, we provide evidence that this assignment was incorrect: although YhdQ does bind to the *copZA* regulatory region (P_{copZA}) *in vitro*, this binding may not be physiologically relevant. Our previously reported genetic studies linking *yhdQ* to the copper-dependent induction of *copZA* were incorrect due to an inadvertent error in strain construction. Here, we present evidence that YvgZ, an ortholog of the recently described copper-sensing metalloregulator CsoR from *Mycobacterium tuberculosis* [88], is the copper-sensing regulator of the *copZA* operon.

4.3 Materials and Methods

4.3.1 Bacterial strains, media, and growth conditions

Bacterial strains used in this study are listed in Table 4.1. *Escherichia coli* DH5α was used for routine DNA cloning [124]. Liquid media were inoculated from overnight pre-culture and incubated at 37°C with shaking at 225 rpm Erythromycin (1 μg/mL) and lincomycin (25 μg/mL) [for MLS (macrolide-lincosamide-streptomycin B) resistance], spectinomycin (100 μg/mL), kanamycin (10 μg/mL), neomycin (10 μg/mL) and chloramphenicol (5 μg/mL) were used for the selection of various *B. subtilis* strains. To determine growth in the presence of copper, strains were cultivated overnight in LB, diluted 1:100 in 5 mL LB, and grown to mid-exponential phase ($OD_{600} \approx 0.4$, Spectronic 21). Three microliters of cells were inoculated into 197 mL LB containing $CuSO_4$ from 0 to 6 mM in a 100-well microtitre plate and growth was monitored after overnight growth with shaking at 37°C using a BioScreen C plate reader.

Table 4.1: Bacterial strains and plasmids used in CSOR REGULATES THE COPPER EFFLUX OPERON *COPZA* IN *BACILLUS SUBTILIS*

Strain or plasmid	Relevant Characteristic(s)	Source or reference
***B. subtilis* strains**		
CU1065	W168 *att* SPβ *trpC2* (″Wild Type″)	[142]
HB7301	CU1065 *yhdQ::kan*	This study
HB7350	CU1065 *csoR::spc*	This study
HB7351	CU1065 *yhdQ::kan csoR::spc*	This study
HB7352	CU1065 *csoR::spc* SPβ (P_{copZA}-*cat-lacZ*)(MLS^R Neo^R)	This study
HB7353	CU1065 *yhdQ::kan csoR::spc* SPβ (P_{copZA}-*cat-lacZ*)(MLS^R Neo^R)	This study
HB7354	CU1065 *csoR::spc amyE::csoR-cat*	This study
HB7355	CU1065 *yhdQ::kan csoR::spc amyE::csoR-cat*	This study
HB7356	CU1065 *csoR::spc amyE::csoR-cat* SPβ (P_{copZA}-*cat-lacZ*)(MLS^R Neo^R)	This study
HB7357	CU1065 *yhdQ::kan csoR::spc amyE::csoR-cat* SPβ (P_{copZA}-*cat-lacZ*)(MLS^R Neo^R)	This study
HB7358	CU1065 SPβ (P_{copZA}-*cat-lacZ*)(MLS^R Neo^R)	This study
HB7959	CU1065 *yhdQ::kan* SPβ (P_{copZA}-*cat-lacZ*)(MLS^R Neo^R)	This study
***E. coli* strains**		
DH5α	ϕ Δ(*lacZ*)M15 Δ(*argF-lac*)U169 *endA1 recA1 hsdR17* (r_K^- m_K^+) *deoR thi-1 supE44 gyrA96 relA1*	[124]
BL21 (DE3)(pLysS)	F^- *ompT* $hsdS_B$ ($r_B^-m_B^-$) *gal dcm* (DE3)/pLysS	Novagen
HE7307	BL21 pGS001	This study
HE8248	BL21 with pET16X containing *yhdQ* cloned into the *Nco*I and *Bam*HI sites	[51]
Plasmids		
pGS001	pET16X containing *csoR* cloned into the *Nco*I and *Bam*HI sites	This study

4.3.2 DNA manipulations

Routine molecular biology procedures were performed according to Sambrook *et al*. [124]. Transformation and specialized SPβ transduction were performed as described by Cutting and Vander Horn [36]. Restriction enzymes, DNA ligase and T4 PNK were all used according to the manufacturer's instructions (New England Biolabs).

4.3.3 Strain construction

Null mutants were generated by allelic replacement via a modified long flanking homology PCR protocol [51, 145]. The resulting PCR products were purified and introduced by transformation into *B. subtilis* wild-type strain CU1065 or appropriate mutant strain with appropriate antibiotic selection. Mutants generated in this study are listed in Table 4.1.

4.3.4 β-Galactosidase assay

The P_{copZA}-*cat*-*lacZ* operon fusion, carried on the SPβ prophage, was introduced by specialized transduction. Overnight cultures were diluted 1:100 in LB liquid medium with or without 0.5 mM $CuSO_4$ and grown to mid-exponential phase. Cells were collected and the expression of β-galactosidase was measured (modified from [103]).

4.3.5 Purification of CsoR

The *yvgZ* (*csoR*) gene was PCR amplified and inserted into the *Nco*I and the *Bam*HI sites of the overexpression vector pET16b (Novagen). This was then introduced into *E. coli* DH5α by transformation. The sequence of the resulting plasmid (pGS001) was verified by DNA sequencing (Cornell Life Sciences Core Laboratories Center) and was introduced into *E. coli* BL21 (DE3)(pLysS). A single colony was grown overnight in 5 mL LB containing ampicillin (100 μg/mL). The overnight culture was used to inoculate 1 L of LB containing ampicillin (100 μg/mL). Cells were incubated with vigorous shaking until an OD_{600} of 0.4 (Spectronic 21) was reached, at which point IPTG was added to a final concentration of 4 mM, and the cells were allowed to grow an additional 2 h. Cells were recovered by centrifugation, resuspended in buffer A (20 mM Tris/HCl (pH 8.0), 100 mM NaCl, 1 mM EDTA, 1 mM DTT, 5%, v/v, glycerol), and sonicated. The extract was clarified by centrifugation and then purified by sequential application to heparin-Sepharose, mono-Q ion-exchange and Superdex-200 size exclusion columns. Purified protein was stored in Buffer A at -80°C for later use. CsoR purity was determined to be ≥95% by SDS-PAGE with Coomassie staining. YhdQ had been purified during previous studies [51].

4.3.6 Electrophoretic mobility shift assays (EMSAs)

PCR fragments containing the *copZA* promoter (246 bp) and the control non-specific *yoeB* promoter (106 bp) were amplified and labeled with T4 polynucleotide kinase (PNK) and [γ-^{32}P]ATP. EMSA reactions were carried out in 10 μL EMSA buffer (20 mM Tris/HCl (pH 8.0), 50 μg/mL BSA, 50 mM NaCl, 1

mM DTT, 5 μg/mL salmon sperm DNA, 5%, v/v, glycerol). Increasing concentrations of CsoR and YhdQ were incubated for 10 min at room temperature with the labeled promoters in both the presence and absence of 10 μM $CuSO_4$ (as indicated). DTT was added to the reaction to reduce Cu^{2+} to Cu^{1+} [14]. The *copZA* promoter was digested with *Bts*I and the control non-specific *ytiA* promoter with *Eco*RI where indicated. All samples were loaded onto a 6% polyacrylamide gel and electrophoresed for 1 h at 90 V in 45 mM Tris/borate buffer (without EDTA), pH 8.0. The gel was dried and imaged on a Storm 840 PhosphorImager scanner (Molecular Dynamics) after overnight exposure of a PhosphorImager screen.

4.3.7 DNase I footprinting

Oligonucleotide primers labeled with T4 PNK and [γ-^{32}P]ATP were used to generate a 246 bp P_{copZA} fragment. PCR with the labeled forward or reverse primer (and a second, unlabeled primer) was used to generate labeled fragments. Footprinting was carried out in 50 μL EMSA buffer. CsoR was added in increasing amounts to the top- or bottom-strand end-labeled PCR product and incubated at room temperature for 20 min. After this binding incubation, 53 μL DNase I reaction mixture (0.06 units/μL DNase I, 5 mM $CaCl_2$, 10 mM $MgCl_2$) was added to digest the labeled DNA. Digestion was performed at room temperature for 2 min and stopped by precipitation of the DNA with 645 μL -20°C absolute ethanol, 50 μL 3 M sodium acetate and 5 μL 1 mg/mL yeast carrier RNA at -20°C for 20 min. DNA was collected by centrifugation, washed with cold 70% ethanol, and the dried pellets were dissolved in 7.5 μL formamide loading buffer. Samples were incubated at 90°C for 3 min before loading. The G+A lad-

der was generated by adding 1 μL labeled promoter to 3 μL formamide loading buffer with 1% formic acid added; the reaction was incubated at 90°C for 20 min. Then 3 μL G+A ladder and 7.5 μL of the DNase I footprinting reactions were loaded onto a 6% polyacrylamide sequencing gel with 6 M urea pre-run in 0.5× TBE electrophoresis buffer at 1500 V for 40 min. The gel was run for 1 h at 1500 V, dried, and imaged on a Storm 840 PhosphorImager scanner (Molecular Dynamics) after overnight exposure of a PhosphorImager screen.

4.4 Results and Discussion

4.4.1 CsoR negatively regulates the *copZA* operon

The *copZA* operon is situated downstream of a candidate σ^A promoter sequence with an overlapping GC-rich pseudo-inverted repeat (Fig. 4.1). As noted previously, P_{copZA} has features similar to promoters regulated by MerR family transcription factors, including a longer than average spacer sequence and an inverted repeat element in the spacer region similar to known MerR-binding sites. These observations led us to investigate the role of MerR like proteins as candidate regulators for *copZA*. Previously, we reported that a disruption of *yhdQ* resulted in reduced expression levels of a P_{copZA} reporter fusion relative to levels in a wild-type background. Together with biochemical studies that demonstrated binding of YhdQ to P_{copZA} we concluded that this protein mediated copper induction of *copZA* and we proposed to rename *yhdQ* as *cueR* [51]. This assignment was supported by the limited similarity (17% identity) between *B. subtilis* YhdQ and *E. coli* CueR [113, 135]. However, we demonstrate here that *yhdQ*

is not involved in the copper-dependent regulation of copper efflux functions, and we will henceforth refer to this gene as *yhdQ* (as presently annotated in the SubtiList database; [107]) rather than *cueR*.

In the course of follow-up studies to determine the structural features of YhdQ required for copper sensing, we were unable to reproduce the previously observed defects in induction of the P_{copZA} reporter fusion in strains lacking YhdQ. Analysis of the original strains revealed an error in strain construction: in the course of introducing reporter fusions by phage transduction, the wrong promoter fusion had been introduced into the *yhdQ* null background. In our newly constructed strains, a *yhdQ* null mutation did not affect copper inducibility of P_{copZA} (Fig. 4.2A).

Concurrent with this discovery, a report appeared describing a new family of copper-sensing regulatory proteins designated CsoR [88]. The prototype for this family of metalloregulatory proteins is the *M. tuberculosis* CsoR protein, which functions as a Cu^{1+}-selective repressor protein and regulates expression of copper efflux systems. Giedroc and colleagues noted that apparent CsoR orthologs are present in many bacteria and they speculated that these might also play a role in regulating copper homeostasis [88]. The predicted CsoR ortholog in *B. subtilis* is encoded by the *yvgZ* gene, which is located immediately upstream of the *copZA* operon (Fig. 4.1). YvgZ of *B. subtilis* shares 33% amino acid identity with *M. tuberculosis* CsoR, consistent with a similar functional role. More importantly, the ligand-coordinating residues shown to be essential for copper-sensing in *M. tuberculosis* CsoR are strictly conserved in *B. subtilis* (C45, H70 and C74). Other conserved residues include Y44 and E90, which have been implicated in the allosteric modulation of the DNA binding

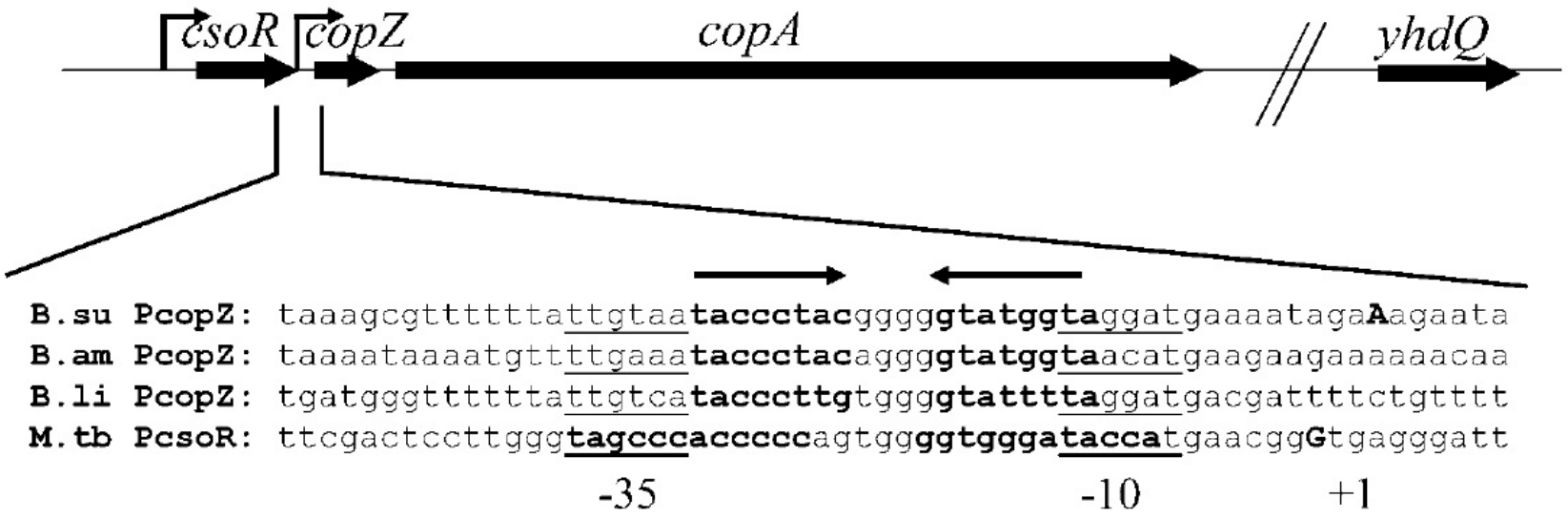

Figure 4.1: Schematic representation of the *csoR-copZA* locus. *csoR* (*yvgZ*) is located immediately upstream of the *copZA* operon and is transcribed from its own promoter. The *yhdQ* (*cueR*) gene is distant from the *copZA* operon. The promoter region between *csoR* and *copZ* has been expanded to illustrate the sequence alignment of *B. subtilis* (B.su), *B. amyloliquefaciens* (B.am), *B. licheniformis* (B.li), and *M. tuberculosis* (M.tb). Conserved -35 and -10 promoter elements are underlined. Bold letters represent the conserved GC-rich pseudo-inverted repeat. The identified +1 sites of transcription [52, 88] are designated by capital letters.

domain in response to bound copper [88]. Previous studies had demonstrated that *yvgZ* is not co-transcribed with *copZA*, nor is it copper regulated [52]. We demonstrate that *yvgZ* is required for the copper-dependent regulation of the *copZA* efflux operon. Hence, we rename this gene *csoR*, to be consistent with the *M. tuberculosis* nomenclature [88].

To determine whether CsoR regulates the *copZA* operon and to investigate the role of YhdQ, a series of allelic replacement mutations were constructed (Table 4.1) and tested for their effect on copper induction of a P_{copZA}-*cat*-*lacZ* promoter fusion (Fig. 4.2A). In the *csoR* null mutant the *copZA* promoter was expressed constitutively (Fig. 4.2A). Complementation of the mutant strain with an ectopically integrated copy of the *csoR* gene restored wild-type regulation. These results suggest that CsoR functions as a repressor for P_{copZA}. In contrast, induction of P_{copZA} upon exposure to copper was unaffected in a *yhdQ* null mutant. Since YhdQ had been previously shown to bind the *copZA* regulatory region [51], we considered the possibility that both proteins might exert a regulatory influence over *copZA* expression. However, the *csoR yhdQ* double mutant was indistinguishable from the *csoR* single mutant (Fig. 4.2A).

Since a *csoR* null mutant expresses copper efflux functions constitutively, we hypothesized that this strain should have a higher tolerance for copper shock. This expectation is supported by the observation that the null mutant has a slightly enhanced ability to grow relative to wild-type when diluted into medium containing high levels of copper (Fig. 4.2B); this is most apparent at concentrations between 5 and 6 mM copper. This effect is rather subtle, consistent with the fact that the *copZA* operon is probably induced even in the wild-type strain under these conditions. In contrast, a *copA* null mutant is unable to

grow in medium containing 2 mM copper [52].

4.4.2 CsoR specifically binds P_{copZA} in the absence, but not the presence, of copper ions

EMSA was used to determine if CsoR is acting as a copper sensing repressor. CsoR bound with high affinity (Kd ≈ 50 nM) to P_{copZA}, but not to the non-specific control fragment (*yoeB*), and this binding was eliminated in the presence of 10 μM $CuSO_4$ and 1 mM DTT (Fig. 4.3A). Under these conditions, DTT is known to reduce Cu^{2+} to Cu^{1+} [14], the presumed inducer by analogy with *M. tuberculosis* CsoR [88]. In parallel EMSA reactions with YhdQ, significant binding was detected to P_{copZA}, as previously reported [51]. Moreover, this binding appeared to be of higher affinity than that for the non-specific control fragment (*yoeB*), suggesting that there is some specificity for the *copZA* promoter DNA fragment. However, the formation of several different mobility complexes (Fig. 4.3B) suggests that there may be multiple YhdQ oligomers bound to this DNA fragment. To further investigate the DNA-binding properties of YhdQ, EMSAs were conducted with two additional control DNA fragments: the *copZA* promoter region digested with *Bts*I (to generate two fragments, one of which lacks the proposed specific binding site) and the non copper-regulated *ytiA* promoter digested with *Eco*RI. Both fragments produced a ladder of shifted complexes (Fig. 4.3C). Taken together, these results suggest that YhdQ binds to DNA in a relatively non-specific manner while CsoR binds specifically to the P_{copZA} region with high affinity.

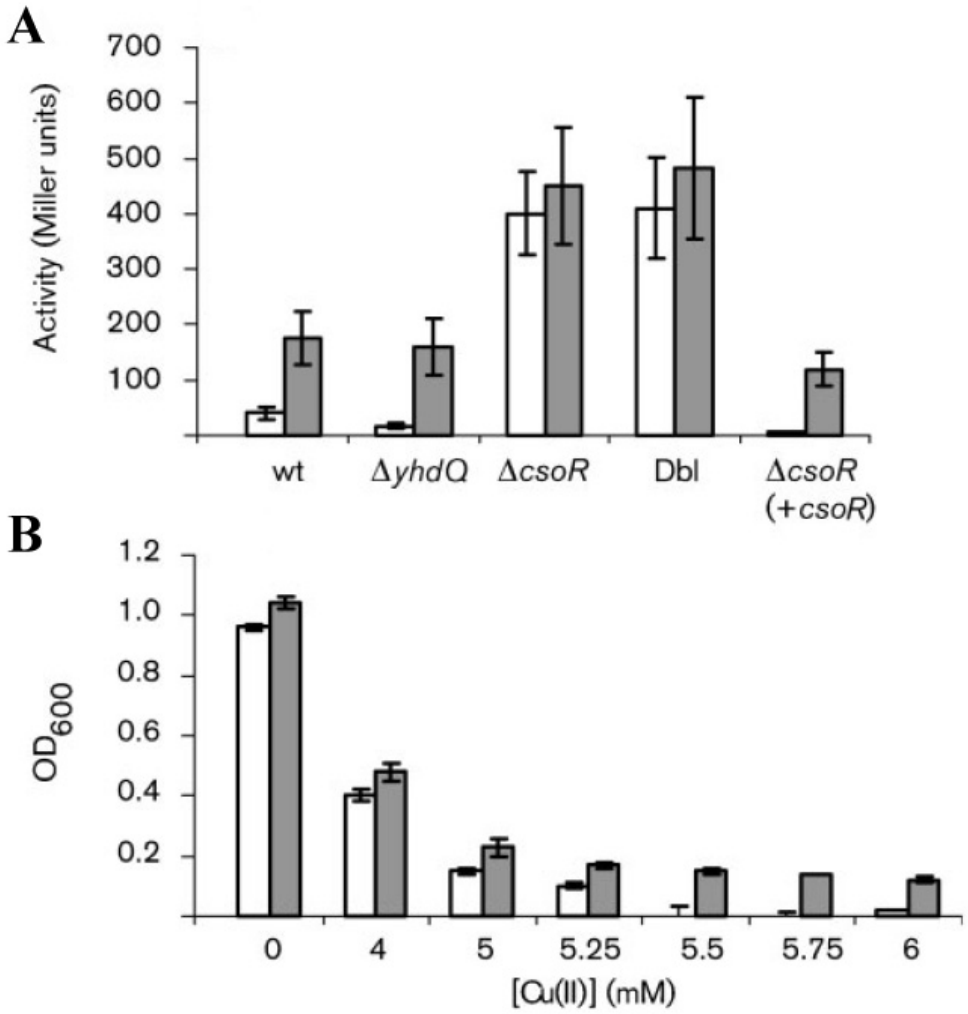

Figure 4.2: Expression of P_{copZA} is affected in a *csoR* null background. **A**. Expression of P_{copZA}-*cat-lacZ* promoter fusion in different null backgrounds with (grey bars) and without (white bars) $CuSO_4$ added to a final concentration of 0.5 mM was measured using β-galactosidase assays. Dbl, Δ*csoR* Δ*yhdQ* double mutant; Δ*csoR* (+*csoR*), *csoR* null mutant complemented ectopically with *csoR*. Results presented are the means ± SD of three experiments where the total n=7. **B**. Growth yield for wild-type (CU1065; white bars) and its isogenic *csoR* null mutant (grey bars) after overnight growth in medium either lacking (0) or supplemented with $CuSO_4$ at the indicated concentration.

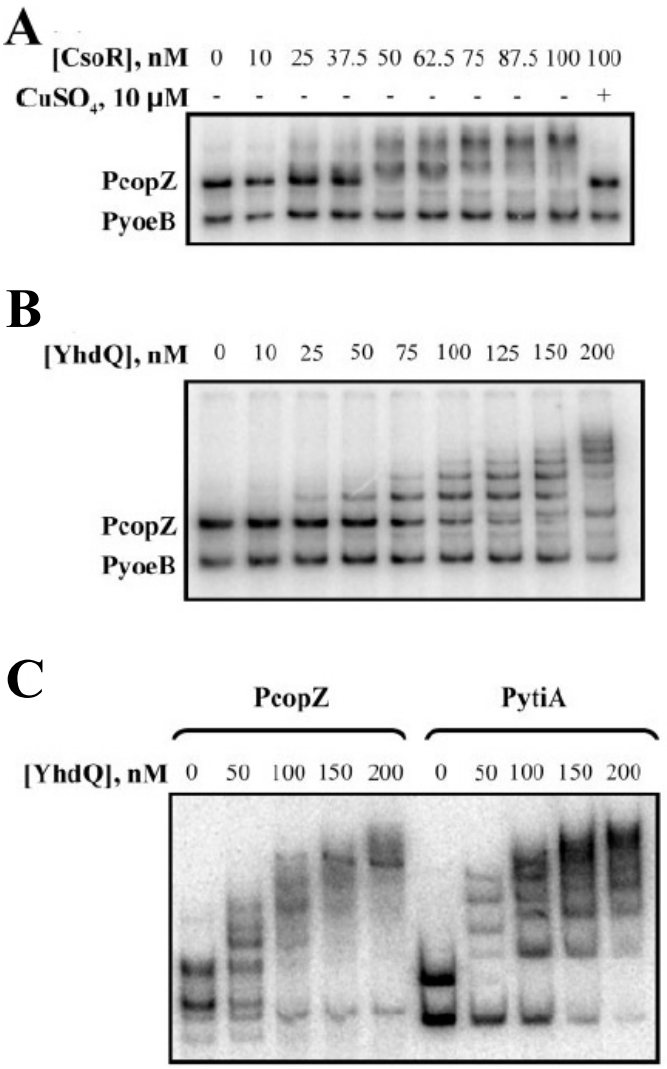

Figure 4.3: CsoR and YhdQ electromobility shift assays. **A**. CsoR EMSA was carried out with increasing amounts of protein and a constant amount of both specific *copZA* promoter and non-specific *yoeB* promoter; 10 μM $CuSO_4$ in the presence of 1 mM DTT was added to the last lane to test the effects of copper on DNA-binding activity. **B**. YhdQ EMSA with increasing amounts of protein and a constant amount of both specific *copZA* promoter and non-specific copper uninduced *yoeB* promoter. **C**. YhdQ EMSA carried out with both specific *copZA* promoter and non-specific *ytiA* promoter. Both promoters were digested with either *Bts*I or *Eco*RI to generate a promoter specific fragment (upper band in 0 lane) and a non-specific fragment (lower band in 0 lane).

4.4.3 CsoR binds to an inverted repeat overlapping the promoter of *copZA*

Using DNase I footprinting, CsoR was found to protect a 25 nt region of the top strand, overlapping the *copZA* promoter. In agreement with the EMSA experiments, the protection of the promoter region is lifted once copper is supplied to the reaction (Fig. 4.4). This result is consistent with the role of CsoR as a repressor. Furthermore, CsoR protects the same general DNA region on the bottom strand over the same range of protein concentrations (data not shown). It is interesting to note that this operator region in *B. subtilis* and its close relatives shares similarity with the *M. tuberculosis csoR* binding site (Fig. 4.1). This GC-rich pseudo-inverted repeat probably mediates CsoR binding and regulation.

4.5 Concluding Remarks

In this study, we have identified the regulator of the *copZA* operon as CsoR (formerly YvgZ). We had previously assigned this role to YhdQ (CueR), a MerR homolog, proposed to function as an activator of copper efflux [51]. This assignment was supported by the observed binding of YhdQ to the *copZA* regulatory region, the loss of P_{copZA} induction in a strain carrying a *yhdQ* mutation, and weak similarity in protein sequence (17% identity) between *B. subtilis* YhdQ and the CueR regulator of copper efflux gene expression in *E. coli*. However, due to an error in strain construction, the previous genetic experiments were incorrect and we now report that there is no effect on copper-dependent regulation at the *copZA* promoter in a *yhdQ* mutant strain. Consistent with our previous find-

ings [51], YhdQ does bind with high affinity to the *copZA* promoter region, but it also binds to several other promoter regions, suggesting that this binding is relatively non-specific and unlikely to be physiologically relevant. Our current results support a model for CsoR as the sole repressor of the *copZA* operon in *B. subtilis* that is responsible for the previously characterized, copper-specific induction of this efflux system [52].

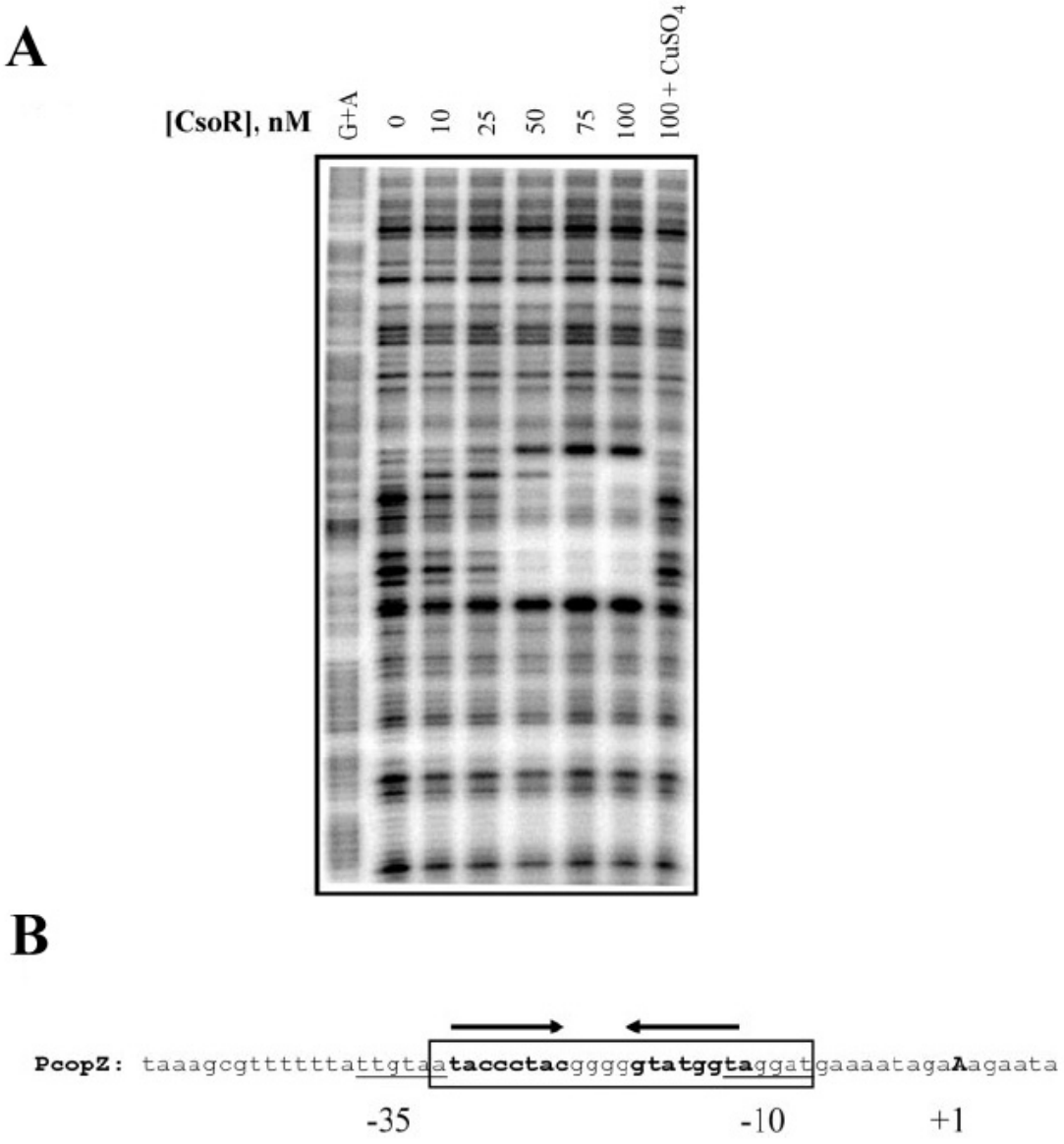

Figure 4.4: The CsoR-binding site overlaps the *copZA* promoter. **A**. DNase I footprinting of the top stand of P_{copZA} with increasing amounts of CsoR. The last lane contains 10 μM $CuSO_4$ in the presence of 1 mM DTT. The G+A ladder was run as a standard; it was calibrated to a dideoxy chain-termination sequencing reaction (data not shown). **B**. Schematic of the *B. subtilis copZA* promoter. The -10 and -35 elements are underlined, the GC-rich pseudo-inverted repeat is in bold, and the protected region as determined by the DNase I footprinting is boxed.

APPENDIX A

DNAX TRANSLATION IS NOT AFFECTED BY FSRA EXPRESSION

A.1 Summary

Initial bioinfomatic and biochemical results indicated a possible role of the sRNA FsrA and the iron-sparing response in the regulation of the production of both γ- and τ-like proteins from the *dnaX* transcript. The line of experimentation described below was carried out to independently confirm the initial results that FsrA was regulating the production of both protein species in an iron inducible manner. These results do not support the initial hypothesis and show no production of the γ-like protein from epitope tagged DnaX constructs.

A.2 Introduction

In *Escherichia coli* and other bacteria, the *dnaX* gene codes for two ATPases which act as "clamp loading" proteins for the β-sliding clamp processivity factor [100]. The γ and the longer τ protein perform unique functions in the DnaX complex important for the tethering of the leading and lagging strand complexes. γ acts as the active subunit in "clamp loading" while τ (with its two additional domains) facilitates the interactions between itself and the helicase present at the replication fork as well as between itself and the α subunit of DNA polymerase III [100]. These interactions ensure the coupling of leading and lagging strand replication.

The γ subunit is encoded by an alternate reading frame that is facilitated by a

translational frameshifting event that leads to premature termination of the full length *dnaX* gene product [48, 100]. The ribosome was discovered to shift to the -1 reading frame when it encountered an oligo(A) region preceded by a stable stemloop secondary structure. The slip into the -1 frame causes the ribosome to encounter a stop codon after the incorporation of an additional amino acid. This programmed frameshift occurs with an efficiency of 40%, leading to the production of the γ subunit [48].

While this particular mechanism described in *E. coli* is highly conserved, it is not the only way possible for generating γ. For example in *Thermus thermophilus*, γ is generated by transcriptional slippage [100]. In *Bacillus* species, the expression of γ has yet to be observed and there has been no obvious mechanism described for its generation. This has lead to the proposal that *Bacillus* may in fact lack γ altogether [17].

The observation that the iron regulated sRNA FsrA could anneal to a region of the *dnaX* transcript about two thirds of the way through the open reading frame raised an interesting hypothesis: FsrA may generate an sRNA:mRNA duplex leading to a translational frameshifting event. This could lead to the production of both the full length τ and the truncated γ subunits. This hypothesis was supported by two studies which independently described a ribosomal frameshifting event in response to sRNA expression [71, 111]. Both studies observed *in vitro* frameshifting dependent upon the anneling and secondary structure formation between the sRNA at an internal binding site of an ORF residing on the target mRNA. Other factors including ”shift prone” sites (particularly poly(A) and poly(U)) on the mRNA just upstream of the binding site also enhanced the rate of translational slippage [71, 111].

While this hypothesis was initially attractive, the results described below not only disagree with the proposed model, they also demonstrate that only the τ subunit is produced from the *dnaX* transcript.

A.3 Materials and Methods

A.3.1 Bacterial strains, media, and growth conditions

Bacterial strains used in this study are listed in Table A.1. *Escherichia coli* DH5α was used for routine DNA cloning [124]. *B. subtilis* CU1065 strains were constructed by using long-flanking homology PCR [21]. Spectinomycin (100 μg/mL), kanamycin (10 μg/mL), and chloramphenicol (5 μg/mL) were used for the selection of the various *B. subtilis* strains unless otherwise indicated. Liquid media were inoculated at 1:100 dilutions from overnight pre-culture and incubated at 37°C with shaking at 225 rpm. Growth media used in this study include LB medium and modified competence medium (MC).

A.3.2 DNA manipulations

Routine molecular biology procedures were performed as previously described [124]. Isolation of *B. subtilis* chromosomal DNA and transformation were carried out as previously described [36]. Restriction enzymes, DNA ligase, and DNA polymerases were all used according to manufacturer's instructions (New England Biolabs). The IPTG inducible N-terminal FLAG tagged DnaX construct was generated from two sequential rounds of PCR and inserted into the pPL82

Table A.1: Bacterial strains and plasmids used in DNAX TRANSLATION IS NOT AFFECTED BY FSRA EXPRESSION

Strain or plasmid	Relevant Characteristic(s)	Source or reference
***B. subtilis* strains**		
CU1065	W168 *att* SPβ *trpC2* ("Wild Type")	[142]
HB2501	CU1065 *fur::kan*	[10]
HB12517	CU1065 *fur::kan fsrA::spc*	This study
HB12591	CU1065 *amyE::*FLAG-*dnaX*	This study
HB12592	CU1065 *fur::kan amyE::*FLAG-*dnaX*	This study
HB12593	CU1065 *fur::kan fsrA::spc amyE::*FLAG-*dnaX*	This study
***E. coli* strains**		
DH5α	ϕ Δ(*lacZ*)M15 Δ(*argF-lac*)U169 *endA1 recA1 hsdR17* (r_K^- m_K^+)*deoR thi-1 supE44 gyrA96 relA1*	[124]
Plasmids		
pPL82	IPTG inducible integration vector into *amyE* locus	[119]

vector. The first round of PCR generated two fragments; the first was made with forward primer 5'TTGCCTGGGCCGAGCTAAC3' (5326) and reverse primer 5'TTTATCATCATCATCTTTATAATCCACGGGTTTGCCCTCCTC3' (5327). This added a FLAG epitope tag just after the *dnaX* start codon. Fragment two was made with forward primer 5'GATTATAAAGATGATGATGATAAAAGTTACCA AGCTTAATATCGAG3' (5328) and reverse primer 5'GCGCGCATGCTCACTCT CTTTCATTTTGTTAG3' (5329). The second round of PCR joined the two fragments from the first round (via the complementary FLAG epitope sequence added by primers 5327 and 5328) and also added an *Xma*I and a *Sph*I to the 5' and 3' ends of the joined fragment, respectively. The joining PCR reaction was carried out using forward primer 5'GCGCCCCGGGGAGGAGGGCAAACCCGTG3' (5330) and reverse primer 5329. The resulting fragment was cloned into vector pPL82, transformed into *E.coli* DH5α, amplified, purified, and digested with *Sca*I (8). Transformation into *B. subtilis* was carried out and integration occurred at the *amyE* locus. The sequences for all mutant constructs were verified by DNA sequencing (Cornell Life Sciences Core Laboratories Center).

A.3.3 Western blot analysis

50 mL cultures were inoculated from overnight LB broth starter cultures and grown to mid-log ($OD_{600} \approx 0.3$ - 0.35; Spectronic 21) in LB broth with and without 0.1 mM IPTG. Cells were recovered by centrifugation at 5000 rpm for 5 min in an Eppendorf 5804R swinging bucket rotor centrifuge. Cells were frozen overnight at -20°C, thawed, and resuspended in TBS (0.5 mL 50 mM Tris/HCl (pH 7.4), 150 mM NaCl, 1 mM EDTA, 1 mM DTT, and 0.1 mM PMSF). Cells

were then sonicated for 3× 8 s bursts with at least one min on ice between each burst. Crude extract was clarified by centrifugation at 14,000 rpm at 4°C. A bradford assay was used to quantify total protein within the crude extract and 25 μg of total protein was used for 8% SDS-PAGE. Protein levels were detected after membrane transfer and western blot analysis using commercially obtained anti-FLAG primary antibodies (Sigma Cat. F7425).

A.3.4 FLAG agarose pull-down

FLAG agarose beads were prepared as per the manufacture's protocol (Sigma Cat. A2220). The initial 200 μL aliquot of FLAG agarose beads yielded 20 μL bead resin, after preparation, the resin was suspended in 100 μL TBS. 250 μL of the crude extracts were added to 750 μL TBS, to which 40 μL of the diluted resin was added. The binding reaction was allowed to incubate overnight at 4°C with rotation. All resin was recovered by centrifugation at 1000 rpm for 5 min at 4°C and was subsequently washed 3× 500 μL TBS. The resin was suspended in a total volume of 50 μL SDS-PAGE loading dye without reducing agent. All samples were incubated at 95°C for 7 min. 8% SDS-PAGE was carried out on 5 μL of each supernatant and 5 μL of each resin sample. Western blot analysis was subsequently carried out as described above.

A.4 Results and Discussion

A.4.1 Initial observations suggest FsrA alters DnaX translation

Both BlastN and TargetRNA were used to explore the possible interaction between the FsrA sRNA and the *dnaX* mRNA [139]. One of the strongest regions of complementarity with FsrA predicted by both methods corresponds to the precise region postulated to be involved in a frameshiting event (Fig. A.1A). This finding suggests an interesting hypothesis: FsrA may generate an RNA duplex with the *dnaX* transcript leading to the pausing of the ribosome during translation. This would allow time for a frameshifting event leading to the production of both γ and τ. To determine if *B. subtilis* γ and τ are in fact generated in response to the expression of FsrA, Prof. Sang Soo Lee, a visiting scholar to the lab, generated an N-terminal FLAG tagged *dnaX* allele and integrated a single copy into the chromosome at an ectopic locus. Western blot analysis for the FLAG epitope tag identified two protein species of the approximate sizes expected for γ and τ (Fig. A.1B). Moreover, the production of the smaller protein (corresponding to γ) was increased in the *fur* mutant, but not in the *fur fsrA* double mutant background. This is consistent with a process stimulated by FsrA and provides the first evidence that *B. subtilis* produces a γ-like protein.

A.

```
FsrA sRNA
3     AGAGAGAAGCUACUCUCUGUUCCCCAACCCCU-CU-AUCAGAUCAAGAUCCG  52
      || :|||||||       ||  |||||||   | || | ||||||||||||||
1338 UCGUUCUUCGA------AC--GGGGUUGACAAAGACUCGUCUAGUUCUAGGC  1295
mRNA (dnaX)
```

B.

Figure A.1: Inital experiment suggests FsrA binding leads to γ production. **A**. Postulated mechanism for the production of τ and γ proteins from the *dnaX* gene in *B. subtilis*. **B**. Western blot of *B. subtilis* DnaX using anti-FLAG primary antibody. Blot carried out in (1) Wild Type, (2) *fur fsrA*, and (3) *fur* genetic backgrounds. This is an unpublished figure courtesy of Dr. Sang Soo Lee and Dr. John D. Helmann.

A.4.2 IPTG inducible N-terminal FLAG tagged DnaX shows no change in response to FsrA

In order to replicate these initial results, a second independent approach was taken to express FLAG-DnaX under an inducible promoter and observe the effect FsrA had on translation. To do this, a FLAG epitope tag was appended via a joining PCR to the N-terminus of the *dnaX* open reading frame and amplified to include its native ribosome binding site. This construct was cloned into pPL82 under the control of the P_{spac} promoter (Fig. A.2A). Crude extracts were collected from actively growing WT, *fur*, and *fur fsrA* strains harboring the N-terminal FLAG-DnaX construct with and without 0.1 mM IPTG. Western blot analysis was carried out and exhibited a single inducible band corresponding to the expected size of the τ-like protein (Fig. A.2B). No inducible band corresponding to the expected size for the γ protein was observed, although there were non-specific bands corresponding to cross reacting material in the expected γ size range.

A.4.3 The γ-like protein cannot be detected by means of FLAG agarose pull-down

In order to ascertain whether any γ-like protein was present in the samples but was being obscured by non-specific proteins, FLAG-agarose linked beads were used to bind and pull down the epitope tagged DnaX translation products. FLAG-agarose beads were added to aliquots of the WT, *fur*, and *fur fsrA* crude extracts to bind the FLAG-DnaX translation products. The beads were

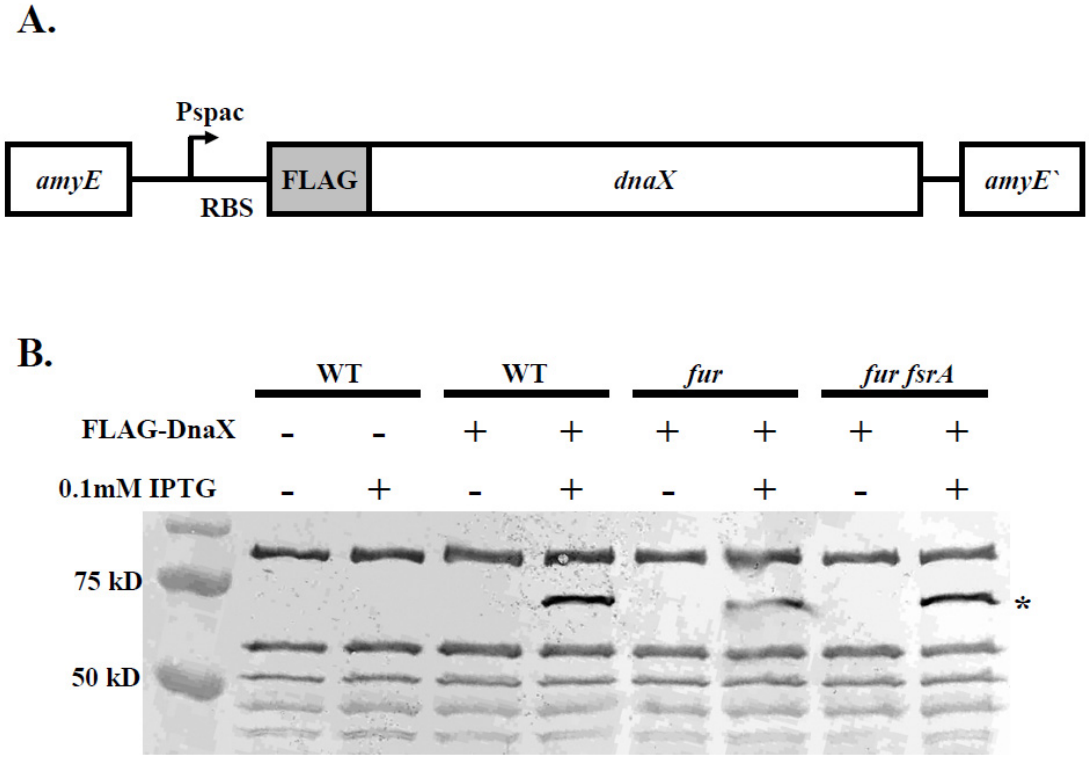

Figure A.2: N-terminal FLAG epitope detection of DnaX. **A**. Illustration of the N-terminal FLAG-DnaX construct integrated at the *B. subtilis* ectopic locus *amyE*. **B**. Western blot of *B. subtilis* pPL82 FLAG-DnaX construct using anti-FLAG primary antibody. The band corresponding to the expected size of the FLAG-DnaX τ product is indicated by the asterisk (*). Cross reacting material used as loading control.

washed and elution was carried out by boiling the beads in SDS-PAGE sample loading buffer without reducing agent. Western analysis of the pull-down exhibited only one strong band corresponding in size to the τ-like protein in both the elutant and bound to the beads indicating the production of only one species of the DnaX protein (Fig. A.3).

A.5 Concluding Remarks

In addition to the experiments presented here, two additional constructs have been generated by Jason Lo (an undergraduate under my supervision), including a C-terminal FLAG epitope tagged construct and an N-terminal HA epitope tagged construct which were tested in the same iron-sparing response mutant backgrounds (data not shown). All three independent attempts to replicate the experimental results of Dr. Lee failed to demonstrate the production of the γ-like protein.

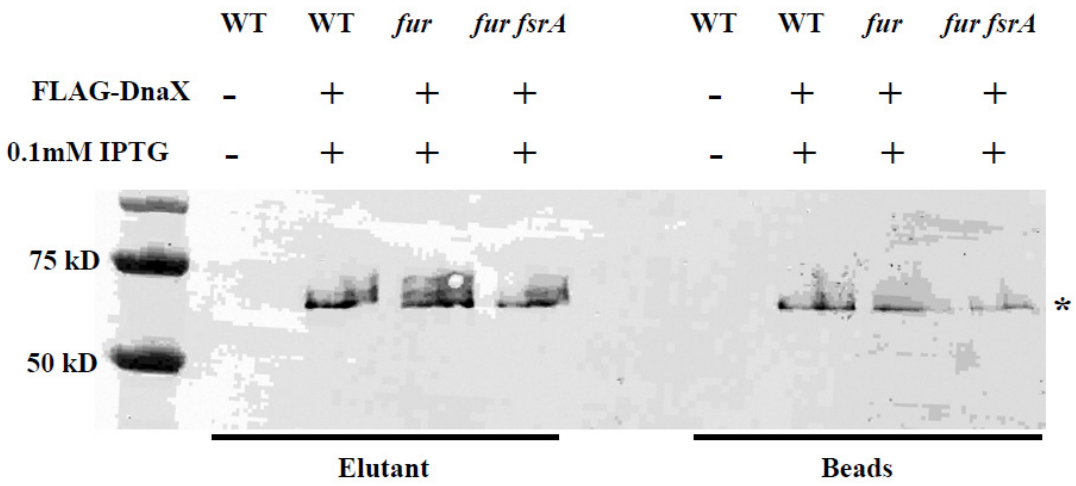

Figure A.3: FLAG agarose pull-down of FLAG-DnaX products. Western blot of *B. subtilis* pPL82 FLAG-DnaX construct using anti-FLAG primary antibody after pulldown with FLAG agarose. The band corresponding to the expected size of the FLAG-DnaX τ product is indicated by the asterisk (*).

BIBLIOGRAPHY

[1] H. Abdul-Tehrani, A. J. Hudson, Y. S. Chang, A. R. Timms, C. Hawkins, J. M. Williams, P. M. Harrison, J. R. Guest, and S. C. Andrews. Ferritin mutants of *Escherichia coli* are iron deficient and growth impaired, and *fur* mutants are iron deficient. *J Bacteriol*, 181:1415–28, 1999.

[2] L. A. Abriata, L. Banci, I. Bertini, S. Ciofi-Baffoni, P. Gkazonis, G. A. Spyroulias, A. J. Vila, and S. Wang. Mechanism of Cu(A) assembly. *Nat Chem Biol*, 4:599–601, 2008.

[3] H. Aiba. Mechanism of RNA silencing by Hfq-binding small RNAs. *Curr Opin Microbiol*, 10:134–9, 2007.

[4] C. Andreini, L. Banci, I. Bertini, and A. Rosato. Zinc through the three domains of life. *J Proteome Res*, 5:3173–8, 2006.

[5] S. C. Andrews, A. K. Robinson, and F. Rodriguez-Quinones. Bacterial iron homeostasis. *FEMS Microbiol Rev*, 27:215–37, 2003.

[6] L. Argaman, R. Hershberg, J. Vogel, G. Bejerano, E. G. Wagner, H. Margalit, and S. Altuvia. Novel small RNA-encoding genes in the intergenic regions of *Escherichia coli*. *Curr Biol*, 11:941–50, 2001.

[7] F. Arnesano, L. Banci, I. Bertini, S. Mangani, and A. R. Thompsett. A redox switch in CopC: an intriguing copper trafficking protein that binds copper(I) and copper(II) at different sites. *Proc Natl Acad Sci U S A*, 100:3814–9, 2003.

[8] A. Bagg and J. B. Neilands. Ferric uptake regulation protein acts as a repressor, employing iron(II) as a cofactor to bind the operator of an iron transport operon in *Escherichia coli*. *Biochemistry*, 26:5471–7, 1987.

[9] N. Baichoo and J. D. Helmann. Recognition of DNA by Fur: a reinterpretation of the Fur box consensus sequence. *J Bacteriol*, 184:5826–32, 2002.

[10] N. Baichoo, T. Wang, R. Ye, and J. D. Helmann. Global analysis of the *Bacillus subtilis* Fur regulon and the iron starvation stimulon. *Mol Microbiol*, 45:1613–29, 2002.

[11] E. Balatri, L. Banci, I. Bertini, F. Cantini, and S. Ciofi-Baffoni. Solution

structure of Sco1: a thioredoxin-like protein involved in cytochrome c oxidase assembly. *Structure*, 11:1313–4, 2003.

[12] L. Banci, I. Bertini, G. Cavallaro, and A. Rosato. The functions of Sco proteins from genome-based analysis. *J Proteome Res*, 6:1568–79, 2007.

[13] L. Banci, I. Bertini, S. Ciofi-Baffoni, L. Gonnelli, and X. C. Su. Structural basis for the function of the N-terminal domain of the ATPase CopA from *Bacillus subtilis*. *J Biol Chem*, 278:50506–13, 2003.

[14] L. Banci, I. Bertini, R. Del Conte, J. Markey, and F. J. Ruiz-Duenas. Copper trafficking: the solution structure of *Bacillus subtilis* CopZ. *Biochemistry*, 40:15660–8, 2001.

[15] A. P. Bhavsar, X. Zhao, and E. D. Brown. Development and characterization of a xylose-dependent system for expression of cloned genes in *Bacillus subtilis*: conditional complementation of a teichoic acid mutant. *Appl Environ Microbiol*, 67:403–10, 2001.

[16] R. G. Brennan and T. M. Link. Hfq structure, function, and ligand binding. *Curr Opin Microbiol*, 10:125–33, 2007.

[17] I. Bruck and M. O'Donnell. The DNA replication machine of a gram-positive organism. *J Biol Chem*, 275:28971–83, 2000.

[18] A. Brush and H. Paulus. The enzymic formation of O-acetylhomoserine in *Bacillus subtilis* and its regulation by methionine and S-adenosylmethionine. *Biochem Biophys Res Commun*, 45:735–41, 1971.

[19] N. Bsat, L. Chen, and J. D. Helmann. Mutation of the *Bacillus subtilis* alkyl hydroperoxide reductase (*ahpCF*) operon reveals compensatory interactions among hydrogen peroxide stress genes. *J Bacteriol*, 178:6579–86, 1996.

[20] N. Bsat and J. D. Helmann. Interaction of *Bacillus subtilis* Fur (ferric uptake repressor) with the *dhb* operator *in vitro* and *in vivo*. *J Bacteriol*, 181:4299–307, 1999.

[21] B. G. Butcher and J. D. Helmann. Identification of *Bacillus subtilis* sigma-dependent genes that provide intrinsic resistance to antimicrobial compounds produced by *Bacilli*. *Mol Microbiol*, 60:765–82, 2006.

[22] T. A. Carrier and J. D. Keasling. Controlling messenger RNA stability in bacteria: strategies for engineering gene expression. *Biotechnol Prog*, 13:699–708, 1997.

[23] Y. Chai, R. Kolter, and R. Losick. A widely conserved gene cluster required for lactate utilization in *Bacillus subtilis* and its involvement in biofilm formation. *J Bacteriol*, 191:2423–30, 2009.

[24] A. Changela, K. Chen, Y. Xue, J. Holschen, C. E. Outten, T. V. O'Halloran, and A. Mondragon. Molecular basis of metal-ion selectivity and zeptomolar sensitivity by CueR. *Science*, 301:1383–7, 2003.

[25] L. Chen, L. P. James, and J. D. Helmann. Metalloregulation in *Bacillus subtilis*: isolation and characterization of two genes differentially repressed by metal ions. *J Bacteriol*, 175:5428–37, 1993.

[26] S. Chillappagari, M. Miethke, H. Trip, O. P. Kuipers, and M. A. Marahiel. Copper acquisition is mediated by YcnJ and regulated by YcnK and CsoR in *Bacillus subtilis*. *J Bacteriol*, 191:2362–70, 2009.

[27] S. Chillappagari, A. Seubert, H. Trip, O. P. Kuipers, M. A. Marahiel, and M. Miethke. Copper stress affects iron homeostasis by destabilizing iron-sulfur cluster formation in *Bacillus subtilis*. *J Bacteriol*, 192:2512–24, 2010.

[28] C. J. Chou, G. Wisedchaisri, R. R. Monfeli, D. M. Oram, R. K. Holmes, W. G. Hol, and C. Beeson. Functional studies of the *Mycobacterium tuberculosis* iron-dependent regulator. *J Biol Chem*, 279:53554–61, 2004.

[29] F. Chu, D. B. Kearns, S. S. Branda, R. Kolter, and R. Losick. Targets of the master regulator of biofilm formation in *Bacillus subtilis*. *Mol Microbiol*, 59:1216–28, 2006.

[30] F. M. Commichau, K. Gunka, J. J. Landmann, and J. Stulke. Glutamate metabolism in *Bacillus subtilis*: gene expression and enzyme activities evolved to avoid futile cycles and to allow rapid responses to perturbations of the system. *J Bacteriol*, 190:3557–64, 2008.

[31] H. J. Conn. The identity of *Bacillus subtilis*. *J Infect Dis*, 46:341–50, 1930.

[32] D. A. Cooksey. Molecular mechanisms of copper resistance and accumulation in bacteria. *FEMS Microbiol Rev*, 14:381–6, 1994.

[33] D. Corbett, S. Schuler, S. Glenn, P. W. Andrew, J. S. Cavet, and I. S. Roberts. The combined actions of the copper-responsive repressor CsoR and copper-metallochaperone CopZ modulate CopA-mediated copper efflux in the intracellular pathogen *Listeria monocytogenes*. *Mol Microbiol*, 81:457–72, 2011.

[34] P. Cornelis, Q. Wei, S. C. Andrews, and T. Vinckx. Iron homeostasis and management of oxidative stress response in bacteria. *Metallomics*, 3:540–9, 2011.

[35] H. Cruz Ramos, T. Hoffmann, M. Marino, H. Nedjari, E. Presecan-Siedel, O. Dreesen, P. Glaser, and D. Jahn. Fermentative metabolism of *Bacillus subtilis*: physiology and regulation of gene expression. *J Bacteriol*, 182:3072–80, 2000.

[36] S. Cutting and P. B. Vander Horn. *Molecular Biological Methods for Bacillus*. Wiley, 1990.

[37] M. J. de Hoon, S. Imoto, J. Nolan, and S. Miyano. Open source clustering software. *Bioinformatics*, 20:1453–4, 2004.

[38] V. de Lorenzo, F. Giovannini, M. Herrero, and J. B. Neilands. Metal ion regulation of gene expression. Fur repressor-operator interaction at the promoter region of aerobacin system of pColV-K30. *J Mol Biol*, 203:875–84, 1988.

[39] H. Ding and R. J. Clark. Characterization of iron binding in IscA, an ancient iron-sulphur cluster assembly protein. *Biochem J*, 379:433–40, 2004.

[40] H. Ding, R. J. Clark, and B. Ding. IscA mediates iron delivery for assembly of iron-sulfur clusters in IscU under the limited accessible free iron conditions. *J Biol Chem*, 279:37499–504, 2004.

[41] C. L. Dupont, S. Yang, B. Palenik, and P. E. Bourne. Modern proteomes contain putative imprints of ancient shifts in trace metal geochemistry. *Proc Natl Acad Sci U S A*, 103:17822–7, 2006.

[42] O. Dussurget, M. Rodriguez, and I. Smith. An *ideR* mutant of *Mycobacterium smegmatis* has derepressed siderophore production and an altered oxidative-stress response. *Mol Microbiol*, 22:535–44, 1996.

[43] M. B. Eisen, P. T. Spellman, P. O. Brown, and D. Botstein. Cluster analysis

and display of genome-wide expression patterns. *Proc Natl Acad Sci U S A*, 95:14863–8, 1998.

[44] M. Emmerling, M. Dauner, A. Ponti, J. Fiaux, M. Hochuli, T. Szyperski, K. Wuthrich, J. E. Bailey, and U. Sauer. Metabolic flux responses to pyruvate kinase knockout in *Escherichia coli*. *J Bacteriol*, 184:152–64, 2002.

[45] M. J. Faulkner and J. D. Helmann. Peroxide stress elicits adaptive changes in bacterial metal ion homeostasis. *Antioxid Redox Signal*, 15:175–89, 2011.

[46] R. A. Festa, M. B. Jones, S. Butler-Wu, D. Sinsimer, R. Gerads, W. R. Bishai, S. N. Peterson, and K. H. Darwin. A novel copper-responsive regulon in *Mycobacterium tuberculosis*. *Mol Microbiol*, 79:133–48, 2011.

[47] E. Fischer and U. Sauer. Large-scale *in vivo* flux analysis shows rigidity and suboptimal performance of *Bacillus subtilis* metabolism. *Nat Genet*, 37:636–40, 2005.

[48] A. M. Flower and C. S. McHenry. The gamma subunit of DNA polymerase III holoenzyme of *Escherichia coli* is produced by ribosomal frameshifting. *Proc Natl Acad Sci U S A*, 87:3713–7, 1990.

[49] M. Fuangthong and J. D. Helmann. Recognition of DNA by three ferric uptake regulator (Fur) homologs in *Bacillus subtilis*. *J Bacteriol*, 185:6348–57, 2003.

[50] A. Gaballa, H. Antelmann, C. Aguilar, S. K. Khakh, K. B. Song, G. T. Smaldone, and J. D. Helmann. The *Bacillus subtilis* iron-sparing response is mediated by a Fur-regulated small RNA and three small, basic proteins. *Proc Natl Acad Sci U S A*, 105:11927–32, 2008.

[51] A. Gaballa, M. Cao, and J. D. Helmann. Two MerR homologues that affect copper induction of the *Bacillus subtilis copZA* operon. *Microbiology*, 149:3413–21, 2003.

[52] A. Gaballa and J. D. Helmann. *Bacillus subtilis* CPx-type ATPases: Characterization of Cd, Zn, Co, and Cu efflux systems. *Biometals*, 16:497–505, 2003.

[53] T. Geissmann, C. Chevalier, M. J. Cros, S. Boisset, P. Fechter, C. Noirot, J. Schrenzel, P. Francois, F. Vandenesch, C. Gaspin, and P. Romby. A search

for small noncoding RNAs in *Staphylococcus aureus* reveals a conserved sequence motif for regulation. *Nucleic Acids Res*, 37:7239–57, 2009.

[54] S. Gottesman. Stealth regulation: biological circuits with small RNA switches. *Genes Dev*, 16:2829–42, 2002.

[55] G. Grass, M. Otto, B. Fricke, C. J. Haney, C. Rensing, D. H. Nies, and D. Munkelt. FieF (YiiP) from *Escherichia coli* mediates decreased cellular accumulation of iron and relieves iron stress. *Arch Microbiol*, 183:9–18, 2005.

[56] A. M. Guerout-Fleury, N. Frandsen, and P. Stragier. Plasmids for ectopic integration in *Bacillus subtilis*. *Gene*, 180:57–61, 1996.

[57] M. Hansson, L. Rutberg, I. Schroder, and L. Hederstedt. The *Bacillus subtilis* hemAXCDBL gene cluster, which encodes enzymes of the biosynthetic pathway from glutamate to uroporphyrinogen III. *J Bacteriol*, 173:2590–9, 1991.

[58] K. Hantke. Regulation of ferric iron transport in *Escherichia coli* K12: isolation of a constitutive mutant. *Mol Gen Genet*, 182:288–92, 1981.

[59] K. Hantke. Iron and metal regulation in bacteria. *Curr Opin Microbiol*, 4:172–77, 2001.

[60] M. D. Harrison, C. E. Jones, M. Solioz, and C. T. Dameron. Intracellular copper routing: the role of copper chaperones. *Trends Biochem Sci*, 25:29–32, 2000.

[61] C. R. Harwood and A. R. Archibald. *Molecular Biological Methods for Bacillus*. John Wiley & Sons Ltd, 1990.

[62] N. Heidrich, A. Chinali, U. Gerth, and S. Brantl. The small untranslated RNA SR1 from the *Bacillus subtilis* genome is involved in the regulation of arginine catabolism. *Nucleic Acids Res*, 62:520–36, 2006.

[63] N. Heidrich, I. Moll, and S. Brantl. *In vitro* analysis of the interaction between the small RNA SR1 and its primary target ahrC mRNA. *Nucleic Acids Res*, 35:4331–46, 2007.

[64] J. D. Helmann and J. W. Lee. Functional specialization within the Fur family of metalloregulators. *Biometals*, 20:485–99, 2007.

[65] J. D. Helmann, S. Soonsanga, and S. E. Gabriel. *Molecular Microbiology of Heavy Metals*. Springer-Verlag, 2007.

[66] P. J. Hill, A. Cockayne, P. Landers, J. A. Morrissey, C. M. Sims, and P. Williams. SirR, a novel iron-dependent repressor in *Staphylococcus epidermidis*. *Infect Immun*, 66:4123–9, 1998.

[67] E. Himelblau, H. Mira, S. J. Lin, V. C. Culotta, L. Penarrubia, and R. M. Amasino. Identification of a functional homolog of the yeast copper homeostasis gene ATX1 from *Arabidopsis*. *Plant Physiol*, 117:1227–34, 1998.

[68] K. J. Hintze and E. C. Theil. Cellular regulation and molecular interactions of the ferritins. *Cell Mol Life Sci*, 63:591–600, 2006.

[69] S. N. Ho, H. D. Hunt, R. M. Horton, J. K. Pullen, and L. R. Pease. Site-directed mutagenesis by overlap extension using the polymerase chain reaction. *Gene*, 77:51–9, 1989.

[70] R. H. Holm, P. Kennepohl, and E. I. Solomon. Structural and functional aspects of metal sites in biology. *Chem Rev*, 96:2239–314, 1996.

[71] M. T. Howard, R. F. Gesteland, and J. F. Atkins. Efficient stimulation of site-specific ribosome frameshifting by antisense oligonucleotides. *Rna*, 10:1653–61, 2004.

[72] T. Iijima, M. D. Diesterhaft, and E. Freese. Sodium effect of growth on aspartate and genetic analysis of a *Bacillus subtilis* mutant with high aspartase activity. *J Bacteriol*, 129:1440–7, 1977.

[73] J. A. Imlay. How oxygen damages microbes: oxygen tolerance and obligate anaerobiosis. *Adv Microb Physiol*, 46:111–53, 2002.

[74] I. Irnov, C. M. Sharma, J. Vogel, and W. C. Winkler. Identification of regulatory RNAs in *Bacillus subtilis*. *Nucleic Acids Res*, 38:6637–51, 2010.

[75] J. F. Jacques, S. Jang, K. Prévost, G. Desnoyers, M. Desmarais, J. Imlay, and E. Massé. RyhB small RNA modulates the free intracellular iron pool and is essential for normal growth during iron limitation in *Escherichia coli*. *Mol Microbiol*, 62:1181–90, 2006.

[76] X. Jian, E. C. Wasinger, J. V. Lockard, L. X. Chen, and C. He. Highly sen-

sitive and selective gold(I) recognition by a metalloregulator in *Ralstonia metallidurans*. *J Am Chem Soc*, 131:10869–71, 2009.

[77] N. S. Juty, F. Moshiri, M. Merrick, C. Anthony, and S. Hill. The *Klebsiella pneumoniae* cytochrome bd' terminal oxidase complex and its role in microaerobic nitrogen fixation. *Microbiology*, 143 (Pt 8):2673–83, 1997.

[78] M. Kaltwasser, T. Wiegert, and W. Schumann. Construction and application of epitope- and green fluorescent protein-tagging integration vectors for *Bacillus subtilis*. *Appl Environ Microbiol*, 68:2624–8, 2002.

[79] D. B. Kearns, F. Chu, S. S. Branda, R. Kolter, and R. Losick. A master regulator for biofilm formation by *Bacillus subtilis*. *Mol Microbiol*, 55:739–49, 2005.

[80] D.B. Kearns, F. Chu, R. Rudner, and R. Losick. Genes governing swarming in *Bacillus subtilis* and evidence for a phase variation mechanism controlling surface motility. *Mol Microbiol*, 52:357–69, 2004.

[81] H. J. Kim, D. W. Graham, A. A. DiSpirito, M. A. Alterman, N. Galeva, C. K. Larive, D. Asunskis, and P. M. Sherwood. Methanobactin, a copper-acquisition compound from methane-oxidizing bacteria. *Science*, 305:1612–5, 2004.

[82] L. W. Klomp, S. J. Lin, D. S. Yuan, R. D. Klausner, V. C. Culotta, and J. D. Gitlin. Identification and functional expression of HAH1, a novel human gene involved in copper homeostasis. *J Biol Chem*, 272:9221–6, 1997.

[83] V. Koronakis, A. Sharff, E. Koronakis, B. Luisi, and C. Hughes. Crystal structure of the bacterial membrane protein TolC central to multidrug efflux and protein export. *Nature*, 405:914–9, 2000.

[84] B. P. Krom, J. B. Warner, W. N. Konings, and J. S. Lolkema. Complementary metal ion specificity of the metal-citrate transporters CitM and CitH of *Bacillus subtilis*. *J Bacteriol*, 182:6374–81, 2000.

[85] F. Kunst, N. Ogasawara, I. Moszer, A. M. Albertini, G. Alloni, V. Azevedo, M. G. Bertero, P. Bessieres, A. Bolotin, S. Borchert, R. Borriss, L. Boursier, A. Brans, M. Braun, S. C. Brignell, S. Bron, S. Brouillet, C. V. Bruschi, B. Caldwell, V. Capuano, N. M. Carter, S. K. Choi, J. J. Codani, I. F. Connerton, A. Danchin, and *et al*. The complete genome sequence of the gram-positive bacterium *Bacillus subtilis*. *Nature*, 390:249–56, 1997.

[86] S. J. Lin and V. C. Culotta. The ATX1 gene of *Saccharomyces cerevisiae* encodes a small metal homeostasis factor that protects cells against reactive oxygen toxicity. *Proc Natl Acad Sci U S A*, 92:3784–8, 1995.

[87] J. M. Liu and A. Camilli. A broadening world of bacterial small RNAs. *Curr Opin Microbiol*, 13:18–23, 2010.

[88] T. Liu, A. Ramesh, Z. Ma, S. K. Ward, L. Zhang, G. N. George, A. M. Talaat, J. C. Sacchettini, and D. P. Giedroc. CsoR is a novel *Mycobacterium tuberculosis* copper-sensing transcriptional regulator. *Nat Chem Biol*, 3:60–8, 2007.

[89] S. Lutsenko and J. H. Kaplan. Organization of P-type ATPases: significance of structural diversity. *Biochemistry*, 34:15607–13, 1995.

[90] Z. Ma, D. M. Cowart, R. A. Scott, and D. P. Giedroc. Molecular insights into the metal selectivity of the copper(I)-sensing repressor CsoR from *Bacillus subtilis*. *Biochemistry*, 48:3325–34, 2009.

[91] L. Macomber and J. A. Imlay. The iron-sulfur clusters of dehydratases are primary intracellular targets of copper toxicity. *Proc Natl Acad Sci U S A*, 106:8344–9, 2009.

[92] L. Macomber, C. Rensing, and J. A. Imlay. Intracellular copper does not catalyze the formation of oxidative DNA damage in *Escherichia coli*. *J Bacteriol*, 189:1616–26, 2007.

[93] U. Mader, S. Hennig, M. Hecker, and G. Homuth. Transcriptional organization and posttranscriptional regulation of the *Bacillus subtilis* branched-chain amino acid biosynthesis genes. *J Bacteriol*, 186:2240–52, 2004.

[94] D. Magnani and M. Solioz. *Molecular Microbiology of Heavy Metals*. Springer-Verlag, 2007.

[95] E. Massé, F. E. Escorcia, and S. Gottesman. Coupled degradation of a small regulatory RNA and its mRNA targets in *Escherichia coli*. *Genes Dev*, 17:2374–83, 2003.

[96] E. Massé and S. Gottesman. A small RNA regulates the expression of genes involved in iron metabolism in *Escherichia coli*. *Proc Natl Acad Sci U S A*, 99:4620–5, 2002.

[97] E. Massé, H. Salvail, G. Desnoyers, and M. Arguin. Small RNAs controlling iron metabolism. *Curr Opin Microbiol*, 10:140–5, 2007.

[98] E. Massé, C. K. Vanderpool, and S. Gottesman. Effect of RyhB small RNA on global iron use in *Escherichia coli*. *J Bacteriol*, 187:6962–71, 2005.

[99] N. R. Mattatall, J. Jazairi, and B. C. Hill. Characterization of YpmQ, an accessory protein required for the expression of cytochrome c oxidase in *Bacillus subtilis*. *J Biol Chem*, 37:28802–9, 2000.

[100] C. S. McHenry. Chromosomal replicases as asymmetric dimers: studies of subunit arrangement and functional consequences. *Mol Microbiol*, 49:1157–65, 2003.

[101] A. L. McLoon, I. Kolodkin-Gal, S. M. Rubinstein, R. Kolter, and R. Losick. Spatial regulation of histidine kinases governing biofilm formation in *Bacillus subtilis*. *J Bacteriol*, 193:679–85, 2011.

[102] M. Miethke, O. Klotz, U. Linne, J. J. May, C. L. Beckering, and M. A. Marahiel. Ferri-bacillibactin uptake and hydrolysis in *Bacillus subtilis*. *Mol Microbiol*, 61:1413–27, 2006.

[103] J.H. Miller. Assay of β-galactosidase. In *Experiments in Molecular Genetics*. Cold Spring Harbor Laboratory Press, 1972.

[104] T. M, T. Franch, P. Hojrup, D. R. Keene, H. P. Bachinger, R. G. Brennan, and P. Valentin-Hansen. Hfq: a bacterial Sm-like protein that mediates RNA-RNA interaction. *Mol Cell*, 9:23–30, 2002.

[105] T. M, T. Franch, C. Udesen, K. Gerdes, and P. Valentin-Hansen. Spot 42 RNA mediates discoordinate expression of the *Escherichia coli* galactose operon. *Genes Dev*, 16:1696–706, 2002.

[106] C. M. Moore and J. D. Helmann. Metal ion homeostasis in *Bacillus subtilis*. *Curr Opin Microbiol*, 8:188–95, 2005.

[107] I. Moszer, P. Glaser, and A. Danchin. Subtilist: a relational database for the *Bacillus subtilis* genome. *Microbiology*, 141:261–8, 1995.

[108] A. Odermatt, R. Krapf, and M. Solioz. Induction of the putative copper ATPases, CopA and CopB, of *Enterococcus hirae* by Ag^{+} and Cu^{2+}, and Ag^{+} extrusion by CopB. *Biochem Biophys Res Commun*, 202:44–8, 1994.

[109] A. Odermatt and M. Solioz. Two trans-acting metalloregulatory proteins controlling expression of the copper-ATPases of *Enterococcus hirae*. *J Biol Chem*, 270:4349–54, 1995.

[110] J. Ollinger, K. B. Song, H. Antelmann, M. Hecker, and J. D. Helmann. Role of the Fur regulon in iron transport in *Bacillus subtilis*. *J Bacteriol*, 188:3664–73, 2006.

[111] R. C. Olsthoorn, M. Laurs, F. Sohet, C. W. Hilbers, H. A. Heus, and C. W. Pleij. Novel application of sRNA: stimulation of ribosomal frameshifting. *Rna*, 10:1702–3, 2004.

[112] M. C. Oosthuizen, B. Steyn, J. Theron, P. Cosette, D. Lindsay, A. Von Holy, and V. S. Brozel. Proteomic analysis reveals differential protein expression by *Bacillus cereus* during biofilm formation. *Appl Environ Microbiol*, 68:2770–80, 2002.

[113] F. W. Outten, C. E. Outten, J. Hale, and T. V. O'Halloran. Transcriptional activation of an *Escherichia coli* copper efflux regulon by the chromosomal MerR homologue, *cueR*. *J Biol Chem*, 275:31024–9, 2000.

[114] K. Papenfort, M. Bouvier, F. Mika, C. M. Sharma, and J. Vogel. Evidence for an autonomous 5′ target recognition domain in an Hfq-associated small RNA. *Proc Natl Acad Sci U S A*, 107:20435–40, 2010.

[115] M. A. Pennella and D. P. Giedroc. Structural determinants of metal selectivity in prokaryotic metal-responsive transcriptional regulators. *Biometals*, 18:413–28, 2005.

[116] E. Pohl, X. Qui, L. M. Must, R. K. Holmes, and W. G. Hol. Comparison of high-resolution structures of the diphtheria toxin repressor in complex with cobalt and zinc at the cation-anion binding site. *Protein Sci*, 6:1114–8, 1997.

[117] K. Prévost, G. Desnoyers, J. F. Jacques, F. Lavoie, and E. Massé. Small RNA-induced mRNA degradation achieved through both translation block and activated cleavage. *Genes Dev*, 25:385–96, 2011.

[118] K. Prévost, H. Salvail, G. Desnoyers, J. F. Jacques, E. Phaneuf, and E. Massé. The small RNA RyhB activates the translation of *shiA* mRNA encoding a permease of shikimate, a compound involved in siderophore synthesis. *Mol Microbiol*, 64:1260–73, 2007.

[119] J. D. Quisel, W. F. Burkholder, and A. D. Grossman. *In vivo* effects of sporulation kinases on mutant Spo0A proteins in *Bacillus subtilis*. *J Bacteriol*, 183:6573–8, 2001.

[120] D. S. Radford, M. A. Kihlken, G. P. Borrelly, C. R. Harwood, N. E. Le Brun, and J. S. Cavet. CopZ from *Bacillus subtilis* interacts *in vivo* with a copper exporting CPx-type ATPase CopA. *FEMS Microbiol Lett*, 220:105–12, 2003.

[121] M. Rehmsmeier, P. Steffen, M. Hochsmann, and R. Giegerich. Fast and effective prediction of microRNA/target duplexes. *Rna*, 10:1507–17, 2004.

[122] C. Rensing and G. Grass. *Escherichia coli* mechanisms of copper homeostasis in a changing environment. *FEMS Microbiol Rev*, 27:197–213, 2003.

[123] H. Salvail, P. Lanthier-Bourbonnais, J. M. Sobota, M. Caza, J. A. Benjamin, M. E. Mendieta, F. Lepine, C. M. Dozois, J. Imlay, and E. Massé. A small RNA promotes siderophore production through transcriptional and metabolic remodeling. *Proc Natl Acad Sci U S A*, 107:15223–8, 2010.

[124] J. Sambrook, E. F. Fritsch, and T. Maniatis. *Molecular Cloning: a Laboratory Manual*. Cold Spring Harbor Laboratory, 2nd edition, 1989.

[125] U. Sauer. Metabolic networks in motion: ^{13}C-based flux analysis. *Mol Syst Biol*, 2:62, 2006.

[126] M. P. Schmitt, B. G. Talley, and R. K. Holmes. Characterization of lipoprotein IRP1 from *Corynebacterium diphtheriae*, which is regulated by the diphtheria toxin repressor (DtxR) and iron. *Infect Immun*, 65:5364–7, 1997.

[127] M. A. Schumacher, R. F. Pearson, T. M, P. Valentin-Hansen, and R. G. Brennan. Structure of the pleiotropic translational regulator Hfq and an Hfq-RNA complex: a bacterial Sm-like protein. *EMBO J*, 21:3546–56, 2002.

[128] A. Sittka, C. M. Sharma, K. Rolle, and J. Vogel. Deep sequencing of *Salmonella* RNA associated with heterologous Hfq proteins *in vivo* reveals small RNAs as a major target class and identifies RNA processing phenotypes. *RNA Biol*, 6:266–75, 2009.

[129] G. T. Smaldone and J. D. Helmann. CsoR regulates the copper efflux operon *copZA* in *Bacillus subtilis*. *Microbiology*, 153:4123–8, 2007.

[130] M. Solioz, H. K. Abicht, M. Mermod, and S. Mancini. Response of gram-positive bacteria to copper stress. *J Biol Inorg Chem*, 15:3–14, 2009.

[131] M. Solioz and C. Vulpe. CPx-type ATPases: a class of P-type ATPases that pump heavy metals. *Trends Biochem Sci*, 21:237–41, 1996.

[132] A. L. Sonenshein. Control of key metabolic intersections in *Bacillus subtilis*. *Nat Rev Microbiol*, 5:917–27, 2007.

[133] M. M. Spiering, D. Ringe, J. R. Murphy, and M. A. Marletta. Metal stoichiometry and functional studies of the diphtheria toxin repressor. *Proc Natl Acad Sci U S A*, 100:3808–13, 2003.

[134] J. V. Stoyanov and N. L. Brown. The *Escherichia coli* copper-responsive *copA* promoter is activated by gold. *J Biol Chem*, 278:1407–10, 2003.

[135] J. V. Stoyanov, J. L. Hobman, and N. L. Brown. CueR (YbbI) of *Escherichia coli* is a MerR family regulator controlling expression of the copper exporter CopA. *Mol Microbiol*, 39:502–11, 2001.

[136] J. V. Stoyanov, D. Magnani, and M. Solioz. Measurement of cytoplasmic copper, silver, and gold with a *lux* biosensor shows copper and silver, but not gold, efflux by the CopA ATPase of *Escherichia coli*. *FEMS Microbiol Lett*, 546:391–4, 2003.

[137] J. Stulke, R. Hanschke, and M. Hecker. Temporal activation of beta-glucanase synthesis in *Bacillus subtilis* is mediated by the GTP pool. *J Gen Microbiol*, 139:2041–5, 1993.

[138] X. Tao, N. Schiering, H. Y. Zeng, D. Ringe, and J. R. Murphy. Iron, DtxR, and the regulation of diphtheria toxin expression. *Mol Microbiol*, 14:191–7, 1994.

[139] B. Tjaden, S. S. Goodwin, J. A. Opdyke, M. Guillier, D. X. Fu, S. Gottesman, and G. Storz. Target prediction for small, noncoding RNAs in bacteria. *Nucleic Acids Res*, 34:2791–802, 2006.

[140] D. Touati. Iron and oxidative stress in bacteria. *Arch Biochem Biophys*, 373:1–6, 2000.

[141] K. I. Udekwu, F. Darfeuille, J. Vogel, J. Reimegard, E. Holmqvist, and E. G.

Wagner. Hfq-dependent regulation of OmpA synthesis is mediated by an antisense RNA. *Genes Dev*, 19:2355–66, 2005.

[142] P. B. Vander Horn and S. A. Zahler. Cloning and nucleotide sequence of the leucyl-tRNA synthetase gene of *Bacillus subtilis*. *J Bacteriol*, 174:3928–35, 1992.

[143] J. Vogel, V. Bartels, T. H. Tang, G. Churakov, J. G. Slagter-Jager, A. Huttenhofer, and E. G. Wagner. RNomics in *Escherichia coli* detects new sRNA species and indicates parallel transcriptional output in bacteria. *Nucleic Acids Res*, 31:6435–43, 2003.

[144] J. Vogel and C. M. Sharma. How to find small non-coding RNAs in bacteria. *Biol Chem*, 386:1219–38, 2005.

[145] A. Wach. PCR-synthesis of marker cassettes with long flanking homology regions for gene disruptions in *S. cerevisiae*. *Yeast*, 12:259–65, 1996.

[146] T. Wakabayashi, N. Nakamura, Y. Sambongi, Y. Wada, T. Oka, and M. Futai. Identification of the copper chaperone, CUC-1, in *Caenorhabditis elegans*: tissue specific co-expression with the copper transporting ATPase, CUA-1. *FEMS Microbiol Lett*, 440:141–6, 1998.

[147] C. Wandersman and P. Delepelaire. Bacterial iron sources: from siderophores to hemophores. *Annu Rev Microbiol*, 58:611–47, 2004.

[148] K.M. Wassarman. 6S RNA: a small RNA regulator of transcription. *Curr Opin Microbiol*, 10:164–8, 2007.

[149] S. Weinberger and C. Gilvarg. Bacterial distribution of the use of succinyl and acetyl blocking groups in diaminopimelic acid biosynthesis. *J Bacteriol*, 101:323–4, 1970.

[150] J. Wennerhold and M. Bott. The DtxR regulon of *Corynebacterium glutamicum*. *J Bacteriol*, 188:2907–18, 2006.

[151] M. Wetzstein, U. Volker, J. Dedio, S. Lobau, U. Zuber, M. Schiesswohl, C. Herget, M. Hecker, and W. Schumann. Cloning, sequencing, and molecular analysis of the *dnaK* locus from *Bacillus subtilis*. *J Bacteriol*, 174:3300–10, 1992.

[152] P. J. Wilderman, N. A. Sowa, D. J. FitzGerald, P. C. FitzGerald, S. Gottesman, U. A. Ochsner, and M. L. Vasil. Identification of tandem duplicate regulatory small RNAs in *Pseudomonas aeruginosa* involved in iron homeostasis. *Proc Natl Acad Sci U S A*, 101:9792–7, 2004.

[153] R. Wimmer, T. Herrmann, M. Solioz, and K. Wuthrich. NMR structure and metal interactions of the CopZ copper chaperone. *J Biol Chem*, 274:22597–603, 1999.

[154] C. C. Winterbourn. Toxicity of iron and hydrogen peroxide: the Fenton reaction. *Toxicol Lett*, 82-83:969–74, 1995.

[155] K. D. Xu, P. S. Stewart, F. Xia, C. T. Huang, and G. A. McFeters. Spatial physiological heterogeneity in *Pseudomonas aeruginosa* biofilm is determined by oxygen availability. *Appl Environ Microbiol*, 64:4035–9, 1998.

[156] R.E. Yasbin and F.E. Young. Transduction in *Bacillus subtilis* by bacteriophage SPP1. *J Virol*, 14:1343–8, 1974.

[157] Q. Z. Ye, S. X. Xie, Z. Q. Ma, M. Huang, and R. P. Hanzlik. Structural basis of catalysis by monometalated methionine aminopeptidase. *Proc Natl Acad Sci U S A*, 103:9470–5, 2006.

[158] C. You, H. Lu, A. Sekowska, G. Fang, Y. Wang, A. M. Gilles, and A. Danchin. The two authentic methionine aminopeptidase genes are differentially expressed in *Bacillus subtilis*. *BMC Microbiol*, 5:57, 2005.

[159] H. Yuan, S. C. Chai, C. K. Lam, X. H. Howard, and Q. Z. Ye. Two methionine aminopeptidases from *Acinetobacter baumannii* are functional enzymes. *Bioorg Med Chem Lett*, 21:3395–8, 2011.

[160] N. Zamboni, S. M. Fendt, M. Ruhl, and U. Sauer. ^{13}C-based metabolic flux analysis. *Nat Protoc*, 4:878–92, 2009.

[161] N. Zamboni, E. Fischer, and U. Sauer. FiatFlux–a software for metabolic flux analysis from ^{13}C-glucose experiments. *BMC Bioinformatics*, 6:209, 2005.

[162] M. Zuker. Mfold web server for nucleic acid folding and hybridization prediction. *Nucleic Acids Res*, 31:3406–15, 2003.